Dynamic Leach Testing of Low- and Medium-pH Injection Grouts to Be Used in Deep Repositories

(Cementitious Materials in Deep Geological Repositories)

Master's Thesis

Tiina Heikola

University of Jyväskylä

Department of Chemistry

Laboratory of Inorganic and Analytical Chemistry

17.10.2008

ABSTRACT

Posiva (Posiva Oy) is planning to deposit spent nuclear fuel in deep repositories. With respect to the long-term safety a suitable chemical environmental is essential. The constructions of underground disposal facility require low-pH cement-based materials, because assured data of the effects of a possible high-pH plume from ordinary cementitious materials is lacking.

The work is comprised of two parts. The literary part reviews the characteristics of cement chemistry and durability aspects of cementitious materials. The experimental part of the work concentrates on the dynamic leach testing of two injection grouts, one low-pH grout and one medium-pH grout. Leach testing was performed in order to study the pH value and chemical composition of the leachates. In order to gain more information on the changes occurring in the leached solids during the test the solid samples were also subjected to investigations.

The literary part begins with discussion of the general aspects of disposal of spent nuclear fuel. Also the influences of cementitious materials to the groundwater and barrier systems, such as bentonite are discussed. The long-term safety of materials is essential in deep geological repository. The second chapter covers the characteristics of cement chemistry, components of cement and hydration reactions of clinker minerals. The durability aspects of cementitious materials are discussed at the end of survey. Finally, the characteristics of low-pH injection grouts are introduced. The use of these materials in the real bedrock conditions has to be carefully evaluated.

Leach testing was performed in a glove-box (N_2 atmosphere) in order to avoid the interference of atmospheric CO_2. Two simulated groundwater solutions, fresh ALL-MR and saline OL-SR, were used as leachates. The object of the work was to evaluate the influence of the water flow on leaching of grout samples. Two flow rates were chosen, higher flow rate of 7.5 mL/h and a lower one of 0.625 mL/h. The sample collection was performed according to a time schedule. The pH value of each leachate sample was measured, but the amount of total organic carbon was determined only for some leachates. Because of the great number of leachate samples some of them were combined before chemical analysis.

Rather expected results were gained. The faster decrease of pH values was noticed in the case of the higher flow rate experiment. A similar decrease was detected in both low- and medium-pH grout leachates. The difference in pH values between two grouts

was greater in the saline leachates for both flow rates. Compared to the pH results gained from earlier static leach testing, the pH of the leachates in present study decreased faster, although the results are not directly comparable since they were performed in different temperatures.[1] The low-pH leachates reached the target pH < 11 in all tests. The medium-pH grout leachates also showed decreasing trend in both solutions at the faster flow rate. However, only a minor decrease was observed at slow flow rate.

The chemical and mineral composition of the grout samples was analyzed by using X-Ray Diffractometry (XRD), thermal analysis (TG/DTA) and X-Ray Fluorescense (XRF). According to the XRD results all the analyzed grout samples were mainly amorphous and, thus, only relatively small amounts of crystalline compounds were detected. The main compound in all the samples specimens was amorphous calcium silicate hydrate gel. The thermal behavior of all the grout samples was relatively similar. The degradation reactions causing mass losses could be divided into seven to nine successive phases. According to the XRF analyses the contents of calcium and silicon in sample specimes had been diminished to some extent. The same effect could be observed in the content of potassium and sodium.

TIIVISTELMÄ

Posivan (Posiva Oy) suunnitelmissa on sijoittaa käytetty ydinpolttoaine syvälle kallioperään rakennettavaan loppusijoitustilaan. Pitkäaikaisturvallisuuden kannalta loppusijoitustilan ja sen ympäristön kemiallisilla ominaisuuksilla on erittäin suuri merkitys. Loppusijoitustilan rakentamista varten tarvitaan matalan pH:n sementtipohjaisia materiaaleja, koska ei ole olemassa varmaa tietoa tavallisten sementtipohjaistenmateriaalien aiheuttaman korkean pH:n vaikutuksista syvällä kallioperässä.

Työ koostui kahdesta osasta. Kirjallinen osuus käsittelee sementin kemiaa ja sen ominaispiirteitä. Kokeellisessa osuudessa keskitytään tarkastelemaan injektointilaasteilla suoritettua dynaamista uuttokoetta. Työn tarkoituksena oli määrittää uuttovesien pH ja kemiallinen koostumus. Lisäksi itse eluutiotestissä olleet kappaleet analysoitiin, jotta voitiin arvioida virtaavan veden vaikutuksia kiinteisiin massoihin.

Kirjallinen osuuden ensimmäisessä kappaleessa käydään yleisesti läpi käytetyn ydinjätteen loppusijoitusperiaatteet. Lisäksi käsitellään sementtipohjaisten materiaalien vaikutusta pohjaveteen ja vapautumisesteiden, kuten bentoniittisaven, toimintakykyyn. Seuraavassa kappaleessa käydään läpi sementtikemian perusteet, sementin komponentit ja klinkkerimineraalien hydrataatioreaktiot. Materiaalien pitkäaikaiskestävyys on erityisen tärkeää syvällä geologisessa loppusijoitustilassa. Tutkielman lopulla käsitellään sementtipohjaisten materiaalien kestävyyttä ja siihen vaikuttavia tekijöitä. Lopuksi käydään läpi matalan pH:n injektointiaineiden tutkimusta ja kehitystä, sekä tarkastellaan niiden käyttöä todellisissa kallioperäolosuhteissa.

Injektointimassojen uuttotesti tehtiin hanskakaapissa, typpiatmosfäärissä, jotta voitiin estää ilman CO_2:n aiheuttamat häiriöt. Uuttotesteissä käytettiin kahta simuloitua pohjavettä: makeaa ALL-MR ja suolaista OL-SR. Dynaamisen uuttotestin avulla pyrittiin selvittää virtaavan veden vaikutus näytekappaleisiin. Virtausnopeuksia oli kaksi: nopeampi 7,5 ml/h ja hitaampi 0,625 ml/h. Näytteenotto suoritettiin ennalta määrätyn aikataulun mukaisesti. Jokaisesta näytteestä mitattiin pH, mutta vain osasta määritettiin orgaanisen hiilen kokonaismäärä. Näytteenottotiheys oli kokeen alussa suuri, joten näytteitä kertyi huomattava määrä. Tämän takia osa näytteistä yhdistettiin ennen kemiallisia alkuaineanalyysejä.

Uuttovesien pH-tulokset olivat melko ennalta odotettuja. Nopeinten uuttovesien pH laski nopeammassa virtauksessa kummankin massan kohdalla ja suurempi ero oli

havaittavissa suolaisessa vedessä. Kun saatuja tuloksia verrattiin aikaisempaan tasapaino- ja diffuusiotestien tuloksiin, huomattiin että pH laski dynaamisessa kokeessa huomattavasti nopeammin.[1] Tulokset eivät kuitenkaan ole suoraan verrattavissa toisiinsa, sillä kokeet suoritettiin eri lämpötiloissa. Matalan pH:n massalla saavutettiin kaikissa testiolosuhteissa vaatimuksissa esitetty uuttoliuoksen pH-arvo testin lopussa. Myös medium pH:n uuttovesien pH laski vaaditulle tasolle nopeammalla virtausnopeudella, mutta vain pieni lasku oli havaittavissa hitaammalla virtausnopeudella.

Laastinäytteiden kemiallinen koostumus sekä mineraalikoostumus analysoitiin röntgendiffraktometrin (XRD), termovaa'an (TG/DTA) ja röntgen-fluoresenssi-spektrometrin avulla (XRF). Röntgendiffraktometrillä saatujen tulosten perusteella voidaan sanoa, että näytteet koostuivat suurimmaksi osaksi amorfisesta kalsiumsilkaattihydraattigeelistä. Kiteisten yhdisteiden osuus näytteissä oli suhteellisen pieni. Näytteiden terminen käyttäytyminen oli melko yhdenkaltaista. Seitsemästä yhdeksään eri massan muutoksen vaihetta voitiin erottaa termovaaka-analyysin aikana. Röntgen-fluoresenssi-spektrometrillä saatujen tulosten pohjalta voitiin arvioida, että näytteiden kalsium- ja piipitoisuus oli vähentynyt uuttokokeen aikana. Myös kalium- ja natriumpitousuudet olivat pienentyneet alkuperäisestä.

PREFACE

This work was carried out at Technical Research Centre of Finland (VTT). It is part of Posiva Oy's project in which the aim is to develop a low-pH injection grout (pH ≤ 11) to be used in deep geological repositories. Publications for this work were obtained by using VTT eLibrary's Journal-software, as well as Posiva's and SKB's report search. Also the search service Google was exploited.

My deepest gratitude belongs to my co-workers at VTT for their help and support. Special thanks to Senior Research Scientist Ulla Vuorinen for the guidance and advices and Laboratory Assistant Kirsti Helosuo for her help in the laboratory. Acknowledgements to Senior Research Scientists Tom E. Gustafsson and Pertti Koskinen at VTT who were a great help in interpretation of the analytical results. I would also like to thank senior assistant Ari Väisänen for his professional advisements and encouragement. Finally, I would express my gratitude to my parents for believing in me and for all the help.

TABLE OF CONTENTS

LIST OF ABBREVIATIONS

The notations used in the report are as follows:

ALL-MR	simulated fresh granitic groundwater
A	Al_3O_3
AFt	general abbreviation for calcium sulfoaluminate hydrate phases (Al_3O_3-Fe_2O_3-tri)
AFm	general abbreviation for calcium aluminate hydrate phases (Al_3O_3-Fe_2O_3-mono)
C_3A	tricalcium aluminate
C_4AF	tetracalcium aluminoferrite
C_4AH_{19}	calcium aluminate hydrate
$C_4A\bar{S}H_{12}$	calcium aluminate monosulphate hydrate
$C_6A\bar{S}_3H_{32}$	ettringite (trisulphate)
CH	calcium hydroxide (portlandite), $Ca(OH)_2$
C_2S	dicalsium silicate
C_3S	tricalcium silicate
CSH or C-S-H	calcium silicate hydrate
DM	dry matter
F	Fe_2O_3
Grout Aid	commercial slurry of silica fume (SF)
H	lower flow rate (0.625 mL/h)
ICP-AES	Inductively Coupled Plasma Atomic Emission Spectrometry
IC	Ion Chromatography
KBS-3V	vertical deposition concept
N	higher flow rate (7.5 mL/h)
NUMO	Nuclear waste management organization of Japan
OPC	ordinary Portland cement
Posiva Oy	Finnish nuclear waste management organisation
SF	silica fume
SKB	Swedish nuclear fuel and waste Management Co
SPL	superplasticizer
SR	sulphate resistant
TG-DTA	Thermo Gravimetric-Differential Thermal Analysis
UF16	Ultra Fine 16 (Commercial injection cement, by Cementa Oy)
W	Water

W/B	water-to-binder ratio
W/C	water-to-cement ratio
XRD	X-Ray Diffractometry
XRF	X-Ray Fluorescence

LITERARY WORK

1 INTRODUCTION

Spent nuclear fuel is planned to be deposited in a deep repository at Olkiluoto, an island on the south western coast of Finland. Posiva Oy (Posiva), owned by the two nuclear power companies, Teollisuuden voima Oy (TVO) and Fortum Power and Heat Oy (Fortum), is responsible for the final disposal of spent nuclear fuel.

Investigations on the suitability of Olkiluoto as location for spent nuclear fuel repository have been ongoing for over fifteen years. The final step in the investigations is the construction of an underground rock characterisation facility, ONKALO, which began in 2004. It will be used to further characterise the bedrock properties, and to test and develop repository construction, operation, and closure technologies. Posiva plans to begin repository operations in 2020. The repository will be constructed in several stages and the total operation period may extend to about 100 years.[2]

One of the main requirements in constructing of the access tunnel is its water-tightness which has to meet the requirement of maximum allowed groundwater inflow of 1-2 L per minute for 100 m of tunnel length. This will be obtained by grouting which seals the fractures and cracks decreasing the permeability of the fracture zones.[3] In addition to the positive affects of grouting it may also cause some harmful chemical effects on the geohydrological environment, such as a high-pH plume resulting from cementitious grouting materials. Another risk is imposed by the organic cement admixtures, which are able to complex radionuclides and thereby enhance their transport.[5] Due to these effects the development and testing of special low-pH grout recipes was started.[6]

The development of a suitable grouting material consisted of several tasks. First the requirements for the materials were set. Development of technical performance of the grouts was done by Kronlöf.[6] The technical properties of the grout mixes were tested and the most promising recipes were then selected to leach testing to assess the leachate pH values.[5] Based on these results, the most promising recipes were also tested in pilot field-test (PFTs) in Finland.[7]

Leaching of cementitious materials has been extensively studied. However, majority of the experiments have been primarily concerned with the degradation of structural materials with standard test not corresponding to the actual environmental conditions. The pH and leaching properties of the low-pH cementitious grouts and a conventional grout as reference were studied by Vuorinen at VTT.[1,5] In the present study, the main

objective was to evaluate the influence of the water flow on the leaching behaviour of grout materials.

2 DISPOSAL

2.1 General aspects

Storing is a consequential step in the management of radioactive waste. In recent years the storages initially intended as temporary facilities have had their lifetimes extended and this has raised some discussion about the important options of a long term waste management. In nuclear countries, radioactive waste results mainly from the civil nuclear power programmes. Produced radioactive waste has to be managed responsibly to ensure public safety, protection of the environment and security from malicious damage now and in the future. In 1995 the International Atomic Energy Agency (IAEA) published The Principles of Radioactive Waste Management, Safety Series No. 111-F. One of the nine principles set forth in that report was that "Radioactive waste shall be managed in such away that will not impose undue burdens on future generations". This statement was based on the commonly excepted ethical aspect that the generation that generates and benefits from activity should make all the arrangement needed for the disposal of the waste.

Although great progress has been made in the developing the technology for geological disposal, no such a repository for high level waste is yet in operation.[8] One geological repository for long lived transuranic waste is in operation: the Waste Isolation Pilot Plant (WIPP) for defence waste in United State of America. Elsewhere the repository projects are at various stages of development. In Finland and Sweden there has been some significant progress only, but in other countries delays has occurred.

The final step in nuclear waste management in Finland is the geological disposal deep in the bedrock.[9] The plan for Finnish nuclear waste management has been developed since 1970s. The first nuclear power plant, Loviisa 1 has been operating since 1977 in Loviisa on Hälsholmen island in Southern Finland. In the beginning of production all the produced high-level nuclear waste from Loviisa power plant was shipped back to the nuclear fuel reprocessing plant Majak in Russia. In 1996 the new nuclear law took effect denying export and import of nuclear waste to Finland. After that all the produced spent fuel has been placed in temporary facilities.

From the beginning it has been an object to build a long term disposal facility in Finland.[10] In 1983 the Finnish Government made a decision on the aims and programme for nuclear waste management. The work was started by investigating a proper location for the final disposal facility. The detailed characterisation was carried out in four

municipalities. In December 2000 the Government made a policy decision in favour of constructing an underground rock characterisation facility in Olkiluoto in the municipality of Eurajoki and in May 2001 Finnish Parliament ratified the Government's policy decision.

The Finnish underground rock characterisation facility for the final disposal of spent nuclear fuel is known as ONKALO. The construction of ONKALO was started in 2004 and it will continue until 2011. The constructions of the final disposal facilities are planned to be started in 2015 and the project will be timed so that the disposal can be commenced in 2020. The total depth of the tunnel will be 520 metres but the final disposal repository will commence at a depth of 200–300 metres (Figure 1). The excavation will be performed with drilling and blasting method. The backfilling and sealing arrangements of the repository aim to re-establishment of the undisturbed conditions in the geosphere. Their main function is to prevent inadvertent intrusion of groundwater into the repository.

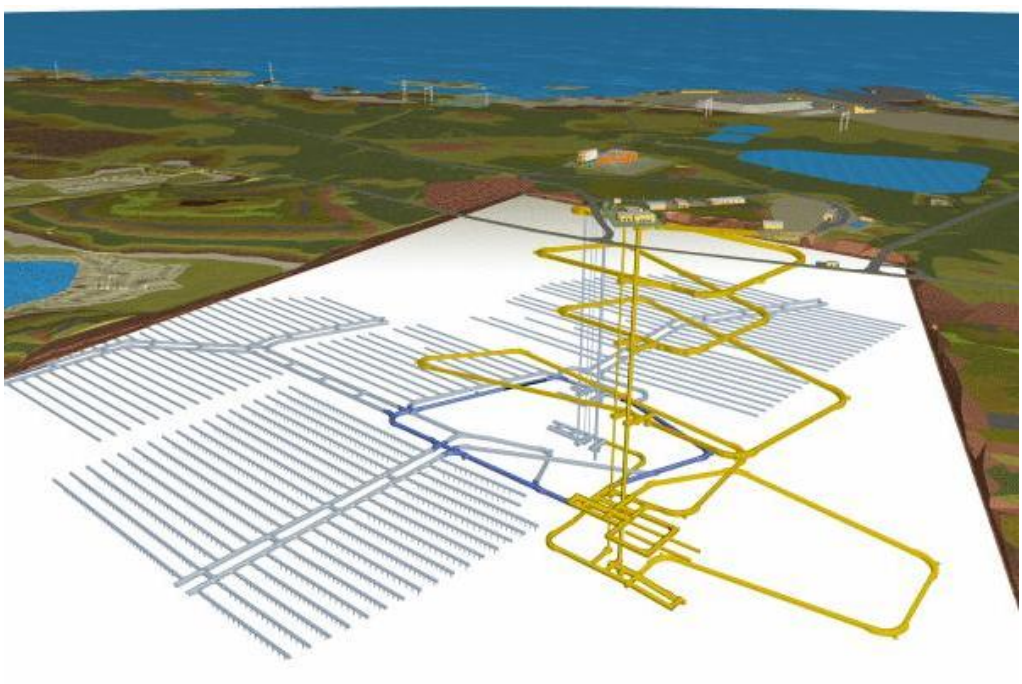

Figure 1. General layout of ONKALO (yellow) and the deep geological repository (blue) according to current design (www.posiva.fi).

According to current plans the tunnels will be back-filled with a mixture of bentonite and aggregate. The spent fuel encapsulated in a tightly fitted iron internal canister inside

an external copper case will be surrounded by compacted bentonite clay in the deposition hole in the intact bedrock. This multi barrier shield will prevent the release of radioactive materials into the bedrock and biosphere. The long-term safety functions of the above introduced components are shown in Figure 2.

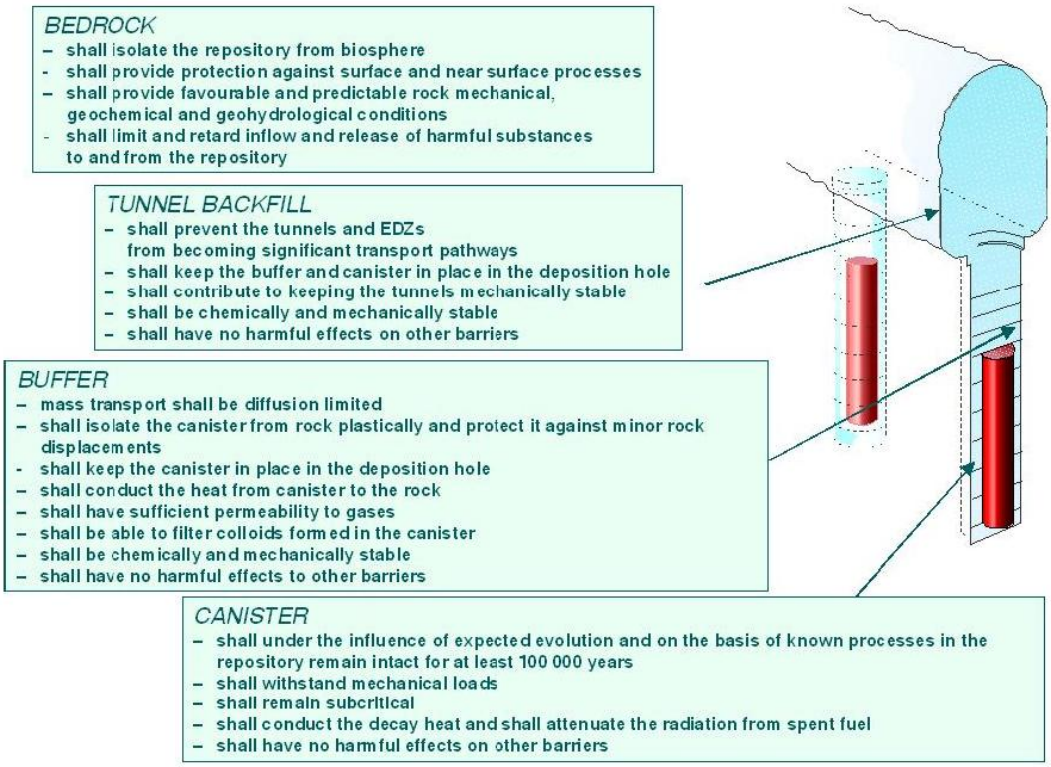

Figure 2. Long-term safety functions of the bedrock and engineered barrier system in the KBS-3V disposal concept.[11]

Water inflow into an underground facility may cause technical, environmental and, safety problems. Therefore it is important to control and restrict the volume of water inflow to a reasonable level. Cement based materials are of special interest in construction and sealing the underground facility. Concrete and cement are planned to be used, for example, as shotcrete and as casting material for rock bolts to reinforce the excavations. In addition, cement and other grouting materials injected into the rock are important means to limit inflow of groundwater into an underground facility.[11] For the sake of long-term safety, a suitable chemical environment is essential. Because there is very little assured data on effects of high-pH plume in saturated repository conditions, the acceptable target pH for injection grout for deep repositories was set at a value ≤ 11.

The crystalline bedrock at Olkiluoto can be divided to three structural types: 1) unfractured rock, 2) individual fractures and 3) brittle deformation zones (fracture zones). These fractured rock masses are the potential flow routes for groundwater. Waters form these zones usually make up the greatest proportion of inflowing water into tunnels. Thus grouting of the fracture zones is an essential task. The expected water flow and groutability of the host rock is dependent on many factors such as, hydraulic conductivity, fracture aperture, contact area, fracture density and occurrence of certain fracture fillings.[12]

An extensive hydrogeochemical sampling has been performed at the Olkiluoto site in order to assess the groundwater conditions. Characteristics of the groundwater vary according to depth (Figure 3). Fresh groundwater is found in the most upper part of the excavations. Brackish groundwater is found at depths varying between -40…-500 m. Below -400…-500 m saline groundwater is observed.[12] Sodium is the main cation in groundwater down to the great depths where it is replaced by calcium. Under brackish saline transition zone (< -500 m) groundwater shifts from sulphidic to methanic conditions. Table 1 represent the variation of geological parameters in groundwater against depth. The hydrochemical conditions in rock environment and groundwater that can decrease the durability of concrete and cementitious materials are pH, carbon dioxide (CO_2), ammonium (NH_4^+), magnesium (Mg^{2+}), chloride (Cl^-), and sulphate (SO_4^{2-}). The hydrochemical conditions of final repository have been evaluated from initial stage to the closure. It has been estimated that at initial conditions the pH is 7.8 – 8.3, ammonium concentration is < 0.05 mg/L, magnesium concentration is 30 – 70 mg/L, and sulphate concentration 0 – 20 mg/L. At closure time the pH value is estimated to be decreased to 6–8, magnesium concentration changed to 10 – 250 mg/L, and sulphate concentration to 0 – 500 mg/L.[12]

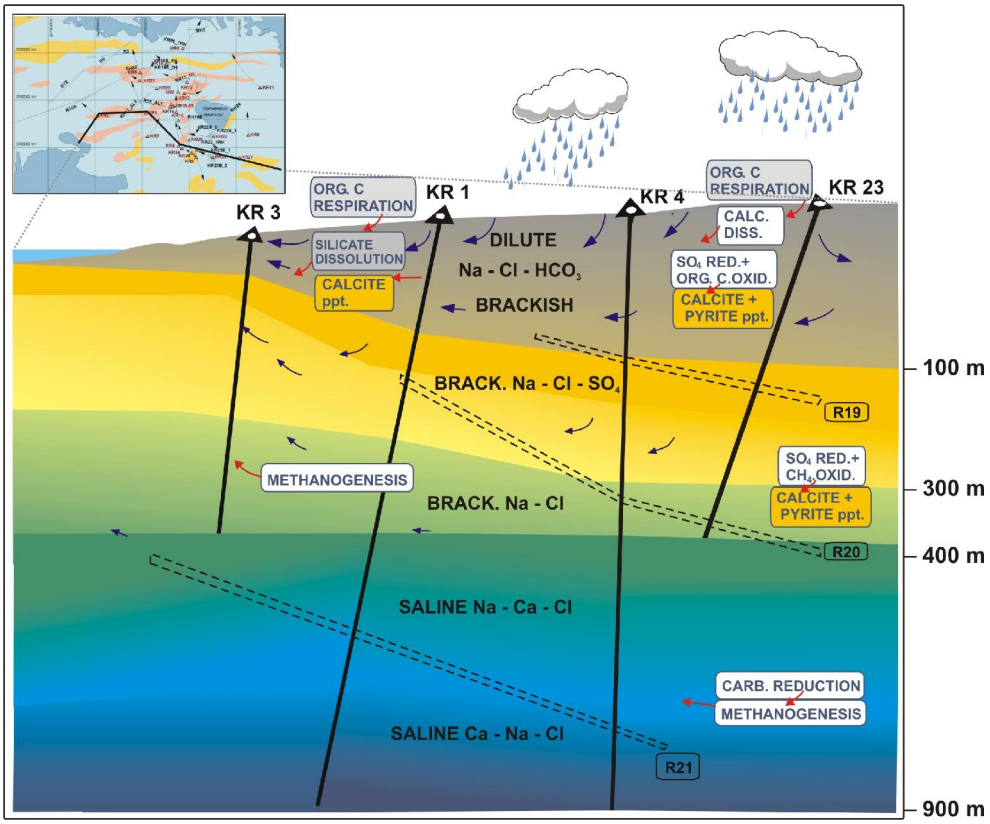

Figure 3. Illustrated cross-section of hydrogeochemical and hydrogeological conditions in the bedrock of Olkiluoto.[13]

Table 1. Vertical variation of the main hydrochemical parameters at Olkiluoto shown against depth.[14]

Depth (m)	Used classification	Water type	Cl (mg/l)	pH	Alkalinity
0	Fresh HCO_3	Ca-Na-Mg-HCO_3-SO_4	<10	5.5	< 0.5
10		Ca-Na-Mg-HCO_3-(SO_4-Cl)	10	7	3
150	Brackish HCO_3	Na-(Ca)-Cl-(HCO_3-SO_4)	2000	7.8	4
200	Brackish SO_4	Na-(Ca)-Cl-(SO_4)	4500	7.5	1
	Brackish Cl	Na-Cl	2700	8.2	0.4
450		Na-Ca-Cl	8000	8	0.2
600	Saline	Ca-Na-Cl	14000	7.8	
1000			50000	7.5	<0.1

2.2 Cement-bentonite interaction

Posiva and SKB are jointly developing backfilling concepts for deposition tunnels and other cavities.[11] Several material combinations and compaction techniques are

considered. The mostly studied and discussed material is a mixture of crushed rock and bentonite (70 wt% and 30 wt%).

The main functions of backfill in the deposition tunnels are to:

- prevent the tunnels and excavation damaged zone (EDZ) around them from becoming significant transport pathways,
- keep the buffering and canister in place in the deposition hole and
- contribute to keep the tunnels mechanically stable.

To fulfil these requirements the backfilling material should have following features:

- a sufficient stiffness and low compressibility,
- a low hydraulic conductivity,
- a sufficient swelling pressure against the possible effects of movements in the backfill,
- no harmful effects on the other barriers and chemical and mechanical stability.

Bentonite is a type of rock containing swelling clay that is chemically and mechanically stable. The major component of bentonite is montmorillonite. Other components are quartz, feldspar, cristobalite, gypsum, calcite, and pyrite. Several different types of bentonite could be used as buffering material in deposition conditions. The two mostly studied materials are: sodium bentonite from Wyoming, United States, (MX-80) and a calcium bentonite from the Greek island Milos (Deponit CA-N).[11]

The performance of bentonite buffer depends on its chemical structure. Montmorillonite has a three layer structure consisting of one octahedrally coordinated sheet between two tetrahedrally coordinated sheets (Figure 4). The octahedral sheets have aluminium and the tetrahedral sheets silicon as the main central cations. Some of these central cations may be substituted by cations of lesser charge (Al^{3+} with Mg^{2+} and Si^{4+} with Al^{3+}), causing a negative charge in the layer. The negative charge is compensated by exchangeable ions in the intercrystallite region. The charge is so weak that the cations can be adsorbed in this region with their hydrate shell. The extent of hydration produces intercrystalline swelling.

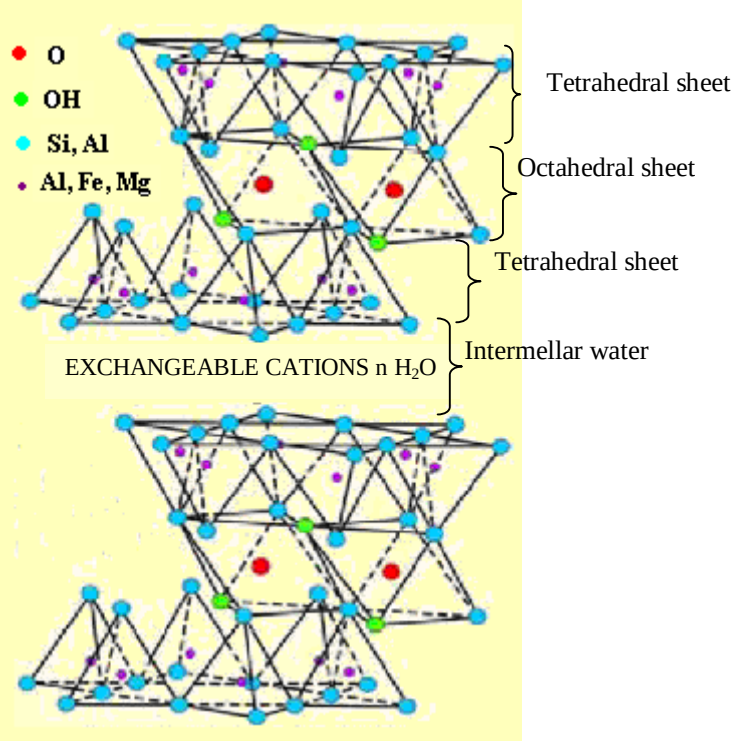

Figure 4. The structure of montmorillonite mineral.[11]

The compacted clay absorbs water into the intermellar spaces reducing the volume of the large pores. The exchangeable cations are bond to the montmorillonite surfaces to maintain the electrical neutrality. The intermellar spaces in montmorillonite are small and only water and exchangeable cation can move within the internal pores (by diffusion) and undergo ion-exchange until equilibrium is reached. The exchangeable cations contribute to the porewater chemistry by this ion exchange process.

The porewater chemistry of bentonite can be defined as the chemistry occurring in the water of the external pores of bentonite.[11] The porewater of bentonite has been extensively studied in many nuclear waste programmes during 20 years, but the general agreement on the composition of it still remains unclear.[15-17] The large swelling pressures of bentonite make it difficult to retrieve representative porewater samples. The chemical evolution of the bentonite buffer is affected by the high temperatures and radiation from the spent fuel, the groundwater composition, the presence of structural materials, such as cement-based grouts, seals, and of microbes.

Use of cementitious materials, especially grouting, can not be avoided in construction of a repository. A high-pH-plume have deleterious impacts on performance of spent fuel, cladding, and host rock, however, the main concern has focused on the effect on

stability of bentonite and thereby on the long-term safety. The high-pH fluids from cementitious materials may affect the effective clay density and clay swelling pressure. The interactions of high-pH solutions with montmorillonite, which is the main mineral component of bentonite, can be converted to non-swelling minerals such as zeolites, resulting decrease in swelling pressure.

Processes affecting the destruction of bentonite due to interaction with cement can be divided in four major classes:[18]

- Mass balance
- Thermodynamic relationships
- Mass transport
- Reaction kinetics

Above-mentioned processes are discussed in more detail in the following sections.

2.2.1 Mass balance

The mass balance control focuses on the relative amounts of cement and bentonite in the near-field of the repository. It evaluates the potential of hydroxyl ions from cement/concrete to deconstruct the properties of bentonite by dissolution of montmorillonite. A simple stoichiometry for dissolution of montmorillonite at high pH is:

$$Na_{0.33}Mg_{0.33}Al_{1.67}Si_4O_{10}(OH)_2 + 4.68\ OH^- + 2\ H_2O \Rightarrow$$
$$0.33\ Na^+ + 0.33\ Mg^{2+}\ 1.67\ Al(OH)_4 + 4\ HSiO_3 \qquad (1)$$

The equation implies that dissolution of one mole of montmorillonite consumes 4.68 moles of hydroxyl ions, and approximately 13 moles of OH^- can be consumed per kg of montmorillonite (MW montmorillonite = 367.02g/mol). MX-80 bentonite contains about 90 wt% montmorillonite, then dissolution of montmorillonite accounts for 0.9 x 12 ~ 13 moles of OH^- per kg of (dry) bentonite. Savage and Benbow[18] have calculated that 1 m^3 of cement could theoretically produce 38 100 moles OH^- ions. The total amount of cement to be used in a repository is believed to be around 9600 tonnes, equivalent to 4800 m^3 of cement paste. Then in theory, this volume of cement could destroy 16 % of dry bentonite used in a spent fuel repository.

The pH 11 was set as a target value for the leach solutions of low-pH grouts. As the pH scale is an inverse logarithmic representation of hydrogen ion (H^+) concentration (activity), each individual pH unit is a factor of 10 different than the next higher or

lower unit. This in mind, OH^- concentration can be expected to be reduced two orders of magnitude between pH 13 and pH 11 and limit the OH-alkalinity of the leachate to a value about 1 mmol/L in pure water.

Low-pH grout mixes would produce roughly 21 000 moles of OH^- ions per cubic metre of grout. Dissolution of 60 % of the montmorillonite in 1 m^3 of bentonite would require all the hydroxyl ion content from approximately 0.52 m^3 of low-pH grout.[18]

Overall the mass balance issue is not that simple. The nature of potential secondary products of cement-bentonite interaction is complicated. They contribute to consumption or generation of OH^- ions, e.g. the precipitation of tobermorite:

$$5\ Ca^{2+} + 6\ HSiO_3^- + 4\ OH^- + 5.5\ H_2O \Rightarrow Ca_5Si_6H_{21}O_{27.5} \qquad (2)$$

which will enhance the pH buffering capacity of bentonite. It consumes the hydroxyl ions and decreases the amount of montmorillonite to be dissolved. On the other hand, precipitation of zeolites such as analcime will generate OH^- ions and potentially increase the amount of montmorillonite dissolution.

$$Na^+ + Al(OH)_4^- + 2\ HSiO_3^- \Rightarrow NaAlSi_2O_6 + 2\ OH^- + 2\ H_2O \qquad (3)$$

The pH conditions will have an effect on the mineralogical alteration of bentonite. At pH > 12 the growth of calcium silicate hydrate solids, such as tobermorite, is dominated (equation 2). At pH < 12 the alteration is typified by zeolites, such as analcime (equation 3) and phillipsite, and tends to extend the scale of alkaline alteration. The amount and types of secondary mineral formation can have a profound effect upon the degree of bentonite alteration.[18]

2.2.2 Thermodynamic relationships

Thermodynamics is the study of energy and its transformations. In geochemistry it can be applied to the equilibrium states of minerals. In general, it might be important to know whether a particular mineral is either dissolving or precipitating. This reaction can be simply defined as:

$$\text{solid mineral} \Leftrightarrow \text{dissolved mineral} \qquad (4)$$

Minerals dissolve and precipitate to minimise the magnitude of Gibbs free energy (G) of the system and bring it to equilibrium. Whether the mineral should be in the solid or dissolved state can be determined by considering the change in Gibbs free energy of the reaction, $\Delta_r G$. While it is difficult to measure absolute values of $\Delta_r G$, it is a common

procedure to calculate the Gibbs free energy for a substance in standard state, $\Delta_f G^0$, from the difference between the Gibbs free energy of the substance and the Gibbs free energy of its constituents. The standard state refers to a pure mineral at some constant temperature and pressure, typically at 25 °C and 101.325 kPa. For any given reaction, there are three conditions of interest:

- $\Delta_r G < 0$, the dissolution reaction will be spontaneous
- $\Delta_r G = 0$, the reaction is in equilibrium
- $\Delta_r G > 0$, the precipitation reaction will be spontaneous.

pH has a great effect on the aqueous speciation of metals and the solubility of minerals. When considered the stability of bentonite in the alkaline solution, the behaviour of silicon is the most important. The variation of silicon speciation and quartz solubility as a function of pH is shown in Figure 5.

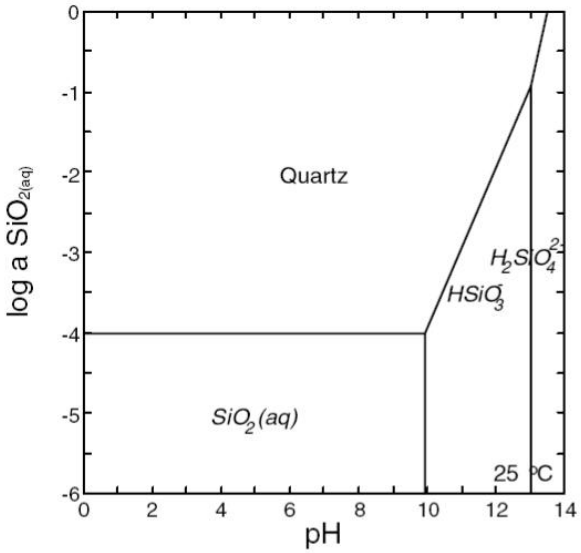

Figure 5. Variation of Si speciation and quartz solubility with pH.[18]

Aqueous speciation of Si is dominated by the neutral species SiO_2(aq) across the large pH range.[18] At this same range the solubility of quartz is also constant at 10^{-4} mol/L. When pH increases above 10, SiO_2(aq) dissociates to produce the charged species $HSiO_3^-$. Correspondingly, the solubility of quartz, increases by three orders of magnitude over that observed in the pH range 1 – 10. At pH > 13, a second dissociation

of SiO_2(aq) occurs. In this pH range, $H_2SiO_4^-$ is the most stable species in aqueous solution, accompanied by further increase in quartz solubility.

The change of silicon speciation with pH has a great effect on hydrolysis reactions of montmorillonite. At pH < 10 the dissolution of one mole montmorillonite generates six moles of hydroxyl ions. At higher pH values dissolution reactions taking place consume hydroxyl ions. From the thermodynamical perspective, the critical boundary for bentonite stability occurs at pH 10, where the notable change in the aqueous speciation of silicon can be detected.[18]

pH < 10: $Na_{.33}Mg_{.33}Al_{1.67}Si_4O_{10}(OH)_2 + 2\ H_2O \Rightarrow$

$$0.33\ Na^+ + 0.33\ Mg^{2+} + 1.67\ Al^{3+} + 4\ SiO_2(aq) + 6\ OH^- \qquad (5)$$

10 < pH < 13: $Na_{.33}Mg_{.33}Al_{1.67}Si_4O_{10}(OH)_2 + 4.68\ OH^- + 2\ H_2O \Rightarrow$

$$0.33\ Na^+ + 0.33\ Mg^{2+} + 1.67\ Al(OH)_4^- + 4\ HSiO_3^- \qquad (6)$$

pH > 13: $Na_{.33}Mg_{.33}Al_{1.67}Si_4O_{10}(OH)_2 + 8.68\ OH^- + 2\ H_2O \Rightarrow$

$$0.33\ Na^+ + 0.33\ Mg^{2+} + 1.67\ Al(OH)_4^- + 4\ H_2SiO_4^{2-} \qquad (7)$$

2.2.3 Mass transport

The driving force for mass transfer is a difference in concentration; the random motion of molecules causes a net transfer of mass from an area of high concentration to an area of low concentration. In repository conditions, the diffusive transfer of hydroxyl ions into the bentonite will be the reaction limiting factor. Rather than diffusing into to the bentonite, cement grout water may flow over the bentonite surface and erode it. Effective diffusion coefficients for solute transport through bentonite are very low, and generally less than 10^{-10} m^2/s.[18] Fick's first law demonstrates that the magnitude of mass transfer by diffusion is dependent on the concentration difference across the medium concerned:

$$F = -D\frac{dC}{dx} \qquad (8)$$

where F = mass flux (mass of solute per unit area per unit time); D is diffusion coefficient (area per unit time); and dD/dx is the concentration gradient.

Use of low-pH grouts with pH ≤ 11 decreases the diffusive transport of hydroxyl ions, because the concentration of OH^- ions leached from the cement paste is much lower compared to OPC cements. Simulations of cement-clay interactions can help predict the alterations in transport occurring in bentonite. Generally simulations predict porosity

decreases in the clay, which would be expected to decrease the rate of mass transport.[19, 20] Also the dissolution of clay coupled with precipitation of secondary minerals can result in a net decrease, not only in porosity, but also effective diffusion coefficient, and hydraulic conductivity.

2.2.4 Kinetics

Montmorillonite is an aluminosilicates mineral for most of which the dissolution rates are accelerated by increasing OH^- concentrations at pH > 8.[21, 22] The rate of dissolution of montmorillonite is a factor of 8 greater at pH 11 than at pH 8 and a factor of 30 greater at pH 13 than at pH 8. Dissolution of one cubic metre of bentonite would thus require ~ 20 000 years at pH 8. If the pH is raised to value 11, it takes around 2 500 years and at pH 13 about 600 years to 1 m^3 of bentonite to be dissolved.[18]

These estimates are based on the theory that dissolution of montmorillonite occurs under far-from-equilibrium conditions, which will not be the case in a repository. In reality, the rate of dissolution would be reduced by approach to equilibrium. The precise mechanism of montmorillonite dissolution close to equilibrium is still uncertain. The presence of dissolved Si (and perhaps Al) may inhibit the dissolution of montmorillonite. Also the potential secondary minerals can have a dramatic effect on the overall montmorillonite dissolution rate. Overall it might be concluded that kinetics would not be the limiting factor in dissolution of montmorillonite at elevated pH.[18]

3 CEMENT

Cement, is an ultra-fine gray powder, which binds sand and rocks into a mass or matrix of concrete. The use of cementitious materials date back long ago. It is not exactly known when prehistoric man first discovered cementing materials, probably soon after he learned to use fire. May be he had made a fire on limestone or gypsum, and the heat of the fire caused part of the rock to change chemically and crumble. The powder mixed with sand and gravel, and when the rain fell down it created a crude form of cement.

In the ancient Egypt heated impure gypsum was used to hold the stone blocks together in the pyramids and buildings.[23] Later the Greeks and Romans used the same method, but added also some sand and gravel to the mix and created an early form of concrete. They noticed that grounding the limestone more finely, they obtained a stronger and longer lasting product. They also discovered that addition of certain volcanic sands produced some new characteristics.

A number of people have contributed to the development of cement, but a British bricklayer Joseph Aspdin in 1824 first patented a product called Portland cement. He used a hard limestone and mixed lime with clay, grinding it to a fine slurry with water. Aspdin's early cement was nothing more than a hydraulic lime, but his patent gave him the priority for the use of the term Portland cement. It was only a proto-Portland cement. It was not until the mid-1840s that the younger son of Joseph Aspdin, William, accidently synthesised the calcium silicates which were the basis of meso-Portland cement. A few years later, Isaac Johnson made the first modern Portland Cement by burning a mixture of chalk and clay at much higher temperatures similar to those used today. Normal Portland cement, as we know it today, is quality calcerous cement manufactured in a rotary kiln. It is a synthetic mixture of calcium silicates and homogeneously prepared mixture of calcareous and argillaceous components. Unlike earlier proto- or meso-Portland cement, normal Portland cement contains a controlled amount of calcium sulphate as a setting retarder.[23]

Nowadays Portland cements made around the world are designed for general construction purposes. In different countries and regions various names are used to define the material, such as Class 42.5 Portland cement in current European and British standards, Types I and II Portland cement in ASTM (American Society for Testing and Materials) used in USA or Ordinary Portland cement (OPC) in former British standards. Standard specifications are based partly on chemical composition or physical properties

such as specific surface area, and partly on performance tests, such as setting time or compressive strength development.

3.1 Chemistry and Structure

Cement is the basic ingredient of concrete, mortar and most non-specialty grouts. It is made from limestone (mainly $CaCO_3$), clay and quartz, which are finely grinded and thoroughly mixed together. The mixing can be carried out either dry or wet. Lime and silica make up about 85 % of the mass. The mix is then heated to temperature about 1450 °C in a cylindrical rotary kiln where partial fusion occurs and produces a clinker. Before using, the clinker has to be cooled down and ground to very fine powder. It is very important to keep the temperature, mixing and grinding conditions, as well as component proportions, constant to obtain a fine product.[24] The clinker is then mixed with a few per cent of calcium sulphate, to make cement. Calcium sulphate, which is commonly referred as gypsum controls the rate of setting and influences the rate of strength development. Typically the clinker has a composition of 67 % CaO, 22 % SiO_2, 5 % Al_2O_3, 3 % Fe_2O_3 and 3 % of other components. The clinker contains four major phases, called alite, belite, aluminate and ferrite, as well as several minor phases, such as alkali compounds and magnesium oxides.[25] Alite is the most important constituent of all normal Portland cement clinker. It makes up 50–70 % of all the cement paste. It is tricalcium silicate (Ca_3SiO_5) and reacts relatively quickly with water. Belite constitutes 15–30 % of normal Portland cement clinkers. The chemical name of belite is dicalcium silicate (Ca_2SiO_4) and it reacts rather slowly with water. Aluminate, tricalcium aluminate ($Ca_3Al_2O_6$) and ferrite, tetracalcium aluminoferrite (Ca_2AlFeO_5) constitutes 5–10 % of normal Portland cement.[24]

The chemical formulae in cement chemistry are often expressed as sums of oxides, for example tricalcium silicate (Ca_3SiO_5) can be written as 3 $CaO{\cdot}SiO_2$. This presentation does not mean that the constituent oxides have any separate existence within the structure. Usually the most common oxides are expressed with only one letter, such as C for CaO or S for SiO_2. In this way tricalcium silicate, Ca_3SiO_5 becomes C_3S. The abbreviations for the most common oxides are:

C = CaO	M=MgO	T =TiO_2
S = SiO_2	K = K_2O	P = P_2O_5
A = Al_3O_3	H = H_2O	F = Fe_2O_3
N = Na_2O	$\overline{S} = SO_3$	$\overline{C} = CO_2$

3.2 Composite Cements

Composite cements also referred as 'blended cements' are hydraulic cements composed of Portland cement and one or more inorganic materials that take part in the hydration reactions and contribution to the hydration product. This definition excludes admixtures, such as $CaCl_2$, that influence the hydration process but do not themselves contribute substantially to the final product. The most important additives are silica fume (microsilica), fly ash (pulverized fuel ash), blastfurnace slag, and natural pozzolanas. Composite cements are used for various reasons. The use of additive materials can give cement desired properties, such as slower and decreased total heat evolution, improved durability or, especially with silica fume, strengths above the normal range.[23] An additional result of using pozzolanas is that the high pH effect of ordinary cement (pH > 12) is greatly reduced. Also some disadvantages may result from the usage of pozzolanic materials, such as reduced workability of the cement mixture and increased concentrations of alkali hydroxides in pore fluid thus causing high pH (< 13) on leaching.[26]

Although additives increase the strength of cement and have other beneficial effect on cement properties, the decreased workability creates problems. Pozzolanas increase the surface area of the cement paste and thus increase the water demand. Increasing the water-cement ratio improves workability but reduces strength, and increases the hydraulic conductivity indirectly reducing the longevity of the cementitious materials. Water reducing agents, also called superplasticizers, allow a given degree of workability to be achieved at a lower w/c ratio. All superplasticizers consist of high molecular weight, water-soluble organic polymers. They disperse cement particles when suspended in water by adsorbing on the surface of the particles causing them to be mutually repulsive due to the anionic nature of the superplasticizers.[26]

3.2.1 Additive Materials

The classification of pozzolanas is difficult because this common name includes so many materials which are quite different in chemical composition, mineralogical nature and geological origin. The common features of these materials are that they contain reactive silica and/or alumina and react when mixed with lime and water. Commonly accepted classification concerns the origin of pozzolanas. They are divided in subdivisions between natural and artificial materials (Figure 6).[23] Artificial materials

usually are residues of some production methods from raw materials having originally no or only weak pozzolanic properties.

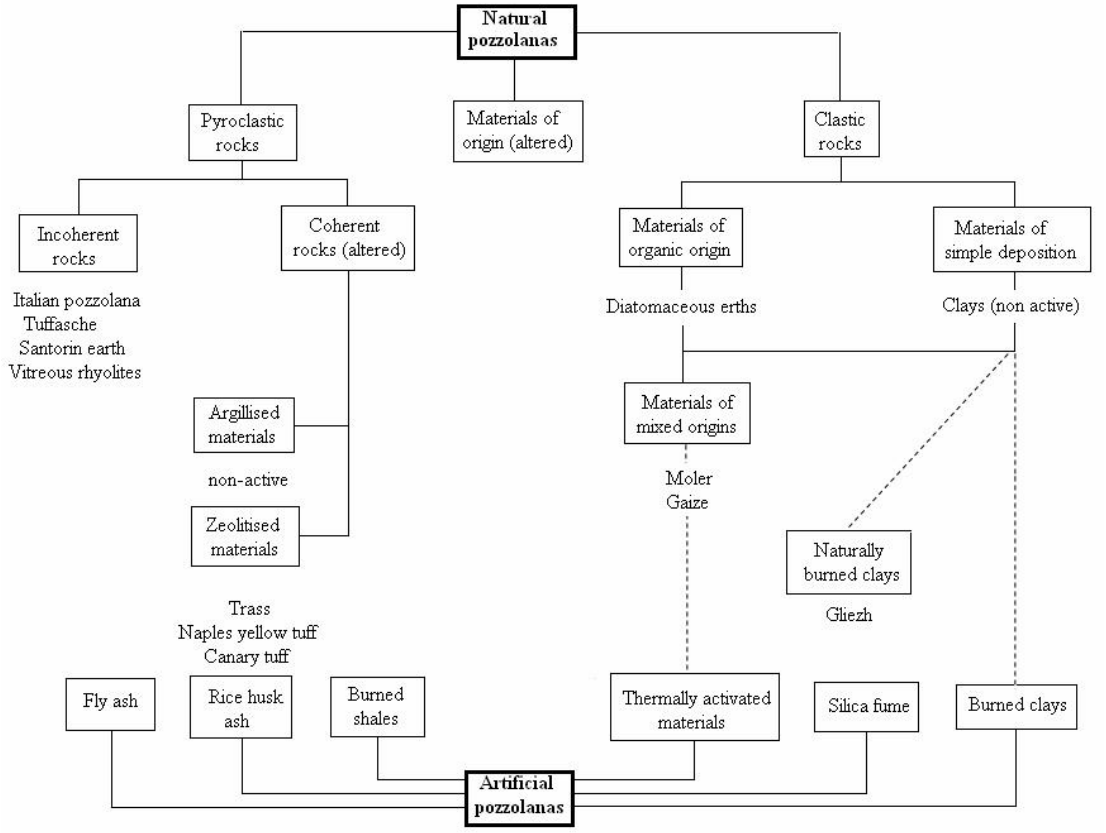

Figure 6. Classification of pozzolanas.[23]

Silica fume (condensed silica fume, microsilica)

Microsilica, also known as silica fume or condensed silica fume, is a fine grey powder which is mostly composed of amorphous silicon dioxide (SiO_2). The primary micro silica particles are spherical and have maximum grain size approximately 0.1–1 μm, which gives large specific surface area. Usually the primary particles will group together and form agglomerations. The use of microsilica in cement paste decreases the workability and increases the water demand. This is the reason why microsilica is often used with superplasticizers. It increases also the internal surface forces, which means an increase in the cohesiveness of the cement. As a result the cement is less sensitive to segregation and this on the other hand is useful for high-fluidity grouts and pumped concrete mixes.[23]

Microsilica is a very reactive pozzolana. It reacts with calcium hydroxide, the product of cement hydration, to produce calcium silicate hydrate (C-S-H). This reaction

decreases the concentration of Ca^{2+} and OH^- ions in the pore solution and lowers the pH of grout leachate. Although this is true the pH does not depend solely on calcium hydroxide. Especially in young concrete sodium hydroxide and potassium hydroxide have even greater influence on the alkalinity. Alkali hydroxides are highly soluble and are easily leached from the concrete or consumed by chemical reactions with weak acids, such as SiO_2.[27] The hydrated C-S-H gel fills the pores and voids within the cement paste and forms bridges between cement grains and aggregate particles. Cement paste with microsilica content usually have improved strength and impermeability which is due to homogeneous and dense structure.

As mentioned earlier especially Portland cement contains small amounts of Na_2O and K_2O, which readily form NaOH and KOH solutions when mixed with water. These highly alkali solutions react with amorphous or poorly crystalline silica particles in aggregates, forming a gel which is able to absorb water and swell, resulting a pressure which can crack the concrete. This is called the alkali silica reaction (ASR).[28, 29] It is worth of noticing the difference between silica fume and silica aggregates. Silica fume can be used to reduce the ASR expansion. It reacts in a pozzolanic manner with cement pore solution to form non-expansive calcium silicate hydrate (C-S-H). However large siliceous agglomerated particles react with alkali hydroxides in the pore solution to form expansive ASR gel.[29] It has been reported by Maas *et al.*[29] that agglomerates smaller than 150 μm in diameter do not contribute to ASR-related expansion. The finer and more reactive the siliceous material is, the faster the evolution of a C-S-H phase during the pozzolanic reaction is. Regardless of the increased reactivity, the microstructure of the C-S-H phase does not change significantly.

Fly ash

Fly ashes fall into subdivision of artificial pozzolanas. Fly ashes result from the burning of bituminous or sub-bituminous coal in power stations. Their chemical composition depends on the mineral composition of the coal gangue, i.e. the inorganic part of the coal. Usually majority of fly ash content consists of silica and alumina. Respectively the lime content is low. The typical particles in fly ash are spherical and glassy and they are classified based on shape, colour, crystallinity and texture. The particle diameters range from < 1 to > 150 μm.[23]

Fly ash cements differ from pure Portland cements in a) the hydration rates, b) calcium hydroxide contents, and c) composition of the hydration products. The use of fly ash

improves the final strength and increases the chemical resistance and durability of cement paste. Due to the smooth spherical shape of fly ash particles, it can also increase workability of cement while reducing water demand and thus increase the durability of the cement-based materials.[24]

Blastfurnace slag

Blastfurnace slag, BFS, is a non-metallic product which consists primary of silicates and aluminosilicates of calcium.[23] In the operation of a blastfurnace the iron oxide is reduced to metallic ion, while the silica and alumina constituents combine with lime and magnesia to form a molten slag which collects on top of the molten iron at the bottom of the furnace. The conversation of a molten slag into widely different products is dependent of the process used in cooling. When molten slag is cooled sufficiently rapidly to below 800 °C, it forms a glass which is a latent hydraulic cement. The ground granulated blastfurnace slag may contain over 95 % of glass.

The composition of slag can vary over a wide range, depending on various factors, such as nature of the ore, the composition of the limestone flux, and the kind of iron being made. In addition, differences between plants can be considerable. Four major constituents of blastfurnace slag are lime, silica, alumina and magnesia. Also some minor components such as ferrous and manganese oxides and sulphides may be present.

Granulated slag alone has a negligible cementing action, but with the presence of a suitable activator, it shows apparent cementing properties. In general, the more basic the slag, the greater its hydraulic activity is in the presence of an alkaline activator.

The use of blastfurnace slag slows down the strength development and the rate of heat evolution in the cement paste. The microstructure of slag cement pastes are quite similar compared to those of pure Portland cement pastes, although decrease in connectivity of the pore system is observed as well as lower calcium hydroxide contents.[24] Portland blastfurnace cements are more resistant to attack by sea water and other chemical agencies than Portland cement. The sulphate resistance of slag-type cements is dependent on the C_3A content of the Portland cement fraction and the alumina content of the slag. The increased resistance is generally associated with the lower content of free calcium hydroxide present in the set cement and the less basic nature of the hydrated calcium silicates.

Natural pozzolanas

The natural pozzolanas do not require any further treatment apart from grinding. They are usually classified in the following manner:

- volcanic, incoherent, rich in unaltered or partially-altered glass,
- tuffs, where volcanic glass has been transformed, entirely or partially into zeolitic compounds,
- sedimentary, rich in opaline diatoms, and
- diagenetic, rich in amorphous silica, resulting from the weathering process of siliceous rocks.[30]

Natural pozzolanas have an accelerating effect on the hydration of calcium silicate. This is due to fineness of the pozzolana particles. Pozzolana addition does not change the composition of the reaction products, although it influences the ratios of the various compounds and their morphology and changes the composition of the pore solution in the cement paste. The main hydrates that are found in the hardened paste are ettringire, tetracalcium aluminate hydrate, monosulfoaluminate, C-S-H, C_2ASH_8, $Ca(OH)_2$ and $CaCO_3$. The incorporation of alkalis into the C-S-H gel reduces the OH^- concentration of the pore solution. Except silica fume, natural pozzolanas do not have an effect on OH^-, Na^+ or K^+ concentrations of the pore solution when the Portland cement has high alkali content. An increase in the silica fume content in the mix decreases the actual concentration values of the ions mentioned above.

3.2.2 Organic Admixtures

Organic admixtures are specially formulated products that are added in small amounts to concrete, mortar or grout during the mixing process in order to modify the concrete properties. Admixtures should be distinguished from additives and additions, such as blastfurnace slag or silica fume, in that these materials are usually solids and added to the cement during its manufacture. The most important organic admixtures are ones added to accelerate or retard setting or hardening, to decrease the water demand to obtain a given degree of workability, or to entrain air in order to increase the resistance to freeze-thaw deterioration.

The organic admixtures are commercial products of fairly ill-defined composition and may contain also some components other than those mentioned in the product safety sheets. It follows that the exact behaviour of the materials is difficult to assess.

Admixtures can be divided into two categories; those that are water soluble and those that are not. The 'solubility' categorisation of admixtures is given in Table 2.[23]

Table 2. Organic admixture categories using solubility as a criterion.[23]

Soluble (water)	**Insoble**
Accelerators	Plasticisers/workability aids: • Solids particulate • Liquid dispersion • Liquid emulsion
Retarders/retarding water reducers	
Water-reducing plasticising/fluidifiers	
Air entrainers	
Superplasticizers	
Air-entraining mortar plasticisers	
Permeability reducers	Pigments
Pumping aids	

Superplasticizers

A mixture of low-viscosity liquid such as water and relatively heavy particles such as cement, sand and aggregates does not remain uniformly mixed once agitation is stopped. Separation of the various phases occurs, resulting segregation and displacement of water. To minimise these effects the water content of the concrete is kept low. Water-reducing agents, also called plasticizers, allow a given degree of workability to be achieved at a lower water/cement ratio, as shown in Figure 7.[3] More powerful water reducers, called superplasticizers, allow w/c ratio to be decreased by up to about 30 %. They are negatively charged polymers and are composed of a variety of different molecules. The molecular weight may vary over a wide range from less than 100 up to 100 000 g/mol. The superplasticizers are usually classified into four categories as follows:

- Sulfonated melamine-formaldehyde condensates (PMS) (Figure 8a),
- sulfonated naphthalene-formaldehyde condensates (PNS) (Figure 8b),
- modified lignosulfonates, and
- other synthetic polymers such as sulfonated polystyrene.[23]

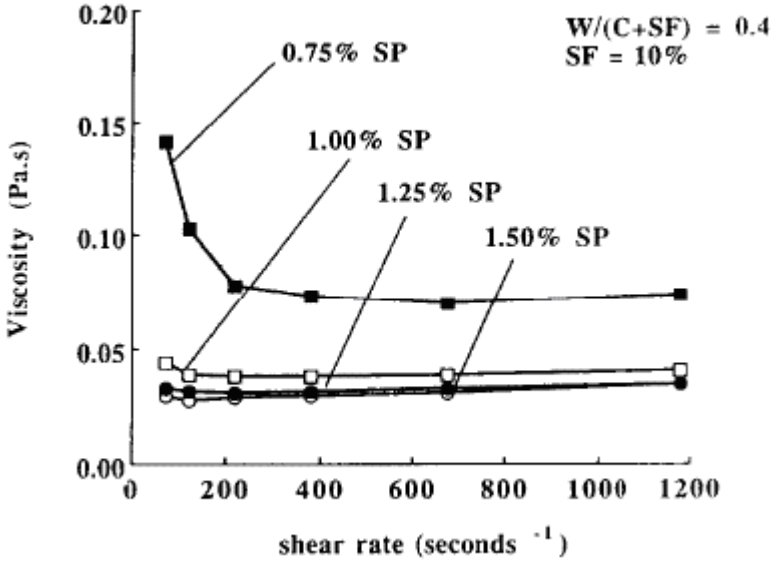

Figure 7. Viscosity versus shear rate for grout containing various amounts of superplasticizers (SPL), with w/b= 0.40 and 10% silica fume.[3]

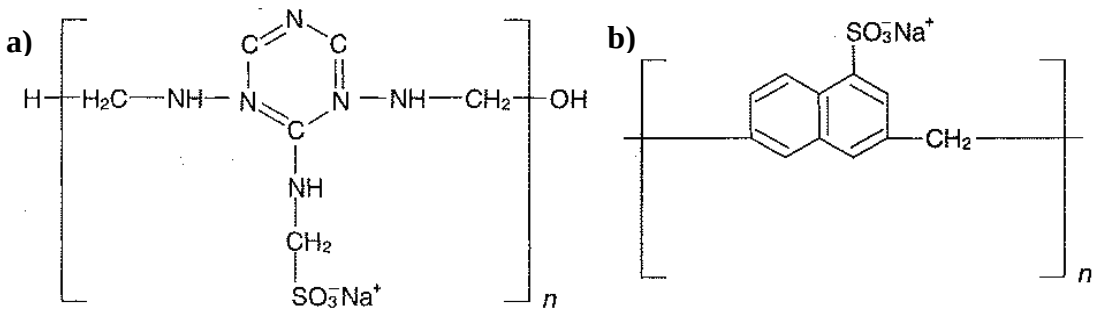

Figure 8. a) Sulphonated melamine-formaldehyde condensate, b) sulphonated naphthalene formaldehyde condensate.[23]

Water reducers adsorb on the cement surfaces, leading to mutual repulsion of individual particles. Mutual particle repulsion leads to a high degree of dispersion, but the polymers employed do not exclude water from the cement surface entirely, and hydration does proceed in a normal manner.[24]

The effect of superplasticizers on cement hydration is mainly due to physical factors rather than chemical interaction. Better dispersion of individual cement grains leads to more efficient hydration and better early strength. The use of superplasticizers (SP) also improves the long-term durability of the cementitious materials by allowing reduced water content leading to improved strength and reduced permeability of the material. In superplasticizer-cement interactions calcium cations act as charge neutralisers by

providing a positively charged site for sorption of negatively charged macromolecules. The most important factor of cement for SP adsorption is the specific area of tricalcium aluminate (C_3A) phase. The amount of adsorbed and incorporated SP strongly increases with the amount C_3A in the cement. The PMS and PNS have a higher affinity to C_3A than PC (polyether polycarboxylate) type of SP. The particle size distribution of cement also has an influence on the retardation of PNS.[31]

3.3 Hydration

In cement chemistry the term hydration refers to a reaction of an anhydrous compound with water.[23] The chemical reactions taking place are usually more complex than simple conversation of anhydrous compounds into the corresponding hydrates. The mixture that is generated when water and cement is mixed together is called a cement paste. Setting is a process in which a 'fresh' cement paste stiffens and looses its deformability without significant development of compressive strength. It is followed by the 'hardening' of the paste in which development of compressive strength occur, this is normally a rather slow process. The final structure of the formed hydrated material on the nanometre and micrometre scale depends on the composition of the original binder, the starting water/cement ratio, temperature, absence or presence of chemical admixtures and finally the hydration time.

3.3.1 Hydration of Portland cement

The hydration of Portland cement consists of a series of chemical reactions between individual clinker minerals, calcium sulphate and water. The progress of the hydration process depends on the rate of dissolution of the involved phases, the nucleation and crystal growth and the rate of water diffusion through the hydrated material already formed.[23] The hydration process of Portland cement paste can be characterised by the four below described stages.

Pre-induction period (first minutes)

Immediately after contact with water, a rapid dissolution of ionic species into the liquid phase and the formation of hydrate phases start.[23] Alkali sulphates present in the cement dissolve completely within seconds, contributing K^+, Na^+ and SO_4^{2-} ions. Dissolution of calcium sulphate introduces Ca^{2+} and SO_4^{2-} ions into the solution. Tricalcium silicate (C_3S) dissolves congruently and a layer of a C-S-H phase precipitates at the surface of cement particles. As the C_3S phase is hydrated the concentration of Ca^{2+} and OH^- ion in

the liquid phase is increased. At the same time, silicate ions enter also the liquid phase, although their concentration remains very low. The fraction of C_3S hydrated during the pre-induction period remains low, probably between 2–100 %. Tricalcium aluminate dissolves and reacts with Ca^{2+} and SO_4^{2-} ions present in the liquid phase, yielding ettringite (AFt) that also precipitate at the cement particle surface. The amount of C_3A hydrated in the pre-induction period varies between 5–25 %. The concentration of Al^{3+} in the liquid phase remains low. The ferrite phases react similarly as C_3A, yielding AFt phase. The fast initial hydration slows down due to the deposition of a layer of hydration products at the cement grain surface.

Induction (dormant) period (first few hours)

During the induction period the hydration rate slows down significantly for a few hours. In this stage the hydration of all the clinker minerals progresses very slowly. During the induction period the concentration of calcium hydroxide in the liquid phase reaches its maximum and then starts to decline. The concentration of SO_4^{2-} remains constant as the fraction consumed in the formation of the AFt phase is replaced by the dissolution of additional amounts of calcium sulphate.

Acceleration period (3-12 hours after mixing)

In this period the hydration rate accelerates again and is controlled by the nucleation and growth of the hydration products.[23] The rate of C_3S and C_2S hydration accelerates and crystalline calcium hydroxide (portlandite) precipitates from the liquid phase reducing the concentration of Ca^{2+} in the liquid phase. Calcium sulphate becomes completely dissolved. Dissolved SO_4^{2-} ions move to AFt phase and their concentration declines in the liquid phase.

Post-acceleration period

Hydration rate slows down gradually, as the amount of still non-reacted material declines and the rate of hydration becomes diffusion-controlled. As the hydration of C_3S and β-C_2S continues the amount of C-S-H phase increases. The AFt phase that has been formed in the earlier stages of hydration starts to react with C_3A and ferrite phases as the concentration of SO_4^{2-} in the liquid phase declines, yielding monosulphate.[23, 25] At sufficiently high initial water/cement ratios the hydration process progresses until all of the original cement becomes consumed. However, a small fraction of larger cement particles may remain un-reacted in mature pastes.

The hydration of each individual phase is characterised quite extensively in literature. **Tricalcium silicate (C_3S)** is considered the most important component of Portland cement. Hydration of tricalcium silicate phase is a rather complex reaction, and it is still not fully understood. The reaction can be described with following equation:

$$2\ C_3S + 6\ H_2O \Rightarrow C_3S_2H_3 + 3\ Ca(OH)_2 \qquad (9)$$

The reaction products are amorphous calcium silicate hydrate phases with CaO/SiO_2 molar ratio less than 3.0, called the 'C-S-H phase' and crystalline hexagonal calcium hydroxide. A typical hydration curve expressing the degree of hydration as function of hydration time for tricalcium silicate ground (special surface area ~ 300 – 500 m^2/kg (Blaine), water-cement ratio ~ 0.5–0.7, at room temperature) is shown in Figure 9.[25]

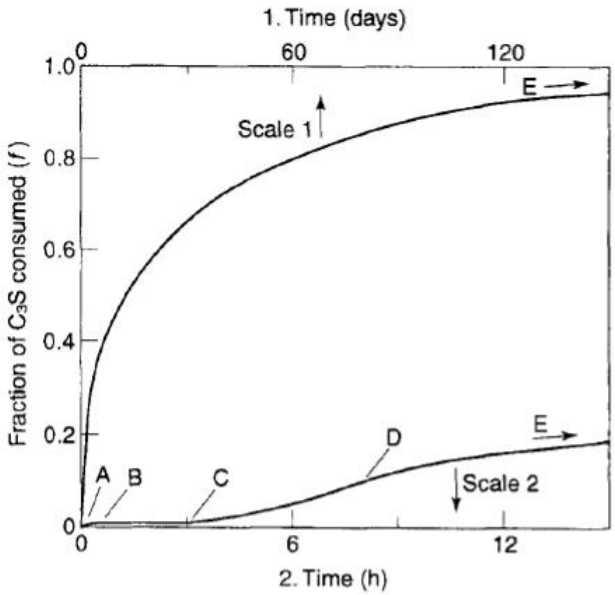

Figure 9. Progress of hydration of tricalcium silicate (C_3S) in paste. A-B: pre-induction period; B-C: induction period; C-D: acceleration period; D-E: deceleration period.[23]

Figure 10 presents the rate of heat formation, changes in Ca^{2+} concentration in solution phase, and the formation of hydration products as a function of time.

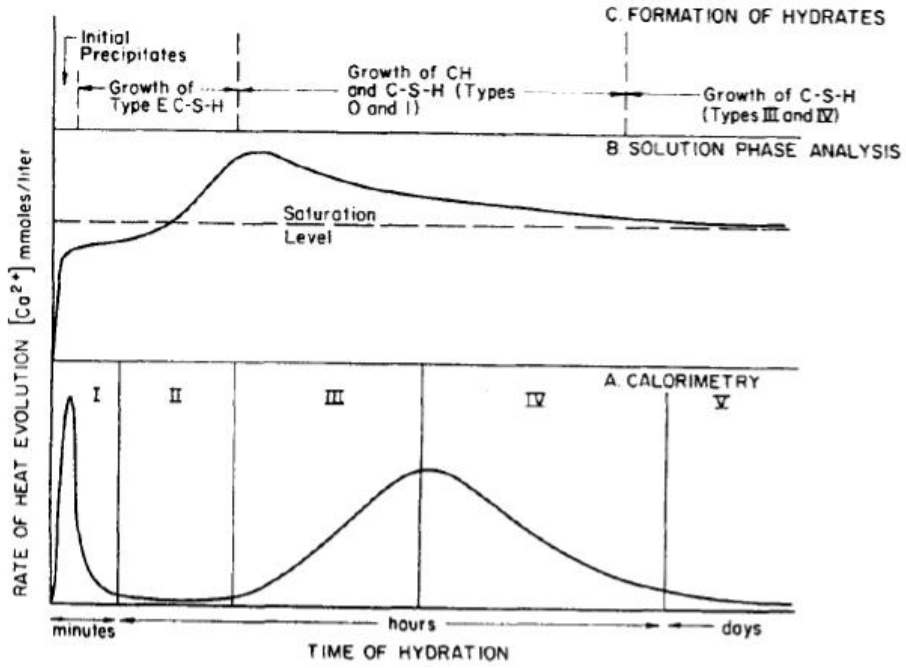

Figure 10. Schematic presentation of processes taken place in C_3S phase as a function of hydration time. A: calorimetric curve; B: solution phase analysis; C: formation of hydrates.[25]

The reactivity of tricalcium silicate depends on a variety of factors. Moderate variations of specific surface area have little effect on the length of the induction period, but prolonged grinding may shorten it. Chemical substances dissolved in the mixing water may also alter the kinetics of hydration. Chlorides (e.g. $CaCl_2$) exhibit an acceleratory effect on the process, whereas phosphates, borates and salts of Zn^{2+} and Pb^{2+} cause retardation. Also, some organic compounds, especially different saccharides may retard the C_3S hydration rate. Certain solid substances may shorten the length of the induction period, while addition of crystalline calcium hydroxide accelerates the hydration rate in the acceleration period. Finally, the rate of C_3S hydration is also dependent on water-solid ratio of the cement paste and ambient temperature.[23]

Upon contact with water, both calcium and silicate ions pass rapidly into solution. Concentrations of calcium, silicate and hydroxyl ions in solution phase of C_3S suspension have been studied extensively (Figure 11).[25] The relatively high silicate concentrations have been observed in pastes only seconds after mixing, but they are transitory and concentrations decreases quickly into a very low level. Contrary to that the concentration of $Ca(OH)_2$ continues to increase during the pre-induction and induction periods.[23]

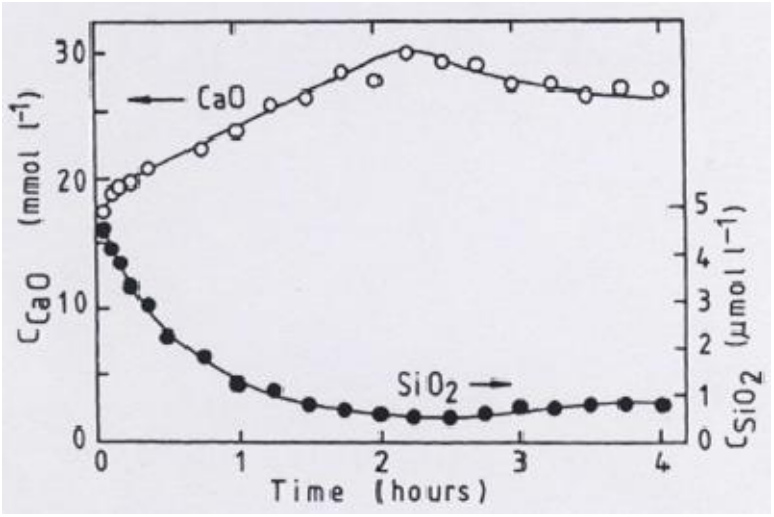

Figure 11. Calcium and silicate ion concentrations (as CaO and SiO_2) in solution phase as a function of time.[25]

Although the hydration of tricalcium silicate phase has been studied extensively, its mechanism is still unclear. Several different theories (e.g. impermeable hydrate layer theory, electrical double-layer theory, nucleation of $Ca(OH)_2$ and C-S-H theories) have been established to explain this phenomenon.[23]

XRD powder evidences show that grains of dicalcium silicate in Portland cement clinkers constitute predominantly or entirely of β-C_2S structure.[24] Hydration reaction of **dicalcium silicate (C_2S)** can be described with following equation:

$$2\ C_2S + 4\ H_2O \Rightarrow C_3S_2H_3 + Ca(OH)_2 \qquad (10)$$

Same reaction products are formed in the hydration process of dicalcium silicate as in the hydration of tricalcium silicate, but relatively more C-S-H phase and less $Ca(OH)_2$ is formed in hydration of C_2S. The reactivity of β-C_2S is rather low compared to C_3S. However, it can be altered by adding suitable doping-agents, by changing the temperature of hydration, or by increasing the fineness of grinding.[23] Figure 12 shows the typical hydration kinetics of β-C_2S hydrated at 20 °C compared to other clinkers. The reaction is characterized by an extended induction period in which the hydration rate is very slow. This period is followed by a gradual increase of the hydration rate and its subsequent slowing down, after reaching a maximum after several days or weeks. According to the available experimental data, it can be stated that the mechanism of

hydration of dicalcium silicate is similar to that of C_3S, even though the whole process progresses more slowly.[23]

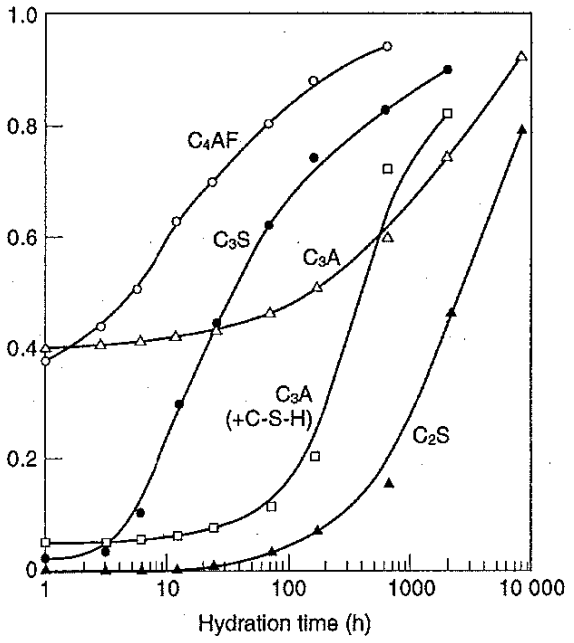

Figure 12. Typical hydration kinetics of pure clinker minerals as a function of time.[23]

Tricalcium aluminate (C_3A) exists in cubic, orthorhombic and monoclinic modifications. The latter two occur only in the presence of different doping agents, such as Na^+. Tricalcium aluminate reacts fast with water to form crystalline hexagonal calsium aluminate hydrate phases which later convert into cubic phases. To retard the fast hydration reaction of C_3A, calcium sulphate is added to Portland cement. In the presence of calcium sulphate the amount of tricalcium aluminate hydrated in the initial stage of hydration is reduced when compared to that consumed in the absence of $CaSO_4$. The first stage of the hydration process is the formation of ettringite (trisulphate) $C_6A\bar{S}_3H_{32}$ (equation 11).[23, 25] Minor amounts of monosulphate ($C_4A\bar{S}H_{12}$) or calcium aluminate hydrate (C_4AH_{19}) may also be formed resulting in an insufficient supply of SO_4^{2-} ions.[23]

$$C_3A + 3C\bar{S}H_2 + 26H \Rightarrow C_6A\bar{S}_3H_{32} \qquad (11)$$

As all the available calcium sulphate is consumed, initially formed ettringite reacts with additional amounts of tricalcium aluminate, yielding calcium aluminate monosulphate hydrate, $C_4A\bar{S}H_{12}$:

$$C_6A\bar{S}_3H_{32} + 2C_3A + 4H \Rightarrow 3C_4A\bar{S}H_{12} \quad (12)$$

As ettringite is gradually consumed, also hexagonal calcium aluminate hydrate, C_4AH_{19}, starts to form. It may be present in the form of a solid solution with $C_4A\bar{S}H_{12}$ or as separate crystals.[23] A complete reaction of C_3A may take several months.

Under comparable conditions the hydration products formed in the hydration of **tetracalcium aluminoferrite phase (C_4AF)** is similar to tricalcium aluminate.[25] The reactivity of ferrite phases may vary in a wide range and seems to depend on the Al/Fe ratio. It generally declines with increasing Fe content. As with C_3A, the hydration is slowed down in the presence of $CaSO_4$. Ferrite phases containing calcium sulphate AFt phase ($C_6(A,F)S_3H_{32}$) is the first main reaction product. In a subsequent reaction step the AFt phase is converted to AFm phase ($C_4(A,F)S_3H_{12}$.

3.3.2 Setting and hardening

Setting is a process in which a 'fresh' cement paste stiffens and looses its deformability without development of compressive strength. It is a physical consequence of reactions between water and cement components. It is followed by the hardening of the paste in which the development of compressive strength and hardness occur.[23, 24] Within minutes after mixing a Portland cement with adequate amounts of water (w/c ~ 0.3–0.7), a flocculation of the cement particles takes place, associated with an increase in a viscosity of the paste. The flocculation is suggested to be derived from weak van der Waals and electrostatic forces between cement particles.[25] As the amount of hydrated material increases, the number of contacts between particles also increases and eventually a continuous, three-dimensional network of solids develops within the paste. As the hydration progresses and the amount of hydrated material increases at the expense of the water-filled pore space, the bonds between solid particles strengthen, resulting in a gradual increase of strength of the set cement paste.

Most investigators believe that the setting process of cement paste is due to a hydration of C_3S and C_3A and formation of C-S-H and AFt, although opinions are not uniform.[23] It has been also postulated that the setting of Portland cement is due to a recrystallisation of primary microcrystalline ettringite into larger crystals. Presence of calcium sulphate regulates the setting of cement paste. If the concentration of Ca^{2+} and SO_4^{2-} ions in the liquid phase is adequate, the amount of C_3A and C_4AF hydrated in the initial pre-induction period is reduced and AFt phase is precipitated at the cement grain

surface during the hydration. Under these conditions the flowability and plasticity of the paste is preserved until the formation of more hydrates causes setting.

3.4 Durability of cement-based materials

Durability is the ability of cement-based materials to resist the deterioration process. It depends on both material properties and the environmental conditions. Degradation includes several various mechanisms such as, alkali aggregation, carbonation, chloride or sulphate attack, interaction with repository materials, leaching, abrasion, and for near-surface concrete possible freeze thaw cycling. Various types of physical and chemical deterioration mechanisms are presented in Figure 13.[36]

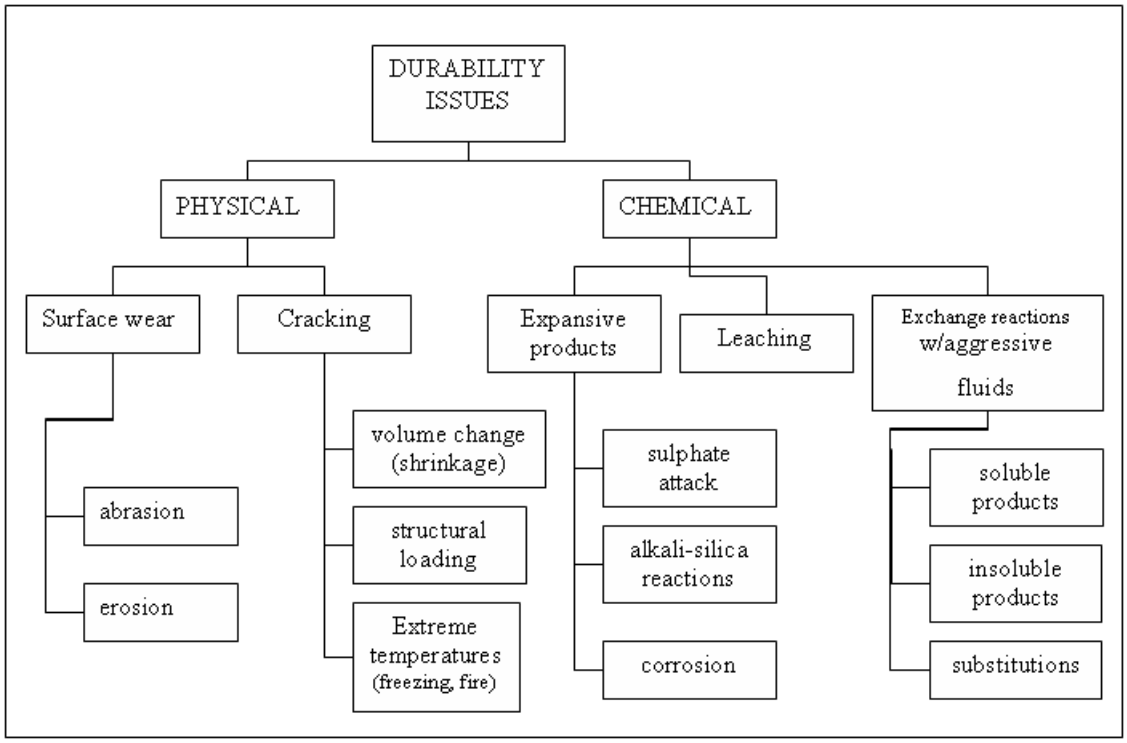

Figure 13. Types of chemical and physical deterioration of cementitious materials.[36]

3.4.1 Permeability

Permeability is a measure of the ability of a porous material to transmit fluids. Permeability of cementitious materials controls the mass transport of deterious agents (i.e. sulphate and chloride) into the cement paste and leaching of cement components from the paste. The coefficient of permeability, K, can be determined from the Darcy's law, as given in equation

$$Q = -KA\frac{\Delta h}{L} \tag{13}$$

where: Q = total discharge (m^3/sec),

K = coefficient of permeability (m/sec),

A = surface area (m^2),

Δh/L = hydraulic head (m/m),

Δh = change in height between two points (m), and

L = distance between points (m).

Both porosity and its geometrical characteristics determine permeability of the hydrated cement paste.[37] Figure 14 shows the relationship between the permeability and capillary porosity. The higher the coefficient of permeability of cement paste, the higher the relatively permeability and thus porosity of the material.[3]

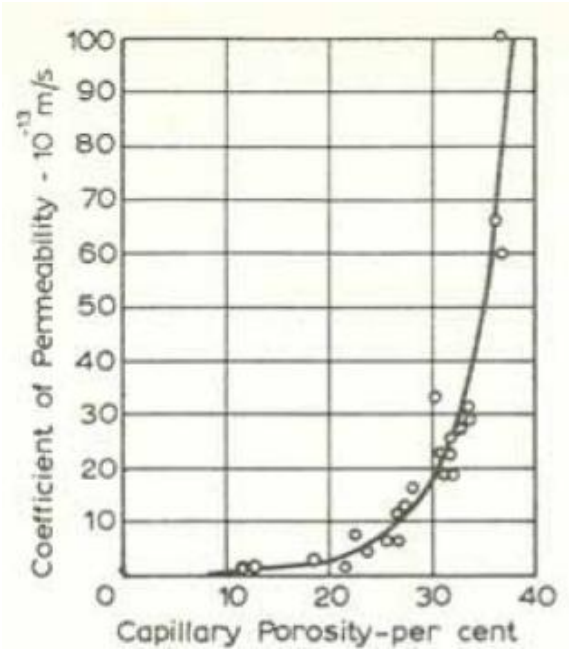

Figure 14. Relation between permeability and capillary porosity of cement paste.[3]

The pore structure of the cement-based materials can be altered by changing the material or mix design, e.g. by reducing the water-to-binder ratio (w/b) of the cement paste.[38] By raising the w/c ratio leaching kinetics increase by increasing the porosity and consequently increasing the diffusion of ions through the material.[39] By adding pozzolanas, such as silica fume, smaller and more discontinuous pores are produced resulting reduced hydraulic conductivity. Addition of silica fume modifies the

nanostructure of the calcium silica hydrate (C-S-H) gel, reducing its porosity. The pozzolanic C-S-H has a porosity of only 19% in comparison with the value of 28% of the conventional C-S-H.[39]

3.4.2 Leaching

In cement-based materials, leaching process consists mainly of transportation of ions from the interior of the material, through its pore system, outwards into the surroundings and vice versa. Solid compounds are dissolved by water that penetrates the (cement) specimen and are transported away, either by a) diffusion based on the concentration gradients, or by b) convection through the flow of water. Transportation is diffusion controlled when the pore size distribution of cement paste is small. As the volume of the flow paths increases it becomes convection controlled (Table 3).[40]

Table 3. Relation of pore radius to permeability coefficient.[40]

Pore radius (m)	**Permeability coefficient (m/s)**	**Transfer**
$< 10^{-7}$	$< 10^{-10}$	Molecular diffusion
10^{-7}—10^{-5}	10^{-10}—10^{-9}	Molecular flow
$>10^{-5}$	$> 10^{-9}$	Viscous flow

Calcium silicate hydrate (C-S-H) gel, portlandite ($Ca(OH)_2$) and alkalis dominate the chemical properties of the aqueous phase in Portland cement pastes. As the leaching process proceeds, it affects the microstructure of the cement paste.[40] The mineralogy of the cement paste is effected and the composition of the pore solution changes as a result of equilibrium shift.

As water penetrates through the cementitious material the pore water will be continually renewed and the rate of leaching will be faster. For cement pastes with low permeability, the limiting factor of leaching will be the rate of the water flow. Haga *et al.*[42] have concluded that the change in the pore structure is related to the type of dissolving hydrate. Dissolution of the primary hydrate such as C-S-H gel and portlandite increases the pore volume and the change becomes larger with longer leaching period. In samples leached for 56 weeks, portlandite was not observed. Instead, ettringite was generated in the surface layer of the samples. It was considered to be a secondary mineral formed in the process of hydrate dissolution. However, in deep repository conditions high chemical content of the groundwater can act as a limit of

leaching. Groundwater may already be heavily saturated in minerals, so it can not remove ions from the concrete.

Decalcification of the cement paste is closely associated with leaching process. As calcium is leached from the cement paste the Ca/Si ratio decreases until a constant value. According to a study of Hidalgo *et al.*[42] polymerization of the C-S-H chain is accompanied with a decrease in Ca/Si ratio and with low Ca/Si ratios aluminium can substitute silicon in the structure.

Leaching mechanism of concrete occurs in a sequence of stages. First the most soluble elements such as alkalis hydroxides, Na^+ and K^+ are removed, followed by the dissolution of portlandite. The next step is dissolution of the calcium-silicate-hydrate gel phases. Finally as the C-S-H gel phases have fully dissolved and its buffering capacity has dropped, other cement phases are dissolved. In an experiment by Lota and Hubbard[40] OPC mortar specimen were exposed to deionised water at a pressure of 2 MPa and a rapid rise of Na content was found in leachates. K content increased almost as rapidly as Na followed by the dissolution of Ca ions into the solution. The initial high pH in the pore solution arose from the high concentration of alkali hydroxides in liquid phase. As the calcium concentration in solution started to decrease the pH value also declined.

The pore water chemistry depends on the solubilities of the solid phases present. Figure 15 presents a schematic illustration of the evolution of pore water chemistry during leaching of the cement paste by pure water. In the beginning, the pore solution is dominated by highly soluble alkali hydroxides and pH is above 13. In the second stage, the pore solution chemistry is controlled by dissolution of calcium hydroxide and pH is buffered at *c.a.* 12.5. At the third step, C-S-H gel and in particular the Ca/Si ratio of the gel determines the pore solution chemistry; pH drops continuously to around 10.8. From this process it can be deduced, that a low pore water pH value can be achieved by reducing the alkali and portlandite content when hydration is completed. Under these conditions, pH is controlled by the C-S-H dissolution: the lower the Ca/Si ratio, the lower the pH.[43]

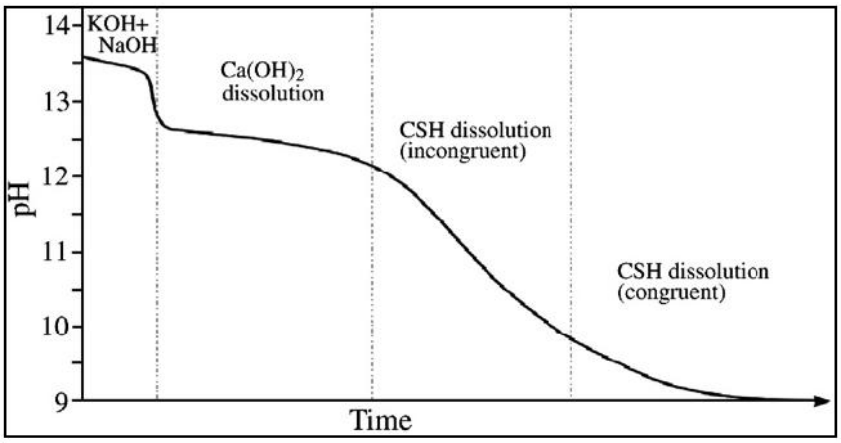

Figure 15. Schematic evolution of pore solution pH during leaching by pure water of sulphate resistant Portland cement.[43]

Some studies have been performed in order to evaluate the influence of the leaching resistance of high (HPC) and ultra-high performance concretes (UHPC) in stagnant or running water test.[27, 44] Alonso *et al.*[27] studied the influence of contact water regime by using a Tank Water Test (TWT) and specifically developed Running Water Test (RWT). In both methods groundwater was used as a leachant. The general trend in the running water test was that the amount of Ca leached was decreased with time. After 12 months of leaching the concentration of calcium in leached solutions from UHPC, stabilised below the Ca concentration in the ground water (0.84 ± 0.04 mmol/l). In HPC samples the leaching concentration stabilised after the first month. The pH values of the leach solutions were alkaline initially (pH > 10.5) but dropped as the dissolution continued. In the tank water test the concentration of calcium leached from all concretes were below that of the Ca introduced by the ground water. Also the pH value of the leachates was near the ground water pH right from the beginning. Vernet *et al.*[44] concluded that the flow type regime and the chemical composition of the solution have significant impact on the mechanism of leaching. The decrease in water flow resulted a slight increase of the amount of calcium leached, but did not change the leaching mechanism mentioned above.

The amount of calcium leached is a good indicator to follow the progression of the leaching process. The composition of leachate will affect and modify the leaching of the components of cementitious materials.[40, 44] For example, in a system where carbonates and bicarbonates are present, Ca values below the initial concentration of the leachate are found, due to the precipitation reaction of calcite. In order to know the real calcium

leached from cementitious materials the amount of calcium precipitated needs to be calculated.

3.4.3 Expansive products

Cement-based materials exposed to sulphate-bearing solutions such as natural ground waters can show signs of deterioration. The two most common types of sulphate attack are physical attack, where the sulphate-containing water enters the surface of the concrete, crystallizes, and causes expansion and cracking, disrupting the hardened concrete; and chemical attack, where sulphate salts react with the Portland cement, causing it to dissolve, soften and loose the initial strength and adhesion.[3, 24]

During sulphate attack, both the portlandite and the aluminate phases in a cement matrix react with sulphate to form insoluble substances with much greater volumes. The extent to which the reactions proceed depends on the conditions, such as ionic strength of the solution and the flow rate.[22] Concrete mixtures prepared with supplementary cementing materials show a better resistance to sulphate attack by reducing their permeability. Pozzolanas reduce the expansion of specimens undergoing sulphate attack by decreasing the amount of portlandite in the cement paste.[3, 45]

Alkali silica reaction (ASR) causes premature deterioration in concrete.[29] Alkali hydroxides present in concrete pore solution react with amorphous or poorly crystalline silica phases in aggregates, forming a gel which absorbs water and expands. Some of the most effective methods of reducing ASR reactions involve replacement of a portion of cement with one or more pozzolanic materials to decrease the permeability and reduce the quantity of alkalis in the concrete.

Corrosion is a problem for steel used together with cement-based materials.[24] The expansion produced by rust formation causes the surrounding concrete to crack and spall. Lowering the pH of a cement mixture can increase the risk of steel corrosion. The high pH of the pore solution stabilizes an oxide film on the steel and inhibits further risks. Chloride ions may cause local breakdown of this passive film, even at high pH and thus cause chloride-induced corrosion in steel rebar.

Gaseous carbon dioxide penetrates the cement-based materials and dissolves in the pore solution, producing CO_3^{2-} and HCO_3^- ions, which react with Ca^{2+} to produce $CaCO_3$ as well as other CO_2-based solid phases. The OH^- and Ca^{2+} ions required to these reactions

are obtained by the dissolution of portlandite and is associated with a drop in the pH value and thus have detrimental effects on reinforced concrete structures.[24, 45]

3.4.4 Exchange reactions with aggressive fluids

Exchange occurs when aggressive fluids react with components of the hardened cement paste. Seawater exposure on concrete provides potential for various types of exchange reactions and types of deterioration to occur simultaneously. The chemical action of seawater on concrete is mainly due to the magnesium sulphate present. Leaching actions remove lime and calcium sulphate while reaction with magnesium sulphate leads to the formation of calcium sulphoaluminate which may cause expansion. The precipitation of magnesium hydroxide may block the pores of the concrete and thus slow down the leaching reactions. The presence of chlorides retards the swelling of concrete in sulphate solutions.[23] Calcium ions may be removed or substituted in various reactions between cement paste and aggressive fluids. Leaching of these materials with time can lead to deterioration of cement-based materials.[3]

3.4.5 Other durability risks

Shrinkage occurs due to the loss of water from a cement-based material. Shrinkage of concrete takes place in two distinct stages: at early and later ages. The early stage is commonly defined as the first day, while the concrete is setting and starting to harden. The long-term shrinkage refers to the concrete at an age of 24 hours and beyond.[2]

The major shrinkage types are drying and autogenous, but in addition the concrete may also be subjected to volume reductions due to thermal changes and carbonation reactions.[3] Drying shrinkage results from loss of water from the concrete. It is dependent on the environmental surrounding of the concrete, especially the temperature and relative humidity (RH). In general, concrete with a high w/c ratio will have higher drying shrinkage because there is more so called free water. Autogenous shrinkage is defined as the macroscopic volume change occurring with no moisture transfer to the surrounding environment. It is a result of chemical shrinkage related to the hydration of cement particles.

If sufficient quantity of water is present in the pores of cement paste, the concrete may be damaged by frost, and especially by repeated cycles of freezing and thawing. The freezing water within the concrete creates hydraulic pressure, causing cracking and fissuring. To resist freeze-thaw deterioration, the hardened concrete must contain an air-void system which provides space to relieve the pressure of the freezing water. Low

permeability and absorption and thus low w/c ration are also important factors affecting the durability of the cement paste.

4 LOW-pH INJECTION GROUTS

Hyper alkaline conditions (pH > 12) of cement pore fluids are considered to have deleterious effects upon the host rock and other engineered barrier system (EBS) materials (especially bentonite, the buffering material) in deep geological repositories of spent nuclear fuel.[11] In Figure 16 is presented a safety assessors view on the assessed impact of different pH regions in deep repository environment and the pH-evolution of the leachates of ordinary Portland cement-based materials. An acceptable pH value lies around 11 when the equilibrium phase no more buffered by is portlandite.

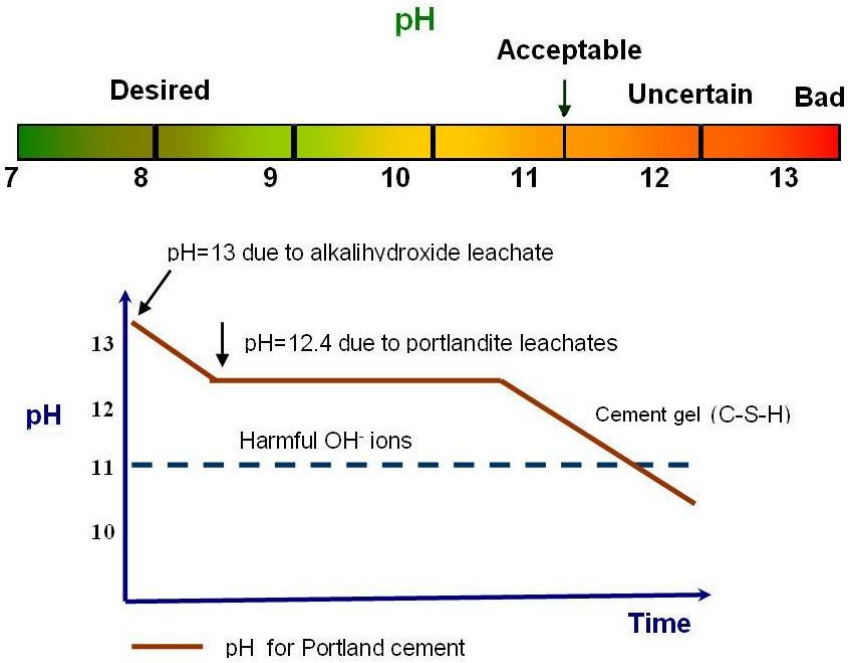

Figure 16. The assessed impact of different pH regions in deep repository environment and the principles for the pH-evolution for Portland cement.[46]

The substitution of cement with other materials will remove the amount of portlandite from the mixture also resulting in lowering the heat of hydration. The lack of free portlandite causes the pH of the pore fluid to be reduced to less than 11. Because low-pH cementitious materials have little, or no free portlandite, they predominantly consist of calcium silicate hydrate (CSH) gel. The high strength and low hydraulic conductivity features make low-pH cementitious materials suitable for use in the repository environment. However, the workability of the low-pH grouts does not fulfil the set requirements (Table 4) without addition of additives such as superplasticizer.

Table 4. Required properties of low-pH cement grouts.[6]

Order of Importance	Property	Requirement	Measuring method
Required Properties	pH	≤ 11	Leaching test
	Penetration-ability b_{min} Penetration-ability b_{crit}	≤ 80 μm ≤ 120 μm	Penetrability meter at 60 min
Desired Properties	Viscosity	≤ 50 mPas	Rheometry at 60 min
	Bleed	≤ 10 %	Measuring glass at 2 hours
	Workability time Shear strength Yield value	≥ 60 min ≥ 500 Pa ≤ 5 Pa	Determined by penetration-ability and viscosity Fall cone at 6 h Rheometry at 60 min
	Compressive strength	≥ 4 MPa	Uni-axial compressive strength at 28 d

4.1 Development

Low-pH injection grouts have been studied since 2002 in a joint project between Posiva, SKB and NUMO. The aim of the project was to achieve at least one well-quantified, tested and approved low-pH injection grout to be used in repository. The development of low-pH grout materials was done at VTT and further optimization by Posiva for ONKALO.[6, 7] The technical performance of different grout mixes was tested before any mixes were chosen for leach testing. Detailed information on the materials, mix characteristics, designing of the mixes and results from their performance are found in Kronlöf's report.[6] The leach and pH testing was done by Vuorinen *et al.*[5] The most promising mixes were then selected to be tested in pilot field testing (PFT1).[7]

Testing and reporting of low-pH grout materials has mainly concentrated on properties of fresh materials rather than the long-term performance. However it has been confirmed in many research studies that the physical and chemical properties of the cementitious material change within time.[41, 47-49] e.g. Haga *et al.*[41] investigated the alteration associated with dissolution of ordinary Portland cement hydrates by subjecting the solid samples to measurement of pore size distribution, bulk density using mercury intrusion porosimetry (MIP) and electron probe microanalysis (EPMA). The mineral and chemical compositions of solid materials were studied by using X-Ray Diffractometry (XRD) and thermal analysis (TG-DTA). Alonso *et al.*[47] evaluated also the changes in the ionic composition and pH of the pore solution at different days of hydration by extracting pore fluid from the solid samples.

The removal of the hydration products can increase the porosity and leaching potential, but again these properties can also decrease due to additional hydration and blocking pores. Some other international studies has also been done on low-pH cementitious materials.[27, 43, 50] Cau Dit Coumes *et al.*[43] and Codina *et al.*[50] have formulated and characterized low-heat and low-alkalinity cementitious materials for radioactive waste repositories. Alonso *et al.*[27] studied the groundwater leaching resistance of high and ultra high performance concretes with two leaching methods based on different convection regimes of the leachate. They used the leachability of calcium as an indicator to follow the progression of the attack.

4.2 Chemical properties

In low-pH cements, the amount of cement is reduced by substituting it with blending materials, such as silica fume, fly ash and blast furnace slag. To attain the defined pH ≤ 11 set for cement grout leachates, the blending materials must comprise at least 50 wt% of dry materials. According to variety of studies the Ca/Si ration of C-S-H of the cement should be lower than 1.1 in order to produce low-pH materials (Table 5).[6, 47, 51]

Table 5. The amount of silica fume needed to produce grout leachates with pH < 11.[6]

Solids in equilibrium	**$[Si]_{aq}$ (mg/L)**	**pH**
Amourphous SH	39.5	6.38
Amourphous SH + CSH (0.8)	117.0	10.17
CSH (0.8)	43.4	10.88
CSH (0.8) + CSH (1.1)	41.1	10.91
CSH (1.1)	31.4	11.03
CSH (1.1) + CSH (1.8)	0.7	12.43
CH + CSH (1.8)	0.5	12.53
CH	0	12.52
SF = Silica Fume	CSH = calcium silicate hydrate	
CH = calcium hydroxide		

Of the possible blending materials silica fume has appeared to be the most promising one in low-pH grouts for deep geological repositories.[7] According to the work by Lagerblad[52] the use of silica fume was found to be an efficient component for lowering the pH of grout leachates. Silica fume reacts with $Ca(OH)_2$, which is one of the main component of pure Portland cement's hydration products. The equilibrium pH of

calcium hydroxide with water is 12.5, and decreasing the amount of $Ca(OH)_2$ in the pore solution lowers the pH to 11 or lower. On the other hand, pH does not depend solely on chemical composition of the materials, but also on the composition of the reaction products formed. As the pozzolanic reactions proceeds the Ca/Si ratio decreases which in turn decreases the pH.

Another positive effect of using silica as a blending agent in cement paste is to produce a grout with low water separation and high penetration as well as enhance the resistance to chemical attack and leaching due to the lower permeability and higher CSH content. Some risk or problems can also occur during the early ages when using high amounts of silica fume. The main concerns of concrete mixtures with high silica fume content are the risk of gel-blocking resulting from decreased penetration-ability, the possibility of silica conglomerates or lumps, and retardation or delayed setting times.[3]

4.3 Characteristics and performance

The low-pH injection grouts will be used in ONKALO and the final repository facilities in order to improve long-term environmental safety. The history of experience with these materials is not very long, so the assumptions concerning the long-term performance are mostly based on similar concrete and cement-based mixtures containing silica fume.

The ingredients of the low-pH injection to be used in the ONKALO are as follows:[3]

- Cement: Ultrafin 16 – sulphate resistant, low alkaline injection microcement, manufactured by Cementa AB in Sweden. Specific surface of 1 600 m^2/kg, C_3A content of 2%, and alkali content of ~ 0.5%.
- Pozzolan: GroutAid – silica fume-based additive for grouting, produced by Elkem ASA Materials in Norway. Minimum SiO_2 content of 86%, solids content of 50%, specific surface area about 15 000 m^2/kg, 90% of particles < 1 μm diameter, pH of 4.5 to 6.5, and no accelerator additive.
- Chemical admixture: Mighty 150 – naphthalene sulphonate based superplasticizer produced by Degussa (now BASF Construction Chemicals).

Very finely-ground microcements are being used in ONKALO for grouting the upper sections of the facility. The particle size in these microcements is usually less than 30 μm in diameter. As a general guide-line, injection filling is possible for maximum

fissures of the sizes three times the maximum grain size in the grout, so the microcement used in ONKALO should be able to fill fissures up to about 100 μm in width.

In sulphate-containing environment sulphate resistant cements improve the expected durability performance of the hardened cement paste.[3] Since sulphate attack on hydrated Portland cement mainly involves the C_3A phase, the sulphate resistant cements are characterized by a reduced C_3A content in clinker. It should, however, be noticed that the sulphate resistance of these cements is not absolute. At very high sulphate concentration (> 200 mg/L), there can still be expansion and deterioration, though more slowly and to a lesser degree compared to Ordinary Portland cements.

As the constructions of ONKALO proceed deeper, the plan is to replace the ordinary high-pH grout with some low-pH injection grout materials. Low-pH injection grouts have better leach resistance and leachates with sufficiently low-pH (≤ 11) compared to ordinary ones.[3]

As mentioned in chapter 3.4, porosity and its geometry determine permeability of the hydrated cement paste. Highly porous materials transmit fluids through the material more readily and decrease the long-term performance. To produce cement paste with maximum density and minimum porosity, it is beneficial to have as low w/c ratio as possible. This can be obtained with superplasticizers. Some leaching tests mentioned by Holt[3] have showed that the use of superplasticizers may increase the total organic load in groundwater. Yet the benefits of material properties and performance gained through the use of superplasticizers outweigh any unfavourable effects of increased organic load.

Some permeability and leaching tests have been performed on low-pH cementitious materials.[5, 27, 53] Vuorinen *et al.*[5] found out that mixtures containing silica fume had promising chemical characteristics (i.e. fast depletion of K, SO_4^{2-} and declining trend of Ca concentration). Onofrei's[53] static leaching test showed that the release of Ca^{2+} was independent of the silica fume addition and the w/b ratio of the cement paste. In dynamic leaching tests the leach rates of Ca^{2+} decreased steadily, indicating the presence of a protective surface layer causing lower solubilities of the cement constituents.

In the deep geological environment it should also be noticed that components present in the granitic bedrock can participate in the cement reactions, as well. Minerals may

precipitate and new secondary minerals may be formed, thus further enhancing the sealing effects of the grout by clogging of fractures.[3] In hydraulic conductivity and permeability tests by Onofrei *et al.*[53] it was noticed that addition of silica fume decreased the apparent hydraulic conductivity (K) of the grout. They concluded that this was a consequence of the decrease in pore size and the decrease in connected capillary pore space. The change in porosity during leaching is mainly attributed to the changes in volume of solids caused by the formation of new hydration products. The results confirm that silica fume grouts have the potential to self-heal and maintain their performance for very long time periods.[3]

The main characteristic difference between the reference and low-pH grouts studied in the experimental part of this report is the increased silica fume content (from 15 % to 40 % by dry weight). Compared to the reference grout mix, the low-pH mixtures have the following characteristics:

- less portlandite (CH) in hydrated cement paste,
- greater homogeneity, due to better fine particle dispersion,
- better penetration into fine fissures,
- better bond to granite bedrock
- possibly higher total porosity, yet with fewer capillary and interconnected pores, and
- better potential for self-healing.

These properties lead to enhanced durability performance, such as lower permeability, better leaching resistance, and greater resistance to chemical attack (especially sulphates).[3] The risks that are associated with the low-pH grout mixtures compared to the reference grout mixes are shrinkage, gel-blocking, and alkali-silica reactions (ASR), although, it has been observed in the accelerated ASR tests that low-pH grout mixes should not posses high ASR reactivity even if unbroken silica granules are present in the mass.[3] However, these reactions are complicated and more accurate information is needed. The total drying shrinkage will likely be higher for the low-pH grout compared to the standard reference one due to its higher w/b ratio and higher total water content, as well as, increased superplasticizer dosage. Yet it will only be a problem if the surrounding environment has substantially lower humidity, but it is assumed that there will be enough groundwater available inside sealed fissures to prevent drying.

It is possible that during further construction of ONKALO, there may be changes in construction techniques or in environmental conditions. Therefore it might be necessary to change the mix design or materials for both reference and low-pH grouts. For instance, the temperature or humidity changes affect the rate of hydration and thus alter the microstructure of cement pastes and long-term performance. One of the main concerns with the Olkiluoto site conditions regarding the performance of the cementitious materials is the groundwater composition. At upper levels of the bedrock (0 – -150 m) it is the presence of bicarbonate (HCO_3) which can react with calcium leached from cement and form precipitable carbonates and change the composition of cementitious material. The precipitation of calcium carbonate may either improve the permeability of grout or decrease it by increasing the leaching of the calcium from the material. The groundwater chloride (Cl^-) content is relatively low in the fresh groundwater at the upper levels (< 10 mg/L) but much higher at greater depths (2 000 – 5 000 mg/L). Chloride attack is a concern because chloride ions react with CH to form soluble products (e.g. calcium chloride) which can be leached away. Hill *et al.*[54] have studied the effect of sodium chloride on the dissolution of C-S-H gels and found out that the concentration of NaCl solution has a strong effect on the Ca concentration. The Ca concentration increased with NaCl concentration in all experiments. At the presence of sulphates (SO_4), especially magnesium sulphate, leaching actions remove lime and calcium sulphate while reactions with magnesium sulphate lead to formation of insoluble products causing expansion and cracking. The pH, acidity, and ammonium (NH_3) contents of the Olkiluoto groundwater are acceptable and should not cause any problems for grout performance.

The influence of organic admixtures of cementitious materials, in other words superplasticizers, in the repository environment has to be carefully evaluated. The role of organic complexing agents in enhancing radionuclide migration has been shown to be undisputed.[34] They may alter the transport properties of radionuclides due to the action of one or more of the following processes:

- increased radionuclide (RN) solubility
- decreased sorption, if the complexants are not themselves sorbed
- increased sorption, if the complexants themselves are sorbed
- decreased rate of transport, if the size of the complexes are sufficient to decrease their diffusion coefficient

- increased rate of transport, if the complexes are sufficiently large to cause size exclusion from small pores.[35]

There are several studies on the environmental concentrations of superplasticizers but estimates of leaching amounts especially from concretes are quite inadequate. The main sources have been industry, wastewater treatment plants, and construction and landfill sites. These environmental studies can give an idea about the behaviour of different compounds of these admixtures, even though they are not directly correlated to the leaching aspects of concrete.[32] Ruckstuhl *et al*.[33] have studied the leaching behaviour of PNS (sulfonated naphthalene-formaldehyde condensate) from a tunnel construction site of the Swiss Federal Railways. When fresh cement containing PNS was applied at construction sites, PNS was leached out into the groundwater. It was noticed that the concentration of PNS in groundwater was up to 58 µg/L about 60 m from the construction site. The leached components were the monomers and the oligomers up to the tetramers. Higher condensed oligomers remained immobilized in the cement matrix.[33]

All the pore water and leaching studies performed have been short-term tests and no long-term tests have been carried out.[31] In order to evaluate the long-term behaviour of superplasticizers in deep geological repository long-term experiments are required.

5 SUMMARY

Posiva's spent fuel management programme consists of the disposal of spent fuel in a deep geological repository at Olkiluoto island. Investigations on the suitability of the site have been ongoing over fifteen years, as a part of these investigations, construction of an underground rock characterisation facility, ONKALO, began in 2004, which may later act as the access tunnel to the repository . Current repository design locates the facility at the depth between -400 and -600 m in the bedrock.

The access tunnels and other cavities in bedrock can have areas with higher hydraulic conductivity than the surrounding rock. Water flows primarily along these network of pathways. By sealing the fractures with cementitious materials, the flow rate of groundwater into the repository can be reduced. The currently used ordinary cementitious grouts may have deterious effects on the engineered barrier system. Therefore, alternative materials are considered to be used. The tunnels will backfilled after the canisters have been placed. The backfilling material is a mixture of crushed rock and bentonite clay. The interactions of ordinary cementitious materials with groundwater may cause a high pH plume. This can change the hydraulic and chemical properties of bentonite leading to the insufficient buffering capacity.

Cement is made from limestone, clay and quartz. It is the basic ingredient in concrete and mortars. The Portland cement clinker contains four major phases called alite, belite, aluminate and ferrite. Also some minor phases are present. The hydration of OPC consists of series of chain reactions that are dependent on each other. Hydration occurs spontaneously when water and cement are mixed together. Setting is a process in which a fresh cement paste stiffens and looses its deformability. It is followed by hardening in which development of compressive strength occurs. The complete hydration of cement paste can take several years.

The properties of Ordinary Portland cement can be altered by using additive materials, such as silica fume (microsilica), fly ash, blast furnace slag or some natural pozzolanas. They can be used to decrease the total heat evolution of hydration, improve durability and decrease the high pH of the cement pore fluids. Besides the positive effects pozzolanas may also create some negative effects, such as reduced workability and increased concentration of alkali hydroxides in cement pore solution. A better workability can be achieved by increasing the w/c ratio but at the same time it reduces the strength and longevity of the cement paste. Water reducing agents, called

superplasticizers, can be used to achieve desired workability at lower w/c ratios. Superplasticisers are negatively charged organic polymers that may leach from cement matrix into groundwater and change the migration of possible radionuclides by forming new complex compounds. Some studies concerning the leaching behaviour of SPs have been conducted.[33, 34]

Durability is the ability of cementitious materials to resist the deterioration process. Degradation includes several mechanisms such as, chloride and sulphate attack, carbonation, leaching, and formation of new secondary minerals. Hydrated cement paste is porous material. Solid compounds are dissolved by water and transported away either by diffusion or by convection through the water flow. The permeability of cementitious materials is a function of porosity, as the porosity increases so does the permeability. Leaching mechanism of cementitious materials occurs in a sequence of stages. First the most soluble elements are removed, followed by the dissolution of portlandite. In the next stage the CSH phases are leached. The pore water chemistry depends on the solubility of the solid phases present. The high chloride and sulphate concentrations in groundwater may be detrimental to cementitious materials. They react with free $Ca(OH)_2$ forming calcium sulphate, which further reacts with hydrated calcium aluminate to form insoluble ettringite. The volume of these new compounds is higher, causing expansion and cracking of the cement paste. All of these deleterious processes decrease the durability of cementitious materials and shorten their lifetime.

The fundamental principle in the development of low-pH injection grouts was to ensure the long-term safety in the repository conditions, because there is not enough information on the influence of possible high-pH plume originating from OPC materials. Testing and reporting on the low-pH grout materials has mainly concentrated on the fresh properties rather than log-term performance. It has been concluded that in order to attain the desired pH (< 11) for cement leachates, the blending materials must comprise at least 50 wt% of dry material. Silica fume has appeared to be the most active blending agent. On the other hand the pH does not depend solely on the chemical composition of the raw materials, but also on the composition of the reaction products. As the pozzolanic reactions proceed the Ca/Si ratio decreases which in turn decreases the pH of the leachates.

The main concern with site conditions regarding performance of the injection grouts is the groundwater composition. Different compound such as, high chloride and sulphate concentrations in groundwater increase the deterioration risk of the injection grouts. The

only bedrock concern is that over long periods of time there can be stress changes in rock with may alter the water tightness of the repository.

EXPERIMENTAL WORK

OBJECTIVE OF THE WORK

Low pH cement-based injection grouts are considered to be used to seal fractures and cracks in the deep geological repository. The possible effects caused by the cementitious materials in the surrounding repository environment have to be carefully evaluated, especially in respect of the long-term safety.[4]

The main objective of this work was to study the effect of water composition and flow rate on leaching behaviour of two freshly mixed cementitious injection grouts. Test was performed at ambient temperature (20 ± 1 °C) in a glove-box in N_2 atmosphere in order to avoid the interference of atmospheric CO_2.

TYÖN TARKOITUS

Matalan pH:n injektointiaineita tullaan käyttämään ydinjätteen loppusijoitustilassa mahdollisten rakovyöhykkeiden injektointiin. Sementtipohjaisten materiaalien käytön vaikutukset tilan ympäristöön, erityisesti pitkäaikaisturvallisuuteen liittyvät seikat, tulee selvittää huolellisesti.

Tämän työn tarkoituksena oli tutkia miten virtaavan veden koostumus ja erityisesti sen virtausnopeus vaikuttavat kahden tuoreelta valetun sementtipohjaisen injektointiaineen uuttumiseen. Koe suoritettiin 20 °C ± 1 °C lämpötilassa hanskakaapissa typpiatmösfäärissä, jossa voitiin välttää ilman hiilidioksidin aiheuttamat häiriöt.

6 METHODS AND PROCEDURE

Dynamic leach testing was used in order to evaluate the influence of the water flow on leaching of two cementitious injection grouts. The experimental setup and need to work inside a glove-box set boundaries to the volume of simulated solutions that could be prepared and handled and also the limits for the flow rates that were possible.

Leaching test was performed inside a glove-box (N_2 atmosphere) in order to avoid the interference of atmospheric CO_2. Two simulated groundwater solutions, fresh ALL-MR and saline OL-SR, were used as leachates. Two flow rates were chosen, a higher flow rate of 7.5 mL/h and a lower one of 0.625 mL/h. Dynamic leach testing was used in order to evaluate the influence of the water flow on leaching of the grout samples. The sample collection of leachates was performed according to a set time schedule. The pH value of each leachate sample collected was measured, but the amount of total organic carbon was determined only for some leachate samples. Because of the large number of leachate samples collected some samples were combined before chemical analyses were performed.

7 MATERIALS AND SOLUTIONS

7.1 Grout samples

Two different injection grouts, medium and low-pH grouts, were subjected to investigation. The grout mixes were prepared by mixing cement, silica fume, plasticizer and water. The cement type was UF16 (Cementa AB), which is a sulphate resistant, chromate reduced and low alkaline injection cement with a specific surface of 1600 m^2/kg. The silica fume used was GroutAid (Elkem) with a minimum SiO_2 content of 86 %. The trade name of the plasticizer was Mighty 150 (Sika Norge AS), which is a naftalenesulfonic acid formaldehyde condensate. Both grout mixes have been tested also earlier in static leach testing by Vuorinen.[1] Table 6 gives the composition and IDs of the grouts. In Table 7 are shown the chemical compositions of cement and silica fume. Detailed information on the materials and results from their technical performance are found in Kronlöfs report.[6]

Table 6. The mix composition and IDs of grout mixes.

Classification of grout	**OPC-type**	**SF type**	**OPC/DM**	**SF/ DM**	**SPL/DM**	**W/DM**	**Grout ID cem-SF-W/DM-SPL**
low-pH	UF16	Grout Aid	0.59	0.41	0.04	1.40	UF-41-14-4
medium-pH	UF16	Grout Aid	0.85	0.15	0.03	1.01	UF-15-10-2.8
OPC = Ordinary Portland cement			SF = Silica Fume				
DM = dry matter			SPL = Superplasticizer				

Table 7. Chemical composition (%) of cement and silica fume.

	CaO	**SiO_2**	**Na_2O**	**K_2O**	**Al_2O_3**	**MgO**	**Fe_2O_3**	**SO_3**	**MnO**	**P_2O_5**	**TiO_2**
cement (UF16)	65.6	22.9	0.08	0.43	3.67	0.79	4.41	1.77	0.23	0.11	0.25
silica fume (Grout Aid)	0.47	93.6	<0.03	0.77	1.13	0.52	0.27	0.09	0.04	0.05	0.01

The mixes were prepared at VTT by Paula Raivio (Contesta Oy). The mixing instrument used was Desoi AKM-70D (1500 W). The mixing order for injection grouts

was the following: cement was added first to a major part of the water and the mixing proceeded for 2 minutes after which SPL was added together with the remaining water. Last microsilica slurry (GroutAid) was slowly added to the mixture. Total mixing time was of about 5 minutes. Directly after mixing the penetration ability of the grout mixes was tested with a filter pump (filter mesh size 100 μm) to ensure that the set penetration requirements were met.[55]

7.2 Leaching solutions

Two simulated groundwater solutions, fresh ALL-MR and saline OL-SL, were used as leachates. The compositions of the leaching solutions are given in Table 8. The solutions were prepared inside the anoxic glove-box in order to avoid interference of atmospheric CO_2. Also all water used in preparation was CO_2-free. This type of simulated water has the advantage, in comparison with deionised water, that the test conditions are more representative of real exposure conditions in resistance studies.

Table 8. Nominal composition of the two stimulated groundwater solutions used.[5]

		Fresh **(ALL-MR)**	Saline **(OL-SR)**
pH		8.80	8.30
Na^+	**mol/L**	$2.3 \cdot 10^{-3}$	0.21
Ca^{2+}	-″-	$0.13 \cdot 10^{-3}$	0.10
K^+	-″-	$0.10 \cdot 10^{-3}$	$0.54 \cdot 10^{-3}$
Mg^{2+}	-″-	$0.03 \cdot 10^{-3}$	$2.3 \cdot 10^{-3}$
Sr^{2+}	-″-		$0.40 \cdot 10^{-3}$
SiO_2	-″-	$0.03 \cdot 10^{-3}$	
HCO_3^-	-″-	$1.1 \cdot 10^{-3}$	
Cl^-	-″-	$1.4 \cdot 10^{-3}$	0.41
Br-	-″-		$1.3 \cdot 10^{-3}$
I^-	-″-		$0.01 \cdot 10^{-3}$
F^-	-″-		$0.06 \cdot 10^{-3}$
B^-	-″-		$0.09 \cdot 10^{-3}$
SO_4^{2-}	-″-	$0.10 \cdot 10^{-3}$	$0.04 \cdot 10^{-3}$

8 EXPERIMENTAL ARRANGEMENT

The experimental set-up consisted of two sets of similar instrumentation, one for each flow rate used. Each set had five components fresh leaching solution, a syringe pump for feeding the leaching solutions into the grout containing syringes, Amani 1000 electrodes for measuring the potential changes of leachates on-line and polyethylene vessels for collecting leachate samples (Figure 17). All the different components of the experimental set-up were connected via plastic tubing.

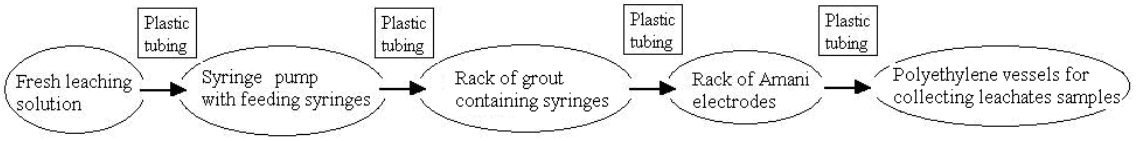

Figure 17. A schematic illustration of the experimental set-up.

The fresh grout mixes were cast in 20 mL plastic syringes (Figure 18). The cement paste was poured into the vertically placed syringes through a casting hole made on the top of each syringe. The vertical syringes were filled almost up to the needle nozzle and a small hole made in the syringe piston at the same level of the needle nozzle. The total volume of cement paste in each syringe was 19 ± 2 cm^3. The flowing leaching solutions attacked the surface of the cast grout materials. After finishing casting the casting holes were sealed with silicone plugs and the syringe racks immediately placed inside steel vessels and flushed with nitrogen. The samples were transferred into the glove-box inside the steel vessels. It took around three hours from casting until everything was set up inside the glove-box and ready for the actual experiment to be started.

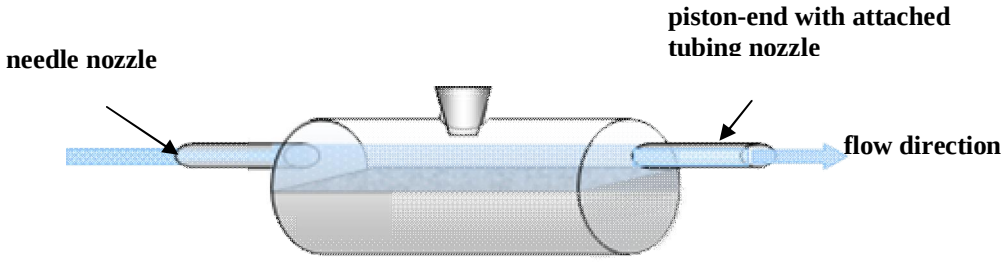

Figure 18. A schematic illustration of a sample syringe with grout mix.

The sampling frequency and collected leachate amount varied along the testing period for both flow rates.

High flow-rate, 7.5 mL/h:

In the beginning of the test sampling of the collected leachates was performed every five hours. After that the sampling frequency was kept around eight hours till the 15th day. Sampling frequency was decreased gradually so that after the 15th day sampling was performed every 16th hour and from the 100th sampling point on, samples were exchanged every other day. When the pH values measured from the leachate samples collected showed rather constant values for a longer time period the flow rate was reduced from 7.5 mL/h to 5.7 mL/h. As the flow rate was reduced, it was possible to decrease the sampling frequency to once in three days. After 93 days from the beginning of the experiment, the flow rate was reduced again from 5.7 mL/h to 2.5 mL/h. Then the leachate sample collection frequency could be changed to once a week. Duration of the entire testing period was 127 days, thus, in total, each grout specimen was leached with approximately 13 600 mL of leaching solution.

Low flow-rate, 0.625 mL/h:

Sampling of the collected leachates was performed every other day till the 18th day of experiment and then decreased to once in four days. From the 19th sampling point on the leachate sample collection frequency was once a week till the end of the experiment. Each grout specimen was leached with approximately 1 390 mL of leaching solution.

The amount of grout in each test was at least 15.2 cm^3, but the amount of grout was more especially in the samples of the higher flow rate experiment (Figure 26).

The actual leaching system running is shown in Figure 19 and Figure 20a. A syringe pump (TSE 200 series) feeding leaching solutions through the sample syringes containing the grout mixes and the Amani electrode rack as well as the leachate collection vials. Amani 1000 electrodes (Figure 20b) are manufactured exclusively by Innovative Instruments, Inc.[56] and they are combination electrodes made entirely of plastic. The tip of the sensor is very small (only 1 mm), so it can be used to measure small sample volumes. The small tip size enabled the on-line mV measurement.

Sample collection was carried out according to planned time schedule. From all solution samples 30 mL was extracted and filtered (0.2 µm) into two 15 mL plastic test tubes in order to remove possible particles or larger colloids present in the leachates. The other 15 mL sample (for cation analysis) was preserved by adding 15 µL of supra pure concentrated HNO_3. After filtration a small aliquot of the filtered leachate sample was used to measure the pH value of the sample with a commercial glass combination electrode (Orion ROSS, Model 8163SC) inside the anoxic glove-box. The measuring electrode was calibrated with adequate commercial pH buffers. Rest of the solution samples were stored in a refrigerator until taken to chemical analyses.

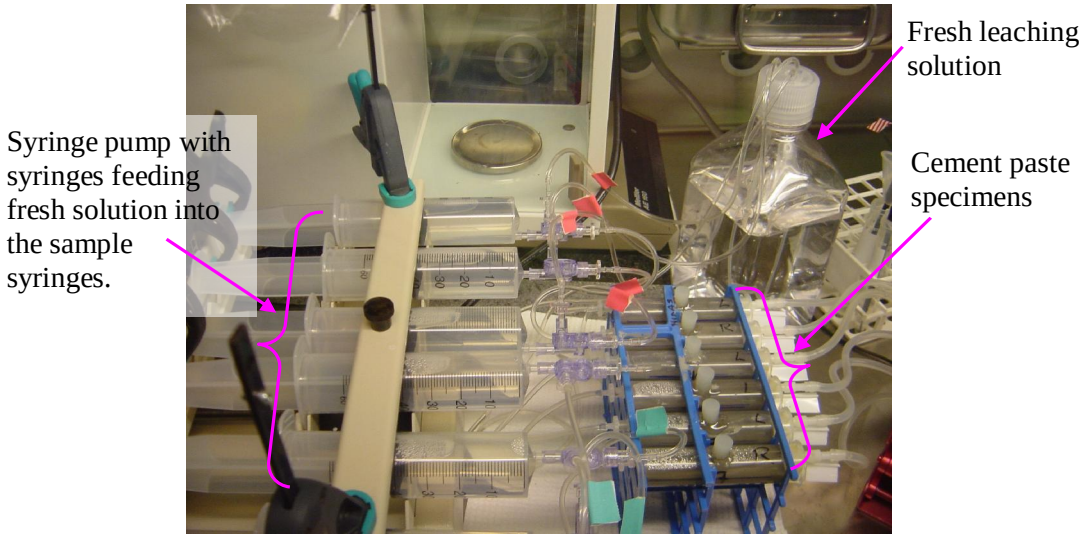

Figure 19. Syringe pump with four syringes feeding water through four grout specimens.

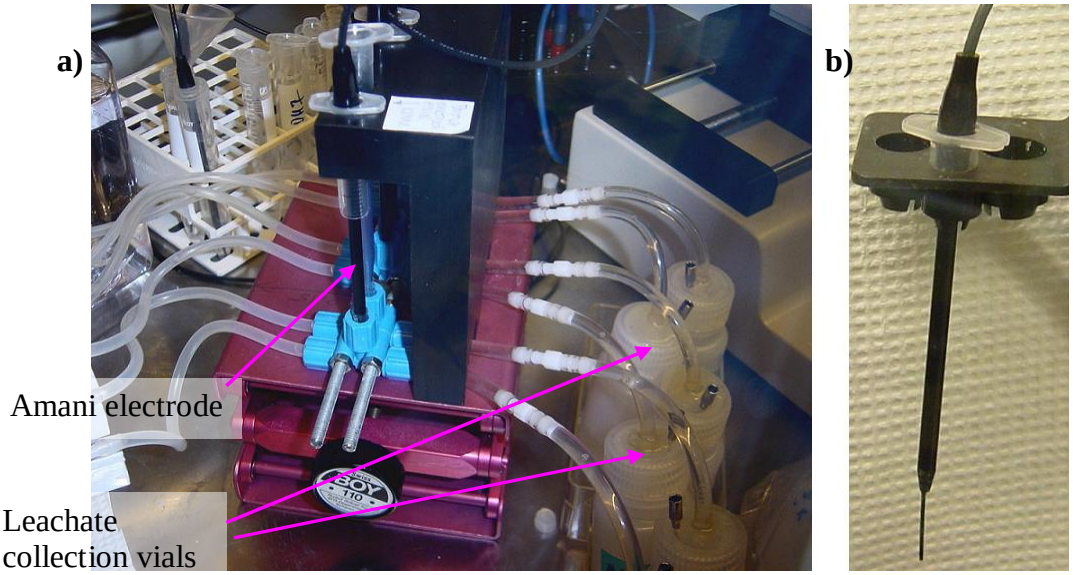

Figure 20. a) On-line potential measurement with amani 1000 electrodes and leachate collection, b) Amani 1000 electrode.

The beginning of the experiment run well, but after a couple of days some precipitate started to form in the experiment with faster flow and more in the case of saline leachate (Figure 21). Later similar precipitates were also formed in the lower flow rate experiment. These precipitates caused some blockage of the flow. There were also some difficulties concerning the three-way syringe valves and the syringe pump itself. At some point it was noticed that the leaching solution flowed back to the feeding bottle instead of the sample syringes. Therefore the syringe valves had to be replaced with new ones. Towards the end of the experiment it became clear that the other syringe pump was not working properly. It was not able to move the syringe pistons and for some time it had to be operated manually, and finally the experiment was stopped.

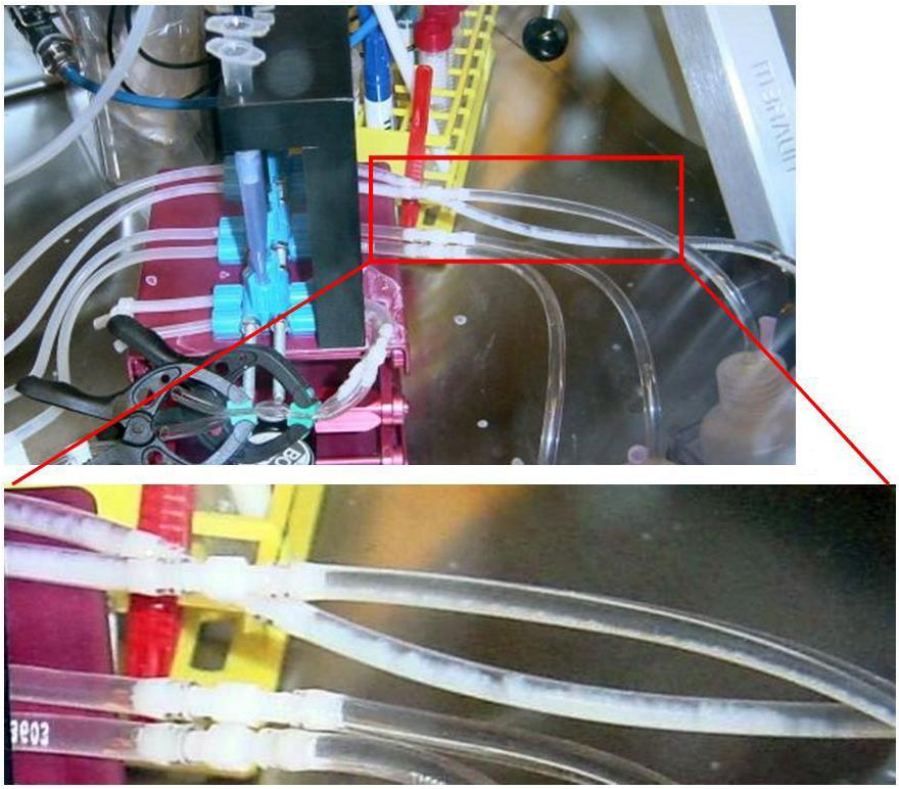

Figure 21. White precipitate in the tubing.

9 RESULTS

9.1 Leach solution results

Dynamic leach testing was continued up to 127 days. The analytical results of the cumulative concentrations of the soluble constituents from the grout samples are given in Figures A1 to A9 in Appendix 1 for both leachates and both flow rates.

9.1.1 pH results

The pH values were measured in both leachates at all sampling points. The results on pH measurement are shown in Figure 22 a-d. Some results from earlier static leach testing are included for comparison purposes (Figure 22 e-f).[1]

As would be expected the flow rate had an influence on the pH values obtained. Faster decrease of pH values was observed in the case of the higher flow-rate experiments, since with faster flow rate the leaching solution was renewed more often and the concentration gradient was greater between the solid sample and the leaching solution. This accelerates the dissolution of the ions from the sample specimen and further decreases the pH value. Similar decrease in pH was detected in both low- and medium-pH grout experiments (Figure 22 a-d). At the end of the leach testing minor decrease was observed in the leachates from the slower flow rate experiments in both fresh and saline leachates, excluding the saline leachates of the low-pH grout. The difference in pH values between the two grouts was greater in the saline leachate for both flow rates. Comparing the results gained from earlier static leach testing[1] the pH values showed faster decrease in the present dynamic leach testing, although the two leach tests are not directly comparable since they were performed at different temperatures which influence the reaction rates.

The influence of the two leachates, fresh and saline, was observed when the results from the experiment of same flow rate were compared. At the end, in the higher flow rate experiments, the pH values in the saline leachate samples were about 0.5 to 1.0 units lower compared to those of the fresh leachates. In the experiment with the lower flow rate (0.625 mL/h) the difference was even more notable. At both flow rates the pH values of the low-pH grouts in saline leachates decreased faster than those in the fresh leachate.

The low-pH grout leachates reached the target pH of 11 in all tests. The medium-pH grout also showed a decreasing trend in both leachates at the faster flow rate. However,

at the slower flow rate only a minor decrease was observed. At the end of the testing the pH values in the leachates were around 11 to 11.5.

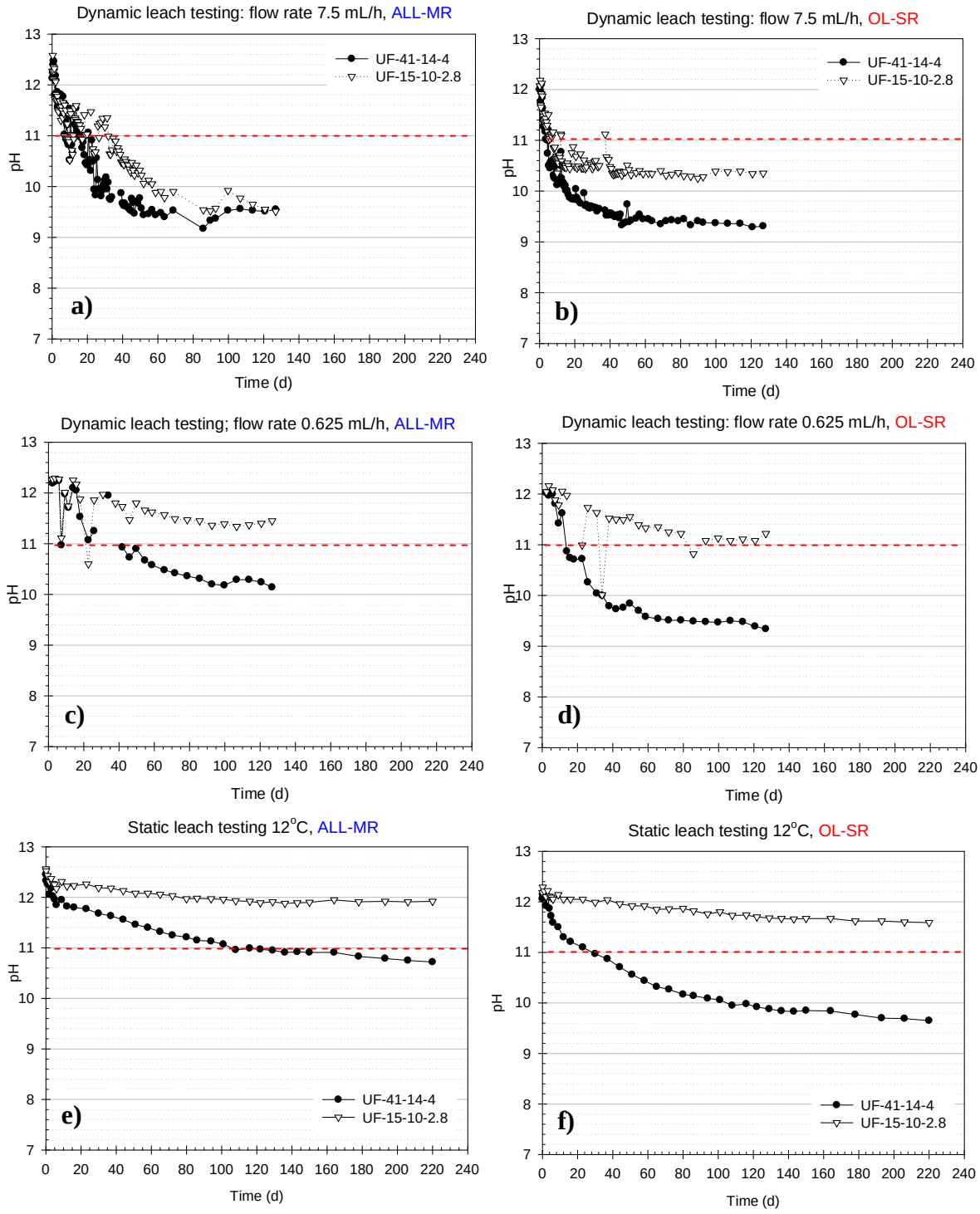

Figure 22. Leachate pH values in fresh (ALL-MR) and saline (OL-SR) leachates for dynamic (sub-figures a-d) and static leach testing (sub-figures e and f).

Due to the difficulties with syringe valves and pumps, the flow rates were not always constant. Some unexpected variation can be observed in the pH values between adjacent sampling points (Figure 22 a-d), which might have arisen from these malfunctions. There was a major temporary decrease in the pH values in the fresh leachates at faster flow around 70 to 80 days time period. The same drop in the pH values was observed in both grout leachates. At the same time the concentrations of Ca, Na, Cl and Mg of the leachates increased substantially (Figure 23). The concentrations of these ions in saline leaching solution are considerably higher than in fresh solution (Table 8). In Table 9 are presented the calculated concentration ratios of Ca, Na, Cl and Mg in the leaching solutions (ALL-MR and OL-SR) and in the doubtful leachate samples. The comparison between the different solutions shows that the concentration ratios of the saline solution and those of the "erroneous" leachates are relatively equal contrary to the ratios of the fresh leaching solution. This indicates that the increase originated from the saline leaching solution introduced accidentally into the sample syringes and therefore four sampling points were excluded from the final results. The calculated ratios also imply precipitation of $MgCO_3$ and $CaCO_3$, since the Ca/Cl and Mg/Cl ratios in the leachates are lower compared to the saline solution. The fresh leaching solution contains 1.1×10^{-3} mol/L of HCO_3^- which can react with Mg and Ca ions present in the solution. The amount of leaching solution flowed through the sample syringes during that time period was around 1.5 L per sample specimen.

Table 9. Calculated concentration ratios of Ca, Na, Mg and Cl in fresh leaching solutions and in the first "erroneous" sampling point (Figure 23) showing high contents of those ions.

Ratio	**ALL-MR**	**OL-SR**	**Leachates**	
			UF-41-14-4	**UF-15-10-2.8**
Na/Ca	17.69	2.10	2.48	3.24
Ca/Mg	4.33	43.48	53.52	47.06
Mg/Cl	0.0214	0.0056	0.0049	0.0053
Na/Cl	1.64	0.51	0.46	0.47
Ca/Cl	0.09	0.24	0.23	0.20

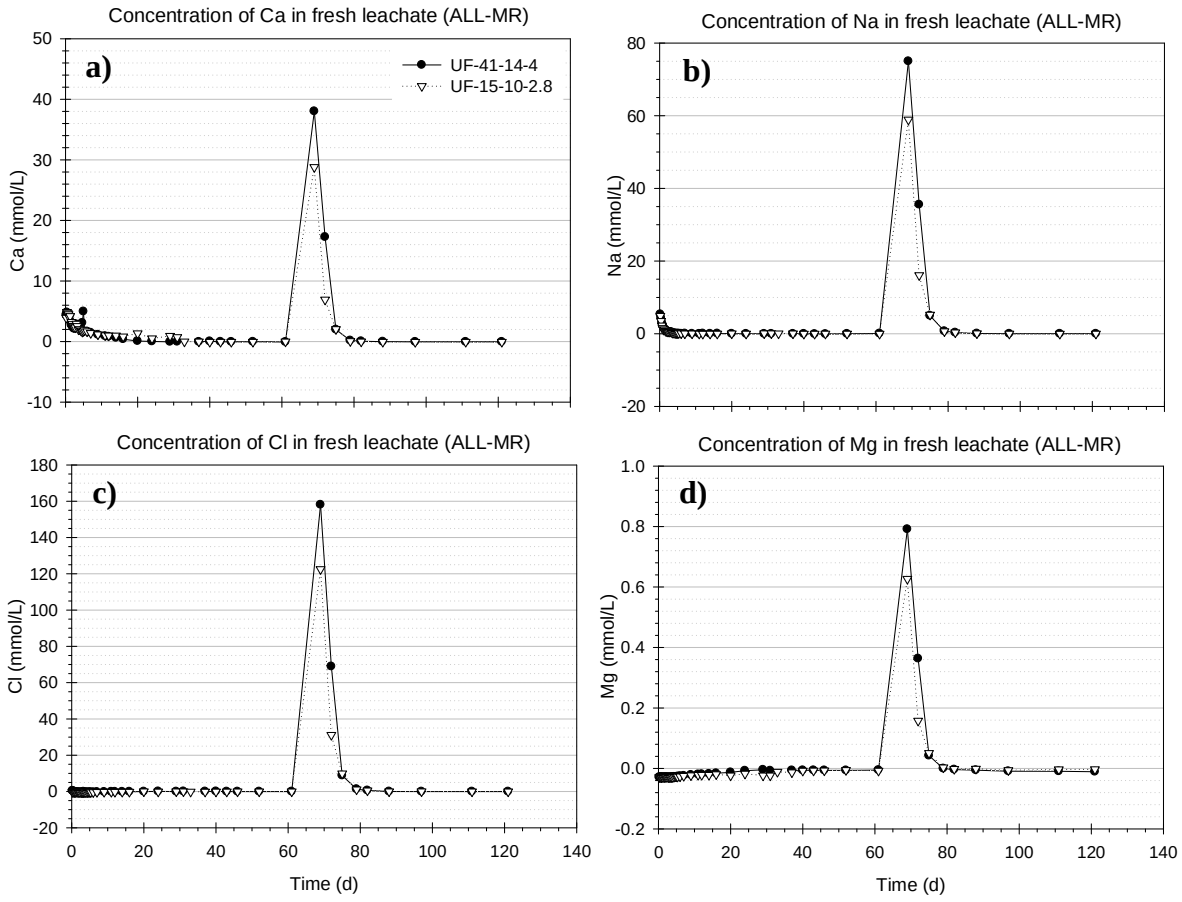

Figure 23. Concentrations of Ca, Na, Cl and Mg in fresh leachates at flow rate 7.5 mL/h. (Note! The legend applies to all the sub-figures.)

The total release of OH^- -ions into the leachates (Table 10) was estimated based on the pH values measured at each sampling point except the four leachate samples in fresh leaching solution at higher flow rate that were ruled out. Also the results from earlier static leach testing are included for comparison purposes.[1] The each specimen in the earlier static leach testing was leached with 1 050 mL of leaching solution. In the present dynamic leach testing the total amount of the leaching solution was 13 600 mL for the higher flow rate and 1 390 mL for the slower flow rate respectively. The pH values were measured in the glove-box at 22 °C temperatures in both experiments. In both experiments the total amount of OH^- ions released was higher in the case of medium-pH grout samples as would be expected, since the medium-pH grout mix contains more portlandite compared to the low-pH one. The comparison between the two leaching solutions showed that more OH^- ions were released from the grout specimens leached with the fresh (ALL-MR) solution. The influence of flow rate

seemed obvious. The release at higher flow rate was at least two times higher compared to the slower in all the experiments. At higher flow rate the leaching solution was more frequently renewed increasing the leaching rate of the cement components.

Table 10. Estimated total release of OH^- ions from each grout specimen in the two leaching experiment (dynamic and static).

		Dynamic leach testing		**Static leach testing**	
Specimen ID		**OH^-**(mmol)		**OH^-**(mmol)	
		higher flow rate	slower flow rate	Temp. 12°C	Temp. 50°C
		ALL-MR			
UF-15-10-2.8	medium-pH	15.4	7.5	9.9	12.2
UF-41-14-4	low-pH	14.2	3.6	3.8	1.1
		OL-SR			
UF-15-10-2.8	low-pH	8.0	4.6	6.2	5.8
UF-41-14-4	low-pH	4.2	1.4	1.8	0.3

Amani 1000 electrodes were used to monitor on-line changes in the mV values during testing. The data was collected with a 16 channel mV measuring instrumentation. Some interferences can be seen in the graphs (Figure 24 a-d) which were partly due to disturbances caused by exchanging the sample collection vials and/or working in the glove-box causing pressure changes as well as disturbing the solution flows, especially when precipitates were present in the tubings. A general observation it can be stated that the experiment with slower flow was more susceptible to interferences.

The comparison between the Amani 1000 and Ross electrodes was quite difficult, because it seemed that there was no correlation between the obtained values. Amani electrodes as well as Ross electrode were calibrated on regular basis. Figure A 1 a–h and Figure A 2 a–b in Appendix 1 present the calibration curves for the Amani 1000 electrodes and Ross electrodes in commercial buffer solutions during the experiment. The slopes of the graphs of Amani electrodes (Table A 1 a in Appendix 1) were quite far from the theoretical value at 20 °C, 58.16 mV/pH unit (Table A 3 in Appendix 5). Amani electrodes A1, A2, A5, and A6 were in the saline leachates (OL-SR) and electrodes A3, A4, A7, and A8 in the fresh leachates (ALL-MR). Two of the electrodes (A1 and A6 in Figure A 1) were relatively constant during the experiment, although

there are fluctuations between different calibration curves. Other electrodes showed more drifting. The calibration curves of Ross glass electrodes seemed better (Figure A 2 a and b in Appendix 1). The slopes (Table A 1 b in Appendix 1) were relatively close to the theoretical value at 22 °C, 58.56 mV/pH unit (Table A 3 in Appendix 5).

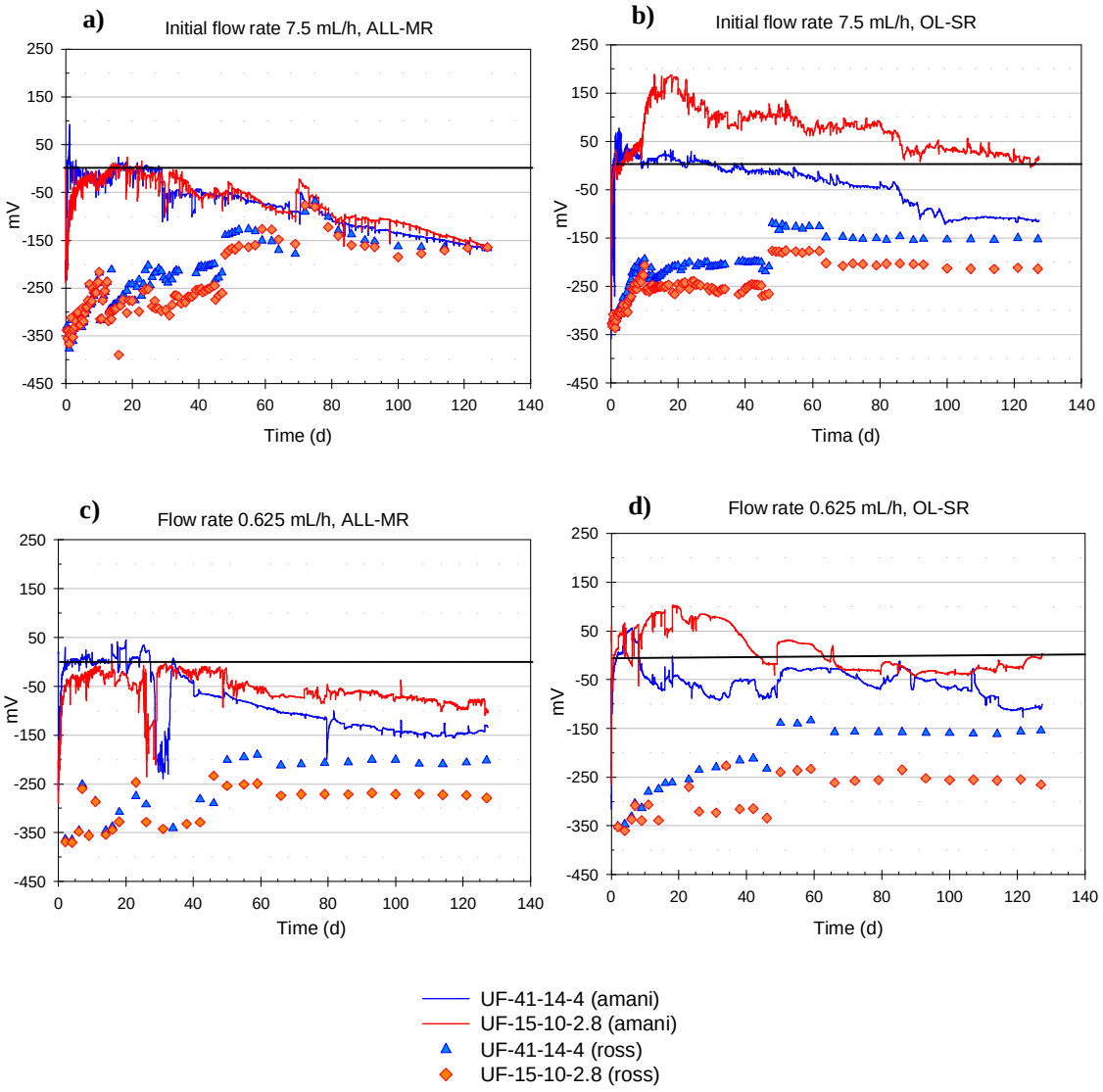

Figure 24. mV measurement of leachates with Ross and Amani 1000 electrodes.

9.1.2 Chemical analysis of leachates

The analysed substances were Na, K, Ca, Mg, Al, Cl^-, SO_4^{2-}, S_{TOT} and Fe. Ion chromatography (IC) was used for the determination of Cl^- and SO_4^{2-} concentrations; K was determined by Flame Atomic Absorption Spectrometry (FAAS) and the rest by

Inductively Coupled Plasma Atomic Emission Spectrometry (ICP-AES). The analyses were performed at VTT.

In all the leachate samples the results of Al and Fe were below the detection limits (for Al 0.1–1.0 mg/L and for Fe 0.02 mg/L). In the experiment with the slower flow rate the initial Mg concentration in both leachates was below the detection limit, but increased during the leach testing. The general observation was that Mg was absorbed or precipitated instead of remaining in the leaching solutions.

As mentioned before in chapter 9.1.1 (page 73) a sudden decrease in the pH values was observed in fresh leachates in higher flow rate around 70 to 80 days and at the same time the concentrations of Ca, Na, Cl and Mg increased considerably. It was deduced that some saline leaching solution instead of fresh one had been introduced into the sample syringes during that time period Due to these rather logical reasons four sampling points were excluded from the results.

Calcium (Ca)

Decrease of Ca content was observed in the beginning of the test in saline leachates at both flow rates (Figure A 3 Appendix 2). Some white precipitation was observed on the surface of the grout samples and in the tubes. This could be part of the explanation of the depletion of calcium from the initial leaching solution. As the leaching of the cement paste proceeds the portlandite starts to dissolve. This increases the concentration of Ca^{2+} and OH^- ions in the liquid phase and leads to the precipitation of $Ca(OH)_2$ (K_{sp} = 7.5×10^{-6} at 25 °C). In the fresh leachates quite fast release was observed in the beginning of the experiment but levelled out rather quickly. This is probably related to the dissolution of portlandite after the alkaline hydroxides are leached from the grout specimens.

Sodium (Na)

Sodium results are shown in Figure A 4 Appendix 2. In fresh leachate Na release was quite similar at both flow rates. Sodium release increased faster in the short period in the beginning of testing and declined later. This supports the fact that alkali hydroxides are highly soluble and easily dissolved.

Contrary to the fresh leachates the results of saline leachates showed depletion of sodium from the initial leaching solution indicating possible diffusion into the grout samples. Depletion was more significant at faster flow rate. At the slower flow rate Na

concentration in both leachates was quite constant throughout the experiment. A slight increase was observed towards the end of testing.

Potassium (K)

Potassium release in both fresh and saline leachates was quite similar (Figure A 5 Appendix 2). In both leachates and at both flow rates the amount of K released was higher in the case of medium-pH grout samples. The influence of the flow rate was not that noticeable in K leaching.

Depletion of both K and Na from the grout specimens was detected also in the chemical analysis (Table 21 and Table 22). Overall, the release patterns of these ions were quite similar except Na in saline leaching solution.

Chloride (Cl)

Absorption of Cl was observed and it was more significant in the case of the saline leachate (Figure A 6 Appendix 2). The saline leaching solution contains much more Cl than the fresh leaching solution (Table 8). Chloride ion diffusion rates are dependent on the water/cement ratio and cement type. The diffusivities lie in the range $0.1–0.2\times10^{-12}$ m^2/s.[23] The physical processes involved in the movement of chloride ions within cement-based materials appear to be closer to exchange of chloride for hydroxyl than to simple diffusion. It has been proposed (e.g. Jones *et al.*[57] and Suryavanshi *et al.*[58]) different mechanisms for the formation of Friedel's salt ($3\ CaO\cdot Al_2O_3\cdot 1/2CaCl_2\cdot 10H_2O$). Dissolution/precipitation and ion exchange contribute to the chloride binding to the solid phase. The lower concentration of free OH^- ions in the blended cement pastes decreases the diffusion of chloride ions due to smaller $OH^- – Cl^-$ exchange capacity. Some proportion of chloride ions might also be present in the pore solution as "free" Cl^- ions.[59]

In the present experiment the effect of the W/DM ratio on the diffusion can also be observed, although this might not be the only explanation. In all cases the absorption of chloride ions is lower on low-pH grouts which have higher W/DM ratio and lower OH^- ion concentration. In the fresh leachates at both flow rates the depletion of Cl is quite small and the concentration in leachates is constant during the experiment.

Sulphate (SO_4^{2-}) and S_{TOT}

A difference between the two leaching solutions was observed. Higher amount of sulphate was released into the saline leachates (Figure A 7 Appendix 2). The results of

fresh leachates showed depletion of SO_4^{2-} as compared to the initial leaching solution in the beginning of testing. After this initial absorption period sulphate was released into the leaching solution especially from low-pH grouts. In the case of medium-pH grout the concentration of leachates stayed at constant level. Generally the low-pH grout released more sulphate than the medium-pH grout.

A quite steady release of sulphate was observed in saline leachates. In the case of medium-pH grout the release was quite small but in the case of low-pH samples the release was more prominent.

Quite similar results were obtained for total sulphur compared to sulphate (Figure A 8 Appendix 2). In both leachates and at both flow rates the release of sulphur from medium-pH grout samples was small. Some absorption of sulphur was observed in the beginning of the test in the fresh leachates.

Silicon (Si)

Silicon results are shown in Figure A 9 Appendix 2. The release of Si between the two grout types correlated with the amount of silica fume in the pastes; higher release of Si from the low-pH grout compared to the medium-pH grout. Si was quite steadily released from low-pH grout into fresh leaching solution during the testing. Dissolution of Si was slightly greater in fresh leaching solution.

An interesting feature was observed in the saline leachates at slower flow rate. A fast initial release of Si was observed. Contrary to the other result a higher amount of Si was released from the medium-pH grout specimen.

Magnesium (Mg)

The general observation is that Mg was absorbed instead of remaining in the leaching solution (Figure A 10 Appendix 2). Absorption of Mg may be due to precipitation of brucite ($Mg(OH)_2$). The pH values of the leachates were high enough (9–10) to brucite to precipitate. Also absorption by CSH gel may also be potential explanation.

In the beginning of the testing the Mg values in the fresh leachate samples were below the detection limit. The results of saline leachates showed higher depletion of Mg from the initial leaching solution. This was an expected result as the saline leaching solution contains much more Mg than fresh solution (Table 8).

Ca/Si

Figure A 11 in Appendix 2 shows the cumulative concentration ratio of Ca/Si. Only in the fresh leachate the results were presentable. During the first ten days of testing calcium release in the fresh leachates was high and the Ca/Si ratio in the leachates increased fast. After an initial high release of Ca the ratio reached a rather steady value but the dissolution of Si into the leachates continued quite steadily and as a result the Ca/Si ratio started to decrease. The difference between the grout types was obvious the Ca/Si ratio was higher in the medium-pH grout leachates.

9.1.3 Total organic carbon (TOC)

The amount of total organic carbon in some leachate samples was determined by using Shimanzu TOC-5000A analyser. The samples for analysis were chosen from the beginning, the middle and the end periods of testing in order to assess the leaching behaviour of possible organic substances (Table 11). The results of TOC analysis are presented in Figure 25. The results show that organic compounds were released in the beginning of testing. The concentration of organics in the leachates decreased and levelled out quite quickly. A clear difference between the two leachates, fresh and saline, was observed. In saline leachates the amount of organic carbon was greater at both flow rates, roughly estimated two times greater. The influence of the flow rate was also significant. The amount of organic carbon in leachates from the slower flow rate was around two times higher compared to the faster flow rate. The difference between the two grout types was noticeable at flow rate 0.625 mL/h. The amount of organic carbon released from medium-pH grout samples was higher compared to low-pH grout. At higher flow rate the difference was quite minor between the two grout types.

Table 11 a,b. The leachate samples selected to the TOC analysis.

a)

Flow rate 7.5 mL/h	
Sampling point	**Time (d)**
1	0.2
2	0.4
3	0.7
7	1.6
21-26	7
85-91	43
102-105	61
113-114	97
117	127

b)

Flow rate 0.625 mL/h	
Sampling point	**Time (d)**
1	2
(7-)8	16
14-16	42
21-22	76
26-27	110

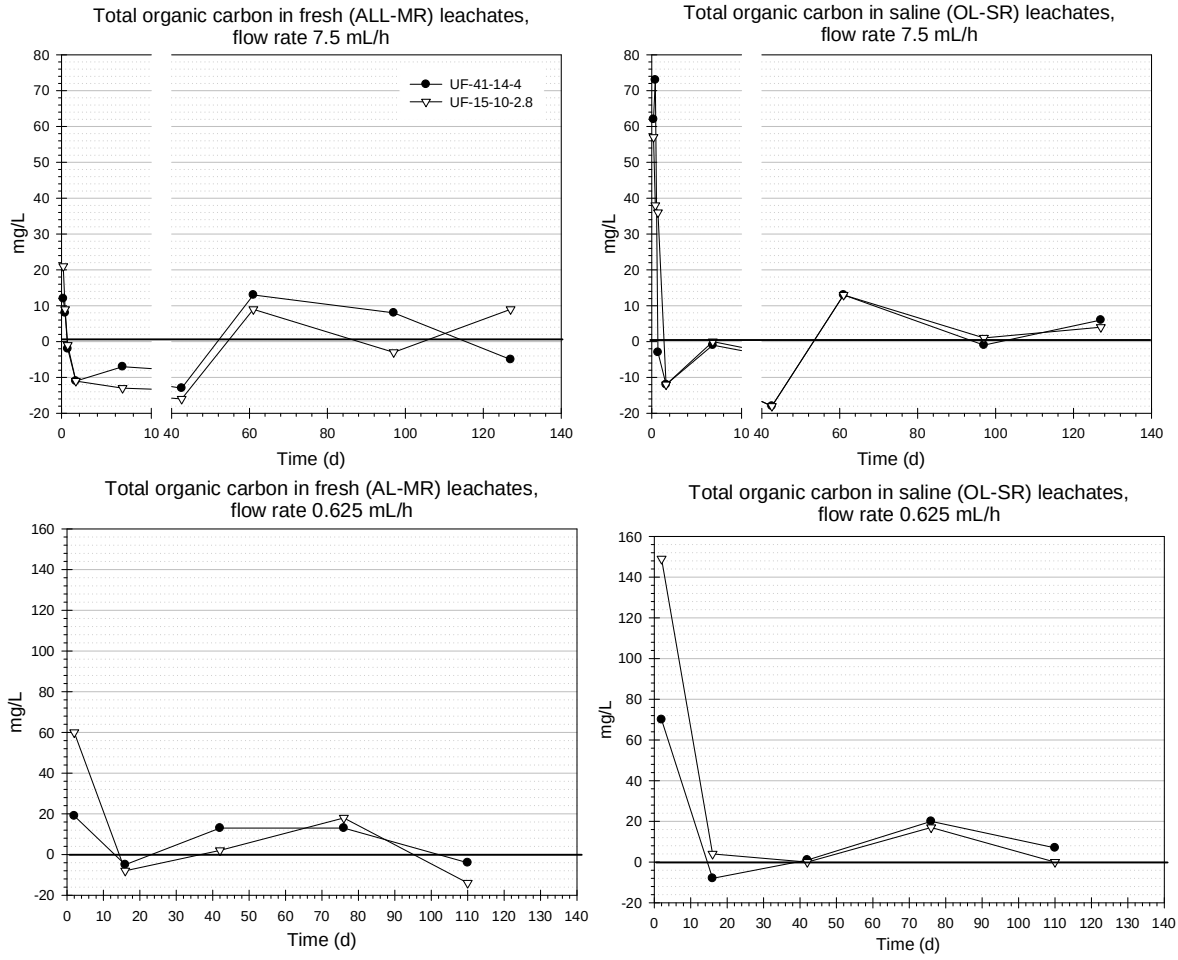

Figure 25. Cumulative results from the total organic carbon (TOC) analysis in fresh and saline leachates at both flow rates. (Note! The legend applies to all subfigures. Different scale in diagrams.)

9.2 Results from solid analyses

After completing the leaching test the grout containing syringes were detached from the system and the out-flow end of the grout specimens were photographed (Figure 26). The upper row shows the specimens leached with the higher flow rate and the lower row specimens leached with the lower flow rate. In some of the specimens different layers can be distinguished, due to the interaction with the leaching solutions. Based on the pictures it can be noticed that the alteration zone in specimens leached with the higher flow rate was more extensive, which implied that the flow rate has had an effect on the leaching process. However, the difference between the two grout types was not quite that clear. In both grout specimens leached with the saline leaching solution with higher flow rate the altered zone appeared to be quite similar. Although in the specimens leached with lower flow rate more definite alteration was detected in low-pH specimen. This was probably due to the fact that the saline leaching solution has been more aggressive leaching agent.

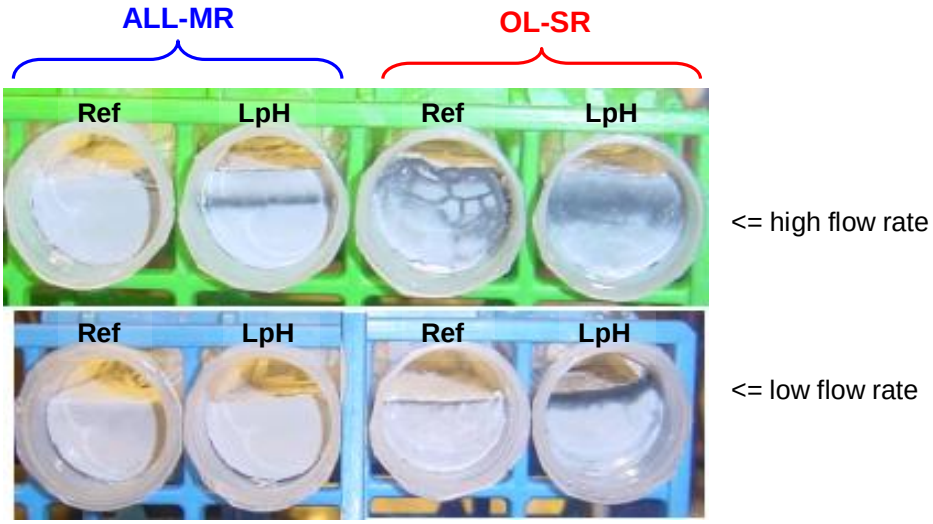

Figure 26. Top line, grout samples leached with higher flow rate (7.5 ml/h) and bottom line, grout samples leached with lower flow rate (0.625 ml/h) (LpH = UF-41-14-4 and Ref = UF-15-10-2.8).

The chemical and mineral composition of the solid samples was analysed by X-Ray Diffractometry (XRD), thermal analysis (TG/DTA) and X-Ray Fluorescence (XRF). The sample syringes were packed inside the glove-box in order to minimise the effects of CO_2 and sent for analyses. First the samples were dried for 14 days at 22 °C inside an exsiccator under vacuum of 20 mmHg. After drying the samples were removed from the syringes and divided in half. The other halves of the samples were then dried further for

7 days at 105 °C in a heating chamber and then split so that the surface layer that had been in contact with the leach solution was separated from the lower layer of the sample. Finally, all the samples were pulverised and subjected to analyses.

9.2.1 Thermal analysis results (TG/DTA)

The TG/TDA analyses were performed with a Mettler TGA 851e –thermobalance. Table 12 gives the analytical parameters of the analyses.

Table 12. The analytical parameters of the TG/DTA analyses.

	UF-41-14-4 / ALL-MR		**UF-15-10-2.8 / ALL-MR**	
(mg)	**N** (7.5 ml/h)	**H** (0.625 ml/h)	**N** (7.5 ml/h)	**H** (0.625 ml/h)
Surface	31.11	33.53	40.79	45.52
Base	34.34	30.25	48.57	49.58
	UF-41-14-4 / OL-SR		**UF-15-10-2.8 / OL-SR**	
	N	**H**	**N**	**H**
Surface	34.97	35.12	46.07	50.87
Base	38.57	35.67	45.69	54.85
atmosphere	air, 50 ml/min			
crucible	Al_2O_3, 150 µl			
heating rate (°C/min)	5			
max temperature (°C)	1 000			

The thermal behaviour of the low-pH grout specimens (UF-41-14-4) was quite similar in all experiments (both leachates and flow rates). Seven successive phases were detected during degradation reactions causing mass loss. The temperature areas of the various phases and the mass losses registered are presented in Table 13 and in Table 14. The thermal curves of the samples are shown in Appendix 3.

The first degradation phase was caused by the evaporation of free moisture still contained in the specimens and by the volatilization of chemically bound water resulting from the disintegration of the C-S-H gel and the AFt- and AFM-phases. It should be noticed that some free water, about 0.5 wt-%, was already evaporated from the samples before the actual thermal analyses were started which could be seen in such a way that the TG-curves did not start from 100 %.

The second and the third phases were probably due to disintegration of the hydration products, mainly of silicate hydrates but possibly also of C-A-H gel, even if the cement used in the grouts was sulphate resistant and, thus, contained only small amounts of

aluminate phase. The burning of the plasticizer used could also explain part of the mass loss taking place during these phases.

It should be noticed that sample specimens UF-41-14-4 did not contain calcium hydroxide. An intensive exothermic peak in the DTA-curves was detected in the samples leached with fresh (ALL-MR) solution at around 850 °C referring to the fact that the samples still contained considerable amounts of unhydrated amorphous silica. At the same time, no exothermic peaks could be detected in the DTA-curves of the samples leached with saline solution. Consequently, the mass loss at high temperatures was also relatively low in samples leached with fresh solution and high in samples leached with saline solution.

The rest of the phases were probably connected to the degradation of very heat-resistant forms of CSH gel. However, part of the mass loss in question could be caused by the decomposition of calcite ($CaCO_3$) assuming that the cement used in the grouts contained some pulverized limestone. It is also presumable that some calcite had been precipitated during the experiment, since the fresh leaching solution contains HCO_3^- which reacts with Ca^{2+} ions present in the liquid phase. The calcite decomposition is probably connected to the sixth phase. In general, the amount of calcite in the samples leached with the saline leaching solution was higher than in the samples leached with the fresh solution, excluding the base samples of the medium-pH grouts.

Table 13. Thermal degradation of the low-pH grout in fresh (ALL-MR) solution.

Phase	**Temperature**	**Mass loss (w-%)**			
		N/surface	**N/base**	**H/surface**	**H/base**
I	25-135	5.27	7.04	5.66	7.17
II	135-290	5.03	5.61	5.64	5.83
III	290-395	1.92	2.26	1.83	2.21
IV	395-560	1.81	1.76	1.87	1.84
V	560-685	0.66	0.56	0.53	0.55
VI	685-810	0.92	0.87	0.89	0.92
VII	810-980	0.10	0.15	0.10	0.21
Total mass loss		15.71	18.25	16.52	18.73

Table 14. Thermal degradation of the low-pH grout in saline (OL-SR) solution.

Phase	Temperature	Mass loss (w-%)			
		N/surface	N/base	H/surface	H/base
I	25-135	6.59	7.22	6.48	7.23
II	135-290	5.24	6.17	5.26	6.29
III	290-400	2.31	2.14	2.21	2.50
IV	400-545	1.67	1.36	1.69	1.39
V	545-725	1.39	1.44	1.48	1.60
VI	725-880	1.82	1.58	1.70	1.47
VII	880-980	0.82	1.28	0.98	1.21
Total mass loss		19.84	21.46	19.80	21.69

The thermal behaviour of the medium-pH grout specimens (UF-15-10-2.8) leached with the fresh leaching solution resembled closely the behaviour of the low-pH grouts (UF-41-14-4) described above. The thermal behaviour of the specimens leached with the saline leaching solution showed slightly different pattern. The mass loss during the first two phases was relatively smaller compared to the specimens leached with fresh leaching solution. The observation made from the medium-pH grout specimens could be divided either into eight (fresh leachate) or into nine (saline leachate) successive phases during which degradation reactions causing mass loss were detected.

The most obvious difference compared to the low-pH grout samples was that the medium-pH grout specimens contained calcium hydroxide, although no distinct reaction referring to calcium hydroxide could be found in the samples leached with saline solution. Some mass loss was registered in the temperature area normally connected to its decomposition. This means that specimens might still contain at least traces of hydroxide. The fourth phase in the degradation process of medium-pH grouts was mainly caused by the decomposition of $Ca(OH)_2$. The hydroxide content in the base samples was higher than in surface samples, which referred to the fact that hydroxide was leached out of the grouts during the test. On the other hand, the decrease in hydroxide content as a function of time in materials containing Portland cement is normal as it is consumed in the complex hydration reactions taking place. It should be noticed that the hydroxide content seemed to be somewhat higher in the samples that were leached with a low rate (code H in the tables) than in the samples that were leached with a high flow rate (code N in the tables).

In the samples leached with saline solution, there seemed to exist a distinct decomposition reaction at the area 250 °C – 360 °C (phase IV), which could not be

found in the samples leached with fresh solution. This reaction was probably connected to the decomposition of the (possibly) chlorine containing calcium aluminate hydrate that was detected in the XRD study of the samples.

The fact that the mass losses of the medium-pH grouts leached with the saline leaching solution were lower during the two first phases than corresponding mass losses in specimens leached with fresh leaching solution indicated that the amount of chemically bound water and free moisture was lower in the specimens leached with the saline solution.

An exothermic phenomenon was observed at 880 °C – 900 °C in the medium-pH grout specimens leached with fresh (ALL-MR) solution. This phenomenon was probably due to crystallization of amorphous silica that had not been reacted during the hydration process. In samples leached with saline solution this phenomenon was not observed, but an exceptionally high mass loss at temperatures > 700 °C, which refers to a high content of very heat-resistant hydration products in these specimens.

Table 15. Thermal degradation of the medium-pH grout in fresh (ALL-MR) solution.

Phase	**Temperature**	**Mass loss (w-%)**			
		N/surface	**N/base**	**H/surface**	**H/base**
I	25-125	4.25	3.36	5.11	4.43
II	125-300	6.63	7.03	6.90	8.02
III	300-420	3.16	2.80	2.97	2.89
IV	420-470	0.60	1.18	0.81	1.47
V	470-570	1.10	0.65	1.12	0.58
VI	570-680	0.85	1.74	0.99	2.15
VII	680-820	0.90	0.69	0.96	0.76
VIII	820-980	0.36	0.73	0.38	0.60
Total mass loss		17.85	18.18	19.24	20.90

Table 16. Thermal degradation of the medium-pH grout in saline (OL-SR) solution.

Phase	Temperature	Mass loss (w-%)			
		N/surface	N/base	H/surface	H/base
I	25-90	3.54	3.52	2.98	3.52
II	90-140	3.38	3.99	3.66	4.19
III	140-250	5.28	4.88	4.65	4.47
IV	250-360	3.38	4.01	4.18	4.06
V	360-515	3.36	3.25	2.84	3.19
VI	515-620	1.15	1.39	1.24	1.22
VII	620-705	0.95	0.88	0.81	0.79
VIII	705-900	2.14	2.19	2.26	2.16
IX	900-980	0.84	0.91	0.75	0.80
Total mass loss		24.02	25.02	23.37	24.40

The total mass losses of the grout samples including the portions evaporated before the actual beginning of the thermal analysis are presented in Table 17 and in Table 18. Also the mass losses after the first degradation phase, i.e. after about 130 °C, are presented in the tables. In addition, Table 17 and Table 18 contain amount of calcium hydroxide in the samples. This was calculated by assuming that all the mass loss in the temperature area 400 °C – 500 °C resulted from the disintegration of calcium hydroxide leading to evaporation of the hydroxide water. However, this was done only to the specimens whose DTG- and DTA- curves showed a clear sign of a separate reaction in the area. Still it should be noticed that some of the mass loss in that area was caused by other factors, such as degradation of C-S-H gel, which means that the values presented for calcium hydroxide in Table 17 and in Table 18 are probably a little too high.

Table 17. Total mass loss, mass loss after 130 °C and $Ca(OH)_2$ content of low-pH grout in both leachates according to thermal analysis.

Leaching solution	Analysed area	total mass loss wt-%	mass loss after 130 °C wt-%	$Ca(OH)_2$ wt-%
ALL-MR				
N (7.5 ml/h)	**surface**	16.3	5.82	-
	base	18.6	7.42	-
H (0.625 ml/h)	**surface**	16.9	5.99	-
	base	19.2	7.66	-
OL-SR				
N (7.5 ml/h)	**surface**	20.3	7.01	-
	base	22.0	7.74	-
H (0.625 ml/h)	**surface**	20.2	6.87	-
	base	22.1	7.65	-

Table 18. Total mass loss, mass loss after 130 °C and $Ca(OH)_2$ content of medium-pH grout in both leachates according to thermal analysis.

Leaching solution	**Analysed area**	**total mass loss wt-%**	**mass loss after 130 °C wt-%**	**$Ca(OH)_2$ wt-%**
ALL-MR				
N (7.5 ml/h)	**surface**	18.0	4.39	2.5
	base	18.3	3.44	4.9
H (0.625 ml/h)	**surface**	19.6	5.46	3.3
	base	21.2	4.76	6.0
OL-SR				
N (7.5 ml/h)	**surface**	24.4	7.34	-
	base	25.4	7.89	-
H (0.625 ml/h)	**surface**	23.7	7.00	-
	base	24.7	8.02	-

9.2.2 Mineral composition of grout specimens (XRD)

The XRD analyses were performed with a Philips PW 1710 –diffractometer by using CuK_α -radiation. A spectrum between 5°–65° (2θ) was produced with a voltage of 50 kV and a current strength of 20 mA.

According to the XRD results all the sample grouts were mainly amorphous and, thus, contained only relatively small amounts of crystalline compounds. The amorphous phase forming most of the samples composed most likely of calcium silicate hydrate gel resulting from the hydration reactions of cement and silica fume with water. The summary of the contents of the crystalline compounds in the samples are presented in Table 19 and in Table 20 and the XRD– diagrams of the injection grout samples in Appendix 4.

Table 19. The content of the crystalline compounds in low-pH grout.

Leaching solution	**Analysed area**	**$Ca(OH)_2$**	**C-S-H**	**C_4AF**	**AFt**	**AFm**	**Ca-Al-Cl**	**$C_{2/3}S/CaCO_3$**
ALL-MR								
N (7.5 ml/h)	**surface**	(+)	++	-	-	-	-	(+)
	base	(+)	++	-	-	-	-	(+)
H (0.625 ml/h)	**surface**	(+)	++	-	-	-	-	(+)
	base	-	++	-	-	-	-	(+)
OL-SR								
N (7.5 ml/h)	**surface**	-	++	-	-	-	-	(+)
	base	-	++	-	-	-	-	(+)
H (0.625 ml/h)	**surface**	-	++	-	-	-	-	(+)
	base	-	++	-	-	-	-	(+)
+++ strong		++ medium		+ weak				
(+) very weak		- not detected						

Table 20. The content of the crystalline compounds in medium-pH grout.

Leaching solution	**Analysed area**	**$Ca(OH)_2$**	**C-S-H**	**C_4AF**	**AFt**	**AFm**	**Ca-Al-Cl**	**$C_{2/3}S/CaCO_3$**
ALL-MR								
N (7.5 ml/h)	**surface**	+	++	-	-	-	-	(+)
	base	++	++	-	-	-	-	(+)
H (0.625 ml/h)	**surface**	+	++	(+)	-	-	-	(+)
	base	++	++	-	-	-	-	(+)
OL-SR								
N (7.5 ml/h)	**surface**	-	++	-	-	-	+	(+)
	base	-	++	-	-	-	+	(+)
H (0.625 ml/h)	**surface**	-	++	-	-	-	+	(+)
	base	-	++	-	-	-	+	(+)
+++ strong		++ medium		+ weak				
(+) very weak		- not detected						

All the samples contained crystalline calcium silicate hydrates. Although their contents were low, they were the main crystalline compounds in all samples, possibly excluding the two base samples from medium-pH grout after leaching with fresh leaching solution (ALL-MR). According to the XRD reflections it is impossible to exactly identify the composition of these hydrates. It seems that their structure is of type $Ca_3(Al,Fe)_2(SiO_4)(OH)_8$ and/or $Ca_{1.5}SiO_{3.5} \times H_2O$. The results would indicate that the compounds detected in the samples would rather be of the latter type.

Portlandite ($Ca(OH)_2$) was detected in all the samples of medium-pH grout leached with fresh leaching solution (ALL-MR). According to the diagrams it is possible that also the low-pH grout samples leached with the same solution contained some portlandite, but even if that was the case its content was very low. As a whole, the amount of calcium hydroxide in the samples was much lower than the level that could have been expected on the basis of their composition (Table 6). It seems that hydroxide was leached out from the grouts during the test and also that the addition of silica fume had reduced the amount of calcium hydroxide in the hydrated cement paste. Part of the diminishing of the hydroxide in the samples could also be due to the normal ageing of the materials.

According to the XRD diagrams it seems obvious that none of the samples contained unhydrated cement minerals. Only in one sample traces of tetra calcium aluminate ferrite (C_4AF) could probably be detected. It is possible that samples contained some calcite, i.e. calcium carbonate. Calcite probably originated from the initial cement used. There is also a strong possibility that Ca^{2+} ions present in the solution phase have reacted with HCO_3^- introduced by the fresh leaching solution and precipitated as calcite.

None of the samples contained AFt phase (i.e. ettringite, $Ca_6Al_2(OH)_{12}(SO_4)_3 \cdot 26H_2O$) or AFm phase (i.e. monosulpfate, $Ca_4Al_2(OH)_{12}(SO_4) \cdot 6H_2O$). Nor was quartz ($SiO_2$) which is sometimes observed with materials containing high amounts of silica such as the low-pH grout mix.

The medium-pH grout samples leached with saline solution contained some crystalline compound that could not be detected in other samples. According to the reflections of the diffraction diagrams the compound in question was a calcium aluminate hydrate, either of the type $Ca_2Al(OH)_7 \cdot 3H_2O$ (hydrocalumite) or, more probably, of chloride containing $Ca_4Al_2O_6Cl_2 \cdot 10H_2O$.

9.2.3 Chemical composition of the grout specimens (XRF)

The XRF analyses were performed with a Philips PW 2404 –spectrometer by using a semi quantitative SemiQ –programme. Fluorine (Z = 9) and all the elements heavier than it excluding the noble gasses were determined. The detection limit of the method was about 0.01 %. The mass losses of the samples in the drying process and in the thermal analysis performed were taken into account when calculating the results of the analyses. The chemical composition of injection grouts is presented in Table 21 and in Table 22. The main components are presented in oxide form, the auxiliary components in element form.

Table 21. Chemical composition of the low-pH grout samples (UF-41-14-4).

	ALL-MR				**OL-SR**			
	H		**N**		**H**		**N**	
	surface	**base**	**surface**	**base**	**surface**	**base**	**surface**	**base**
	wt-%	**wt-%**	**wt-%**	**wt-%**	**wt-%**	**wt-%**	**wt-%**	**wt-%**
	29.3	28.5	23.8	27.6	25.3	23.4	22.8	24.1
CaO	0.56	0.50	0.76	0.51	0.80	0.44	1.23	0.45
MgO	38.3	34.5	44.6	36.2	32.9	29.4	34.8	30.2
SiO_2	1.84	1.59	2.18	1.73	1.52	1.36	1.80	1.39
Al_2O_3	0.08	0.05	0.17	0.09	0.90	0.54	1.10	0.55
Na_2O	0.13	0.15	0.22	0.13	0.08	0.11	0.09	0.09
K_2O	2.66	2.31	3.09	2.22	2.29	1.79	2.33	1.84
Fe_2O_3	1.27	1.38	1.13	1.39	1.00	1.18	0.95	1.20
SO_3	0.04	0.03	0.04	0.03	0.03	0.02	0.03	0.02
P	0.04	0.06	0.05	0.08	1.94	1.61	2.10	1.66
Cl	0.07	0.07	0.10	0.07	0.07	0.05	0.07	0.06
Ti	0.07	0.07	0.10	0.07	0.07	0.05	0.07	0.06
Cr	-	-	-	0.01	-	0.01	-	-
Mn	0.13	0.12	0.15	0.12	0.11	0.10	0.12	0.09
Zn	0.01	0.01	0.02	0.01	0.01	0.01	0.01	0.01
Sr	0.01	0.01	0.01	0.01	0.03	0.02	0.03	0.01
Zr	0.01	-	0.01	0.01	0.01	0.01	0.01	0.01
Ba	-	-	-	-	-	-	-	-
Br	-	-	-	-	0.03	0.02	0.03	0.02
l.o.i.-1	8.47	10.7	6.55	10.9	12.9	18.2	11.9	16.6
l.o.i.-2	16.9	19.2	16.3	18.6	20.2	22.1	20.3	22.0
Total	99.82	99.18	99.18	99.71	100.12	100.37	99.70	100.30

l.o.i.–1 The mass loss of the sample powder as it was dried at 105 °C in a heating chamber.
l.o.i.–2 The mass loss of the sample powder in thermal analysis at 1000 °C.

Table 22. Chemical composition of the medium-pH grout samples (UF-15-10-2.8).

	ALL-MR				**OL-SR**			
	H		**N**		**H**		**N**	
	surface	**base**	**surface**	**base**	**surface**	**base**	**surface**	**base**
	wt-%	**wt-%**	**wt-%**	**wt-%**	**wt-%**	**wt-%**	**wt-%**	**wt-%**
CaO	36.6	39.2	37.0	41.5	34.3	34.3	31.4	34.0
MgO	0.61	0.51	0.68	0.50	0.57	0.47	0.76	0.46
SiO_2	24.2	21.9	26.7	21.2	19.3	18.4	23.3	18.2
Al_2O_3	2.27	1.93	2.49	1.87	1.94	1.73	1.94	1.72
Na_2O	0.02	0.01	0.03	-	0.33	0.18	0.47	0.14
K_2O	0.03	0.03	0.05	0.03	0.03	0.03	0.03	0.02
Fe_2O_3	3.54	3.03	3.78	3.33	2.76	2.54	3.03	2.78
SO_3	1.77	1.54	2.02	1.57	1.45	1.32	1.41	1.29
P	0.04	0.03	0.04	0.04	0.03	0.02	0.03	0.03
Cl	0.06	0.12	0.14	0.31	2.96	2.88	2.50	3.04
Ti	0.11	0.10	0.12	0.10	0.10	0.08	0.09	0.09
Cr	-	0.01	0.01	0.01	0.01	0.01	0.01	0.01
Mn	0.17	0.15	0.18	0.18	0.14	0.13	0.14	0.14
Zn	0.01	0.01	0.01	0.01	0.01	0.01	0.01	0.01
Sr	0.01	0.02	0.01	0.02	0.01	0.02	0.02	0.02
Zr	0.01	-	0.01	0.01	0.01	0.01	0.01	0.01
Ba	-	0.03	-	-	-	-	-	-
Br	-	-	-	-	0.04	0.04	0.04	0.04
l.o.i.-1	9.69	10.5	8.64	11.1	11.9	14.1	11.5	13.8
l.o.i.-2	19.6	21.2	18.0	18.3	23.7	24.7	24.4	25.4
Total	98.74	100.32	99.91	100.08	99.59	100.97	101.09	101.20

l.o.i.–1 The mass loss of the sample powder as it was dried at 105 °C in a heating chamber.
l.o.i.–2 The mass loss of the sample powder in thermal analysis at 1000 °C.

According to the result of XRF analyses it seems that due to leaching the content of calcium diminished to some extent. The result was more distinct in the higher flow rate experiments where the content of CaO in the base samples was higher compared to the surface samples. The same effect could be seen more clearly in the content of potassium and also of sodium regarding the samples that had been exposed to fresh leaching solution (ALL-MR). On the other hand the content of chlorine, probably as chloride, was significantly higher in the samples that had been leached with saline solution (OL-SR). These samples contained also small amounts of bromine which is present in the saline solution as well.

In general, it seems that the saline leaching solution is more efficient leaching agent since the content of almost all components is higher in the samples leached with fresh solution. When comparing the surface and base samples of the same sample specimen it can be stated that more compounds have been leached from the surface. In general, it can be stated that the content of CaO and SO_3, was higher in the medium-pH specimens after leaching compared to the low-pH specimens. The results might have originated from the fact that the initial content of these compounds was higher in the medium-pH grouts (Table 6 and Table 7). The SiO_2 content on the other hand was higher in the low-pH grout samples, as would be expected since the amount of silica fume was higher in the low-pH grout mix (Table 6). The higher silica fume content in the low-pH grout mix reduces its porosity. More deterious Cl^- and SO_4^- ions can diffuse into the medium-pH grout specimen. This trend was also noticed in present work, since the content of chloride and sulphate ions was higher in the medium-pH specimens compared to the low-pH samples.

10 SUMMARY AND MAIN CONCLUSIONS

Two cementitious grout mixes, low- and medium-pH grouts, were subjected to dynamic leach testing. The fresh grout mixes were cast in 20 mL plastic syringes and leached with two stimulated groundwater solution. The experiment was carried out in an anoxic glove-box at ambient box-temperature 20 ± 1 °C up to 127 days.

It is a generally known fact that leaching of cementitious materials occurs in a sequence of stages. At first the most soluble elements such as alkali hydroxides are removed from the solid sample. In the next step the calcium hydroxide (i.e. portlandite) is dissolved followed by the dissolution of the calcium-silicate-hydrate (C-S-H) gel phases. In a final stage other cement phases, such as ettringite are dissolved. As the leaching process of cementitious materials proceeds, the pH value of the leachates decreases respectively.

In the present work rather expected results were gained. Faster decrease of the pH values was noticed in the case of the higher flow rate experiment. A similar decrease was detected in both low- and medium-pH grout leachates. The difference in the pH values between the two grouts was greater in the saline leachates for both flow rates. Compared to the pH results gained from earlier static leach testing[1], the pH of the leachates in present study decreased faster, although the results of the two tests are not directly comparable since they were performed at different temperatures. The low-pH leachates reached the target pH < 11 in all tests. The medium-pH grout leachates also showed decreasing trend in both solutions at the higher flow rate. However, only a minor decrease was observed at slower flow rate and the pH values did not reach the target pH. The reason for the lower pH values at higher flow rate experiment is that the leaching solution was more frequently renewed and a higher concentration gradient was developed between the solid material and the solution, thus increasing the dissolution of ions from the solid matrix and decreasing pH of the leachates respectively. The difference between the two leaching solutions arises from the higher ionic strength (~ 0.5 M) of the saline leaching solution compared with that of the fresh solution (~ 0.003 M) which contributes to higher decrease in the pH values of leachates.

According to the results from the chemical analysis of the leachates and the solid samples it can be stated that calcium and silicon were leached from the grout samples. The same effect was detected for potassium and also for sodium regarding the samples that were leached with the fresh leaching solution (ALL-MR) although, the results of the saline leachates showed depletion of Ca from the initial leaching solution. Based on

the results gained from the thermal analysis it can be concluded that the low-pH grout mixes did not contain portlandite at the end of the experiment contrary to the medium-pH samples. However, the amount of portlandite in these sample specimens was considerably low and only traces of hydroxide could be found.

The proportion of silicon dioxide in low-pH grout mix was higher compared to the medium-pH mix. This was rather expected result since the initial amount of microsilica in the low-pH grout mix was greater. The amount of chlorine in the initial saline leaching solution is significantly higher compared to the fresh solution. In all the cases chloride showed depletion from the initial solution and was absorbed by the grout samples. Probably due to this high concentration of chloride in the leaching solution some chloride containing calcium aluminate hydrate was detected in the XRD study of the medium-pH grout mixes leached with the saline solution.

The total sulphur content in the medium-pH grout samples was higher compared to the low-pH samples according to the results from XRF analysis. The same conclusions could be made from the chemical analysis of the leachates also. In all the cases more sulphate was leached from the low-pH grout samples. Overall, the sulphur release was quite low. After the initial release, the amount of sulphur in the leachates remained steady at least in case of the medium-pH mix.

Only a quantitative analysis of the total organic carbon of the leachates was performed. The samples were chosen from the beginning, the middle and end periods of testing. In general the amount of organic carbon released from the grout samples was highest at the beginning of testing. The difference between the two leaching solutions is notable. In the saline leachates the amount of organic carbon is higher at both flow rates, roughly estimated two times higher. It also seems clear that more organics were leached at the slower flow rates in both leaching solutions. These results might imply that the organics present in grout mixes have relatively high molecular weight, since it has been shown that only the monomers and oligomers up to the tetramers of organic condensates will elute from cement matrix.

11 REFERENCES

1. J. Hansen, P. Juhola, K.Koskinen, M. Vuorio, A. Lehtinen, J. Mattila, U.Sievänen, P. Karttunen, P. Raivio, M. Arenius, T. Lyytinen, U. Vuorinen, S. Partamies and P. Pitkänen, Groundwater inflow management in ONKALO – the future strategy, Posiva Working Report 2008-44, Posiva Oy, Olkiluoto, Finland, to be published.

2. B. Miller and N. Marcos, Process Report-FEPs and scenarious for a spent fuel repository at Olkiluoto, Posiva Report 2007-12, Posiva Oy, Eurajoki, Finland, 2007.

3. E. Holt, Durability of low-pH injection grout - A literature Survey, Posiva Working Report 2007-57, Posiva Oy, Olkiluoto, Finland, 2008.

4. T. Vieno, J. Lehikoinen, J. Löfman, H. Nordman and F. Meszaros, Assessment of disturbances caused by construction and operation of ONKALO, Posiva Report 2003-06, Posiva Oy, Olkiluoto, Finland, 2003.

5. U. Vuorinen, J. Lehikoinen, I. Harutake, T. Yamamoto and M. Cruz Alonso, Injection Grout for Deep Repositories Subproject 1:Low-pH Cementitious Grout for Larger Fractures, Leach Testing of Grout Mixes and Evaluation of the Long-Term Safety, Posiva Working Report 2004-46, Posiva Oy, Olkiluoto, Finland, 2005.

6. A. Kronlöf, Injection Grout for Deep Repositories - Low-pH Cementititous Grout for Large Fractures: Testing Technical Performance of Materials, Posiva Working Report 2004-45, Posiva Oy, Olkiluoto, Finland, 2005.

7. U. Sievänen, P. Raivio, U. Vuorinen, J. Hansen, J. Norokallio and P. Syrjänen, Optimisation of Technical Properties of Low-pH Cementitious Injection Grout Laboratory Tests and Pilot Field Test 3, Posiva Working Report 2006-85, Posiva Oy, Olkiluoto, Finland, 2006.

8. IAEA, The long term storage of radioactive waste: safety and sustainability, A position paper of international experts, International Atomic Energy Agency, Austria, 2003.

9. K. Rasilainen and S. Vuori, Käytetyn ydinpolttoaineen huolto Suomalaisen suunnitelman pääpiirteet, VTT Tiedotteita 1953, VTT, valtion teknillinen tutkimuskeskus, Espoo, Finland, 1999.

10. T. McEwen and T. Äikäs, The site selection process for a spent fuel repository in Finalnd - Summary report, Posiva Report 2000-15, Posiva Oy, Helsinki, Finland, 2000.

11. B. Pastina and P. Hellä, Expected Evolution of a Spent Nuclear Fuel Repository at Olkiluoto, Posiva Report 2006-05, Posiva Oy, Olkiluoto, Finland, 2006.

12. U. Sievänen, Preliminary estimations of water inflow and grouting conditions at Olkiluoto site, Posiva Working Report 2003-11, Posiva Oy, Olkiluoto, Finland, 2003.

13. U. Sievänen and R. Riekkola, Controlling of groundwater inflow into ONKALO and the deep repository at Olkiluoto Summary Report, Posiva Working Report 2003-51, Posiva Oy, Olkiluoto, Finland, 2003.

14. P. Pitkänen, S. Partamies and A. Luukkonen, Hydrogeochemical interpretation of baseline groundwater conditions at the Olkiluoto site, Posiva Report 2003-07, Posiva Oy, Olkiluoto, Finland, 2004.

15. A. Muurinen and J. Lehikoinen, Porewater chemistry in compacted bentonite, Posiva report 99-20, Posiva Oy, Helsinki, Finland, 1999.

16. J. Bruno, D. Arcos and L. Duro, Groundwater-bentonite interaction, TR-99-29, SKB, Swedish Nuclear Fuel and Waste Management Co, Stockholm, Sweden, 1999.

17. A.M. Fernández, B. Baeyens, M. Bradbury and P. Rivas, Analysis of the porewater chemical composition of a Spanish compacted bentonite used in an engineered barrier, *Phys. Chem. Earth, Parts A/B/C,*. **2004**, *29*, 105-118.

18. D. Savage and S. Benbow, Low-pH Cements, SKI Report 2007:32, Swedish Nuclear Power Inspectorate (SKI), Stockholm, Sweden, 2007.

19. E.C. Gaucher, P. Blanc, J. Matray and N. Michau, Modeling diffusion of an alkaline plume in a clay barrier, *Appl. Geochem.*, **2004**, *19*, 1505-15.

20. D. Savage, M. Stenhouse and S. Benbow, Evolution of near-field physico-chemical characteristics of the SFR repository, SKI Report 00:49, Swedish Nuclear Power Inspectorate (SKI), Stockholm, Sweden, 2000.

21. J. Cama, J. Ganor, C. Ayora and C.A. Lasaga, Smectite dissolution kinetics at 80°C and pH 8.8, *Geochim. Cosmochim. Acta,*. **2000**, *64*, 2701-17.

22. F.J. Huertas, E. Caballero, C. Jiménez de Cisneros, F. Huertas and J. Linares, Kinetics of montmorillonite dissolution in granitic solutions, *Appl. Geochem.*, **2001**, *16*, 397-407.

23. P. Hewlett, *Lea's Chemistry of Cement and Concrete, Fourth Edition;* 4pp. 1092. Butterworth-Heinemann, 2004.

24. H.F.W. Taylor , *Cement Chemistry, second edition;* 2pp. 480. Thomas Telford Ltd, 1997.

25. H. Viirola and P. Raivio, Portlandsementin hydrataatio, VTT Tiedotteita 2041, VTT, valtion teknillinen tutkimuskeskus, Espoo, Finland, 2000.

26. M. Gascoyne, Influence of grout and cement on groundwater composition, Posiva Working Report 2002-07, Posiva Oy, Helsinki, Finland, 2002.

27. C. Alonso, M. Castellote, I. Llorente and C. Andrade, Ground water leaching resistance of high and ultra high performance concretes in relation to the testing convection regime, *Cem. Concr. Res.*, **2006**, *36*, 1583-94.

28. X. Hou, L.J. Struble and R.J. Kirkpatrick, Formation of ASR gel and the roles of C-S-H and portlandite, *Cem. Concr. Res.*, **2004**, *34*, 1683-96.

29. A.J. Maas, J.H. Ideker and M.C.G. Juenger, Alkali silica reactivity of agglomerated silica fume, *Cem. Concr. Res.*, **2007**, *37*, 166-74.

30. Barnes, *Structure and Performance of Cements;* 2pp. 592. Taylor & Francis, 2007.

31. M. Hakanen and H. Ervanne, The influence of organic cement additives on radionuclide mobility, Posiva Working Report 2006-06, Posiva Oy, Olkiluoto, Finland, 2006.

32. H. Ervanne and M. Hakanen, Analysis of cement superplasticizers and grinding aids a literature survey, Posiva Working Report 2007-15, Posiva Oy, Olkiluoto, Finland, 2007.

33. S. Ruckstuhl, M.J.-. Suter and W. Giger, Sorption and mass fluxes of sulfonated naphthalene formaldehyde condensates in aquifers, *J. Contam Hydrol.*, **2003**, *67*, 1-12.

34. M.J. Keith-Roach, The speciation, stability, solubility and biodegradation of organic co-contaminant radionuclide complexes: A review, *Sci. Total Environ.*, **2008**, *396*, 1-11.

35. Nirex Ltd, Technical Note, Potential areas of future geosphere research, Nirex, UK, 2006.

36. P.K. Mehta and P.J.M. Monteiro, *Concrete: Structure, Properties, and Materials;* 2 Subpp. 496. Prentice Hall College Div, 1992.

37. A. Aït-Mokhtar, O. Amiri, P. Dumargue and S. Sammartino, A new model to calculate water permeability of cement-based materials from MIP results, *Adv. Cem. Res.*, **2002**, *14*, 43-9.

38. S. Kamali, M. Moranville and S. Leclercq, Material and environmental parameter effects on the leaching of cement pastes: Experiments and modelling, *Cem. Concr. Res.*, **2008**, *38*, 575-85.

39. D.P. Bentz, O.M. Jensen, A.M. Coats and F.P. Glasser, Influence of silica fume on diffusivity in cement-based materials: I. Experimental and computer modeling studies on cement pastes, *Cem. Concr. Res.*, **2000**, *30*, 953-62.

40. T. Ekström, *Leaching of concrete;* Lund Institute of Technology Division of Building Materials, Lund, Sweden.

41. A. Hidalgo, S. Petit, C. Domingo, C. Alonso, and C. Andrade, Microstructural characterization of leaching effects in cement pastes due to neutralization of their alkaline nature Part I: Portland cement pastes, *Cem. Concr. Res.*, **2007**, *37*, 63-70.

42. K. Haga, M. Shibata, M. Hironaga, S. Tanaka and S. Nagasaki, Change in pore structure and composition of hardened cement paste during the process of dissolution, *Cem. Concr. Res.*, **2005**, *35*, 943-50.

43. C. Cau Dit Coumes, S. Courtois, D. Nectoux, S. Leclercq and X. Bourbon, Formulating a low-alkalinity, high-resistance and low-heat concrete for radioactive waste repositories, *Cem. Concr. Res.*, **2006**, *36*, 2152-63.

44. C. Vernet, C. Alonso, C. Andrade, M. Castellote, I. Llorente and A. Hidalgo, A new leaching test based in a running water system to evaluate long-term water resistance of concretes, *Adv. Cem Res.,* **2002**, *14,* 157-68.

45. F.P. Glasser, J. Marchand and E. Samson, Durability of concrete — Degradation phenomena involving detrimental chemical reactions, *Cem. Concr. Res.,* **2008**, *38,* 226-46.

46. Ed. A. Bodén and U. Sievänen, Low-pH Grout for Deep Repositories – Summary Report from a Co-operation Project between NUMO (Japan), Posiva (Finland) and SKB (Sweden), Posiva Working Report 2005-24, Posiva Oy, Olkiluoto, Finland, 2006.

47. M.C. Alonso, L. Fernández, J.L. Garcia and A. Hidalgo, Low-pH Cementitious Materials Design and Characterisation, *12th International Congress on the Chemistry of Cement,* 8.-13.7.2007, 2007

48. J.J. Chen, J.J. Thomas, H.F.W. Taylor and H.M. Jennings, Solubility and structure of calcium silicate hydrate, *Cem. Concr. Res.,* **2004**, *34,* 1499-519.

49. A. Moropoulou, A. Cakmak, K. Labropoulos, R. Van Grieken and K. Torfs, Accelerated microstructural evolution of a calcium-silicate-hydrate (CSH) phase in pozzolanic pastes using fine siliceous sources: Comparison with historic pozzolanic mortars, *Cem. Concr. Res.,* **2004**, *34,* 1-6.

50. M. Codina, C. Cau-dit-Coumes, P. Le Bescop, J. Verdier and J.P. Ollivier, Design and characterization of low-heat and low-alkalinity cements, *Cem. Concr. Res.,* **2008**, *38,* 437-48.

51. S.A. Stronach and F.P. Glasser, Modelling the impact of abundant geochemical components on phase stability and solubility of the $CaO-SiO_2-H_2O$ system at 25 ^oC: Na^+, K^+, SO_4^{2-}, Cl^- and CO_3^{2-}, *Adv. Cem. Res.,* **1997**, *9,* 167-81.

52. B. Lagerblad, Leaching performance of concrete based on studies of samples from old concrete constructions,TR-01-27, SKB, Swedish Nuclear Fuel and Waste Management Co, Stockholm, Sweden, 2001.

53. M. Onofrei, M.N. Gray, W.E. Coons and S.R. Alcorn, High performance cement-based grouts for use in a nuclear waste disposal facility, *Waste Management.* **1992**, *12,* 133-54.

54. J. Hill, A.W. Harris, M. Manning, A. Chambers, and S.W. Swanton, The effect of sodium chloride on the dissolution of calcium silicate hydrate gels, *Waste Management.*, **2006**, *26*, 758-768.

55. P. Raivio and J. Hansen, Technical Performance of Cementitious Grouting Materials for ONKALO - Laboratory Tests 2006, Posiva Working Report 2007-76, Posiva Oy, Olkiluoto, Finland, 2007.

56. I. Innovative Instruments, pH Sensors: The Amani Series, http://www.2in.com/products/ph-sensors/ph-sensors.html (2008, 03/11)

57. M.R. Jones, D.E. Macphee, J.A. Chudek, G. Hunter, R. Lannegrand, R. Talero and S.N. Scrimgeour, Studies using 27Al MAS NMR of AFm and AFt phases and the formation of Friedel's salt, *Cem. Concr. Res.*, **2003**, *33*, 177-82.

58. A.K. Suryavanshi, J.D. Scantlebury and S.B. Lyon, Mechanism of Friedel's salt formation in cements rich in tri-calcium aluminate, *Cem. Concr. Res.*, **1996**, *26*, 717-27.

59. F. Barberon, V. Baroghen-Bouny, H. Zanni, B. Bresson, J.-B. d'Espinose de la Caillerie, L. Malosse, and Z. Gan, Interactions between chloride and cement-paste materials, *Magn. Reson. Imaging*, **2005**, *23*, 267-272.

60. D.C. Harris, *Quantitative Chemical Analysis;* 5 Har/Cdrpp. 899. W.H. Freeman & Company, 1998.

61. H. Galster, *pH Measurement: Fundamentals, Methods, Applications, Instrumentation;* pp. 356. Wiley-VCH Verlag GmbH, 1991.

62. J.J. Barron, C. Ashton and L. Geary, The effects of temperature on pH measurement, Technical Services Department, Reagecon Diagnostics Ltd, Ireland.

APPENDIX 1

Calibration of Amani and Ross electrodes

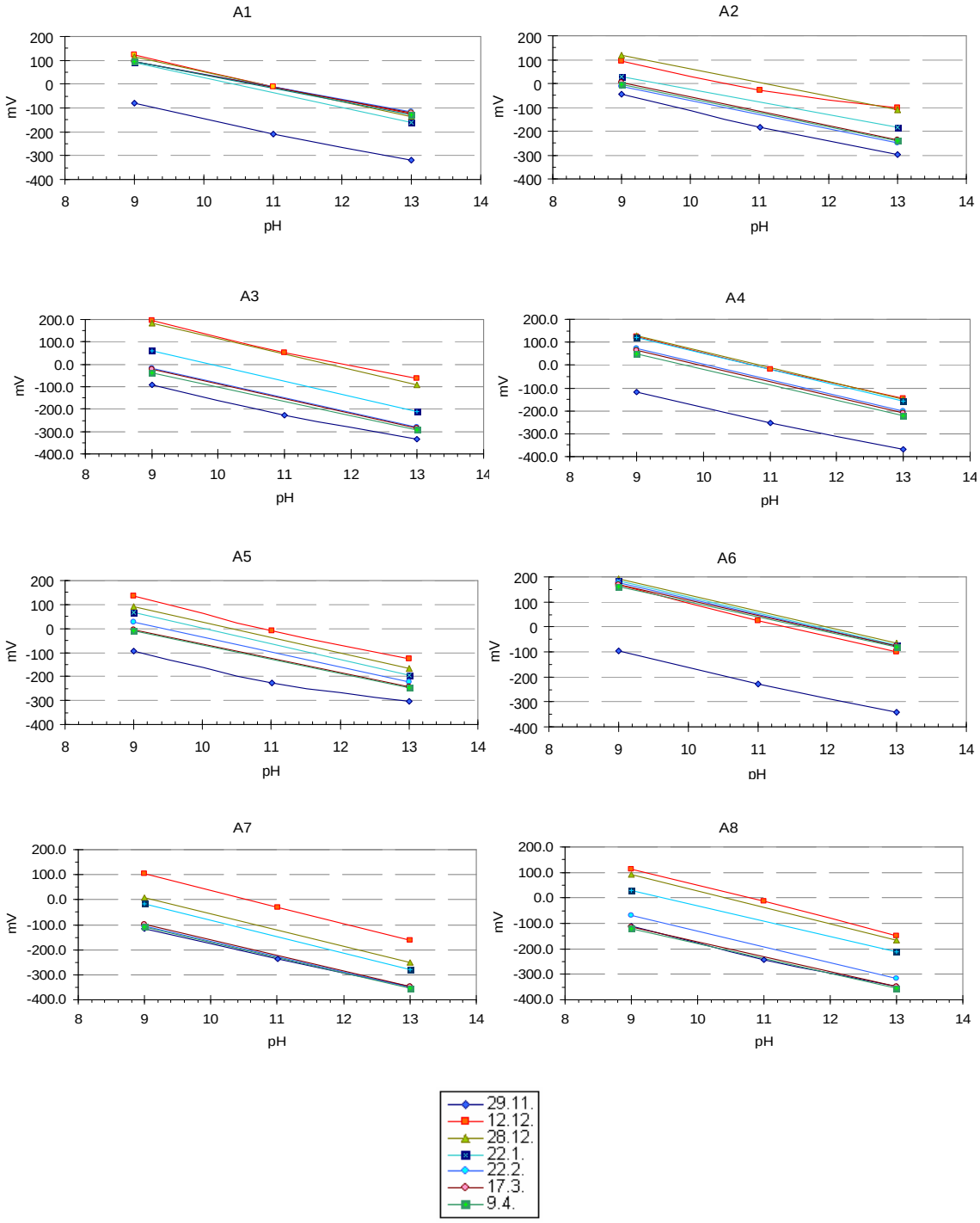

Figure A 1. Calibration curves of eight Amani 1000 electrodes during the experiment (Note! Legend applies to all sub-figures).

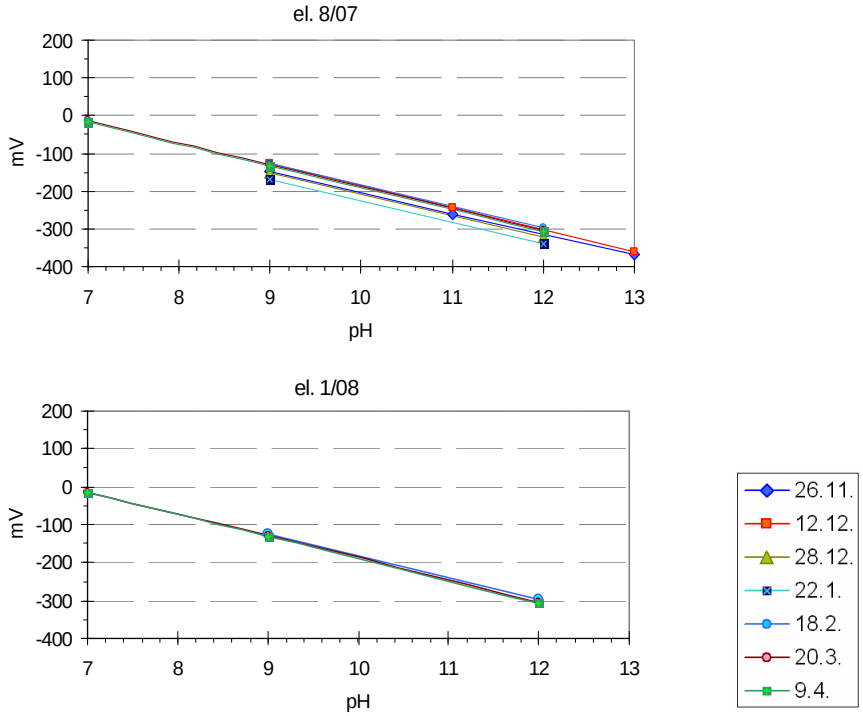

Figure A 2. Calibration curves of two glass electrodes (Ross) used during the experiment (Note! Legend applies to both sub-figures).

Table A 1. a) The slopes of the graphs of Amani electrodes and b) the slope of the two Ross electrodes used.

a)

date	**A1**	**A2**	**A3**	**A4**	**A5**	**A6**	**A7**	**A8**
29.11.07	-60.0	-63.2	-61.4	-62.0	-52.7	-61.1	-57.8	-59.7
12.12.07	-62.1	-50.0	-64.1	-68.0	-65.5	-67.2	-67.1	-65.9
28.12.07	-62.4	-57.4	-68.9	-69.4	-65.1	-64.1	-64.8	-64.1
22.1.08	-63.5	-53.5	-67.8	-69.8	-65.7	-64.6	-65.5	-59.5
22.2.08	-52.7	-55.2	-65.8	-68.5	-62.3	-63.6	-61.7	-61.1
17.3.08	-53.8	-59.9	-66.6	-68.8	-59.6	-61.9	-62.7	-59.1
9.4.08	-55.2	-59.1	-64.3	-66.9	-59.4	-60.5	-61.2	58.6

b)

	Ross 7/08	**Ross 1/08**
26.11.07	-55.9	
12.12.07	-59.2	
28.12.07	-56.7	
22.1.08	-57.7	
18.2.08		-57.0
20.3.08		-58.2
9.4.08		-58.2

APPENDIX 2

Analytical results of leachates

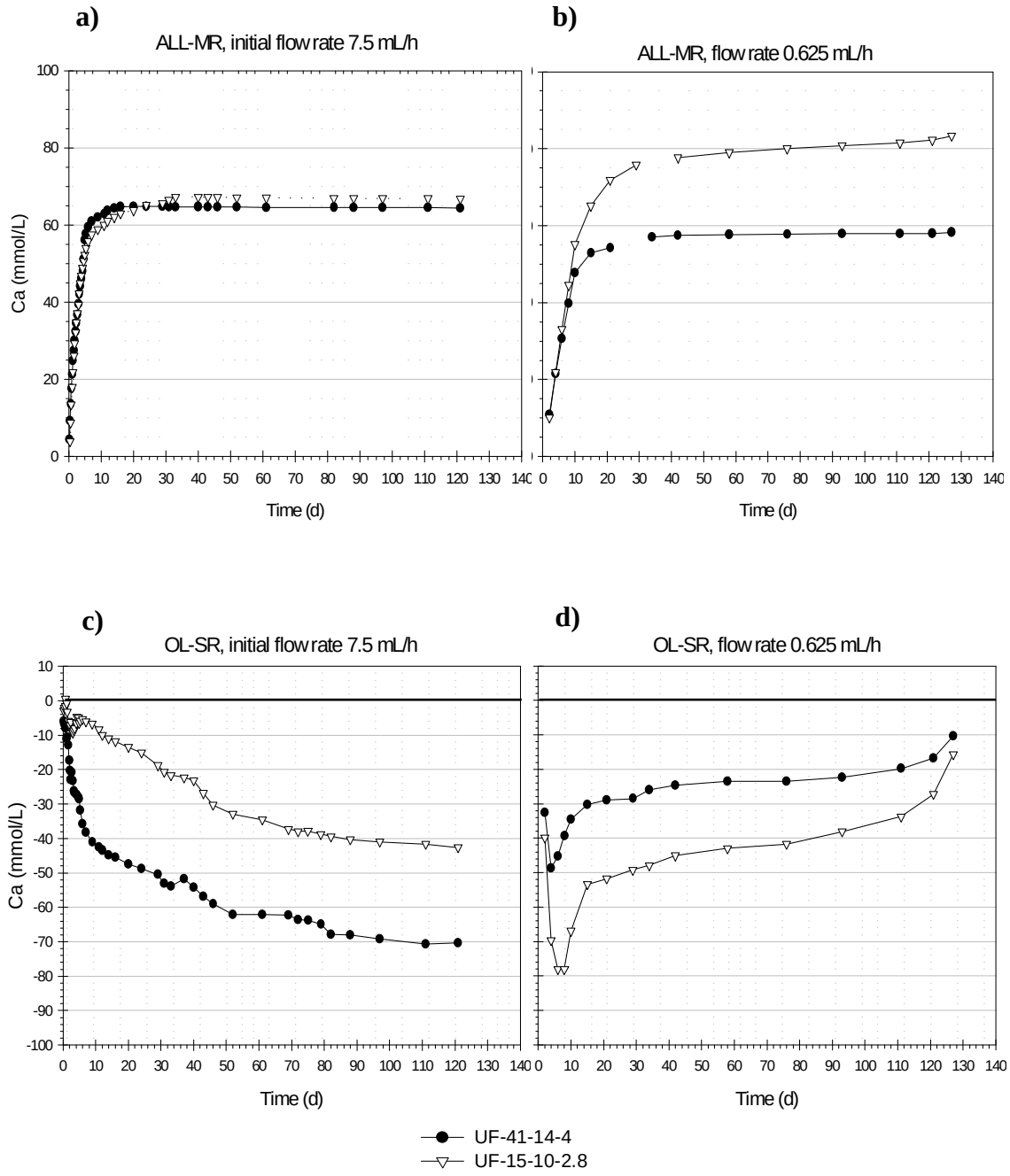

Figure A 3. Cumulative concentrations of Ca in fresh (ALL-MR) and saline (OL-SR) leachates. Note! The legend applies to all sub-figures. The sub-figures a and b have same x-axis as well as sub-figures c and d.

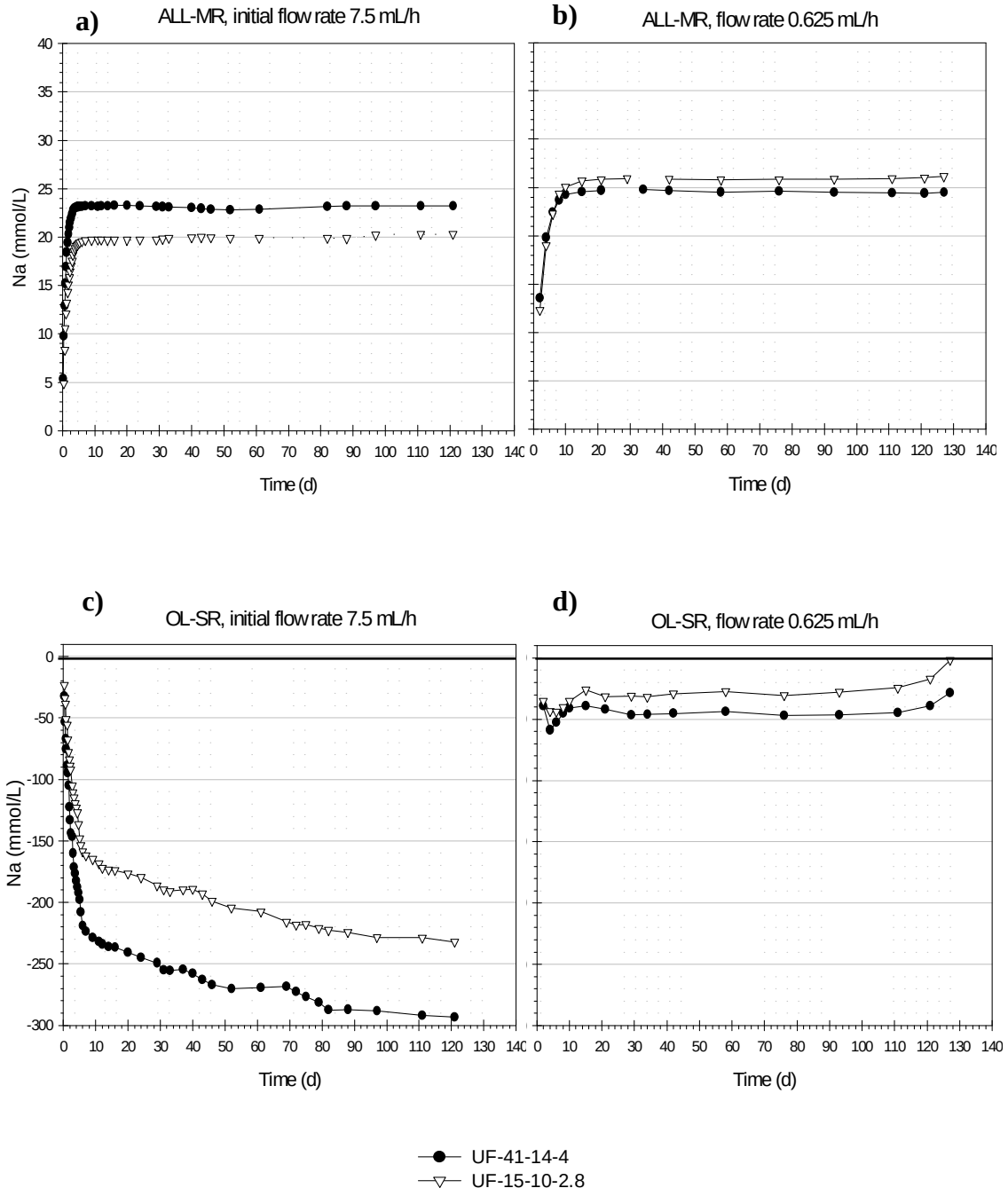

Figure A 4. Cumulative concentrations of Na in fresh (ALL-MR) and saline (OL-SR) leachates. Note! The legend applies to all sub-figures. The sub-figures a and b have same x-axis as well as sub-figures c and d.

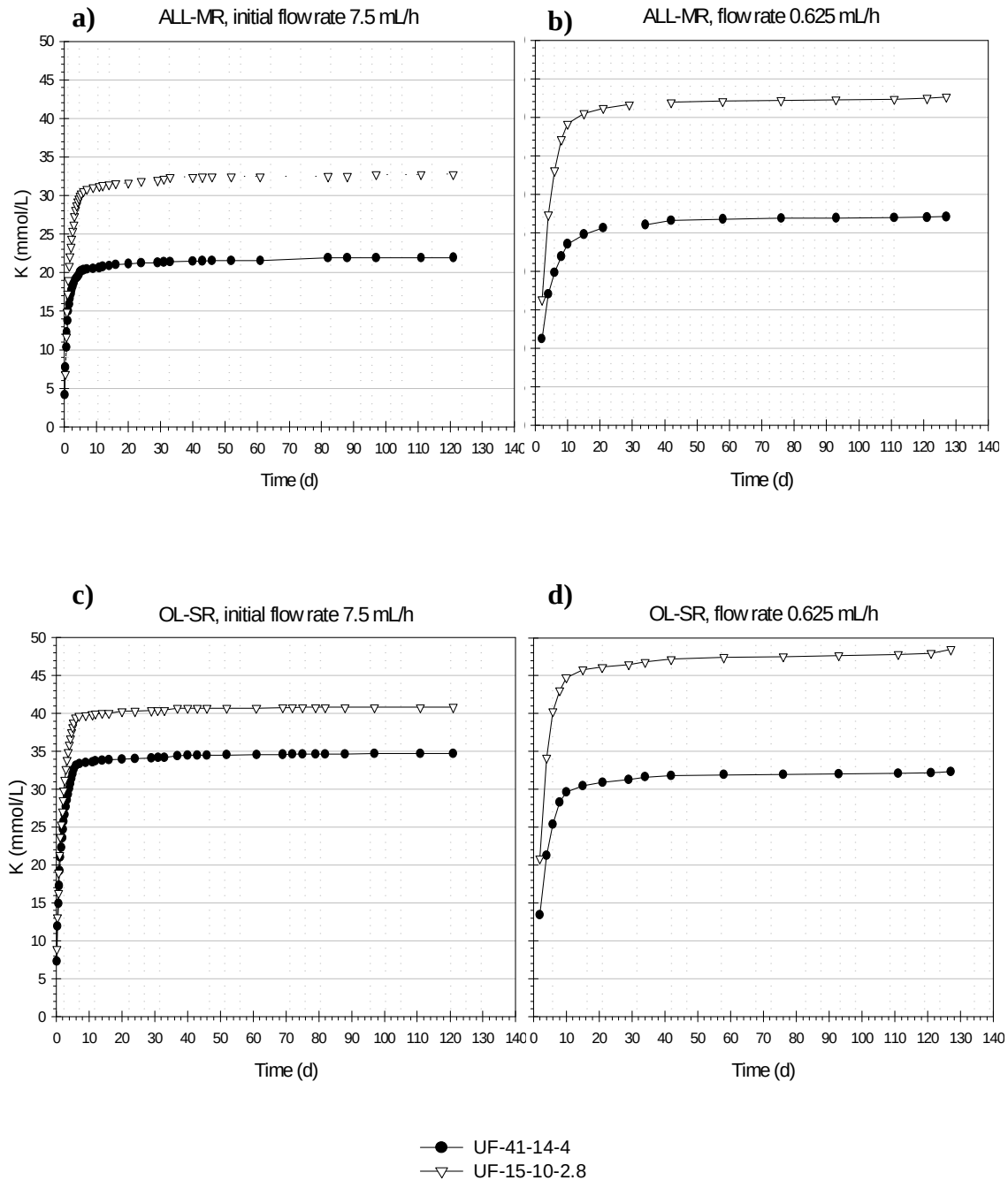

Figure A 5. Cumulative concentrations of K in fresh (ALL-MR) and saline (OL-SR) leachates. Note! The legend applies to all sub-figures. The sub-figures a and b as well as sub-figures c and d have same x-axis.

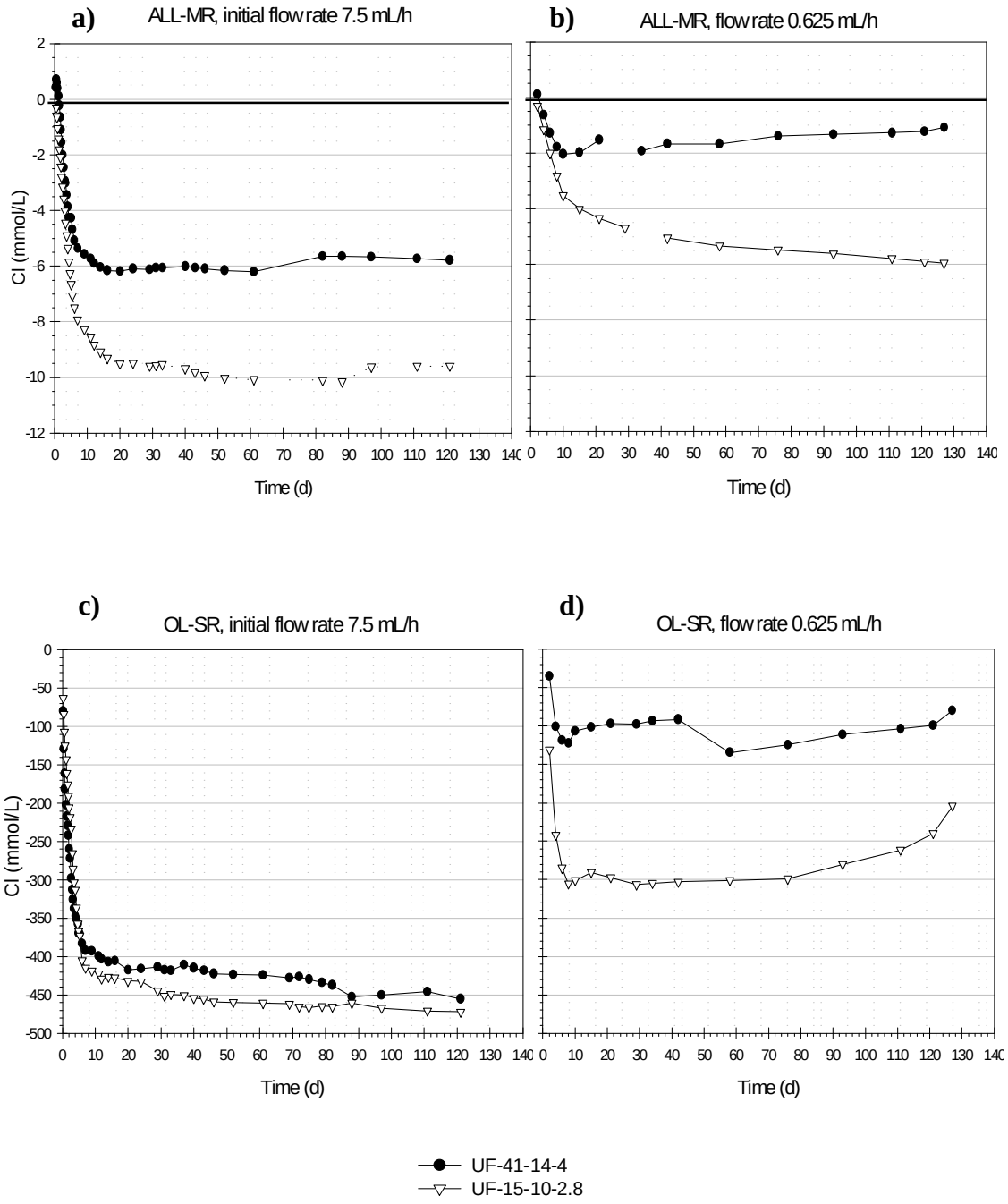

Figure A 6. Cumulative concentrations of Cl in fresh (ALL-MR) and saline (OL-SR) leachates. Note! The legend applies to all sub-figures. The sub-figures a and b have same x-axis as well as sub-figures c and d.

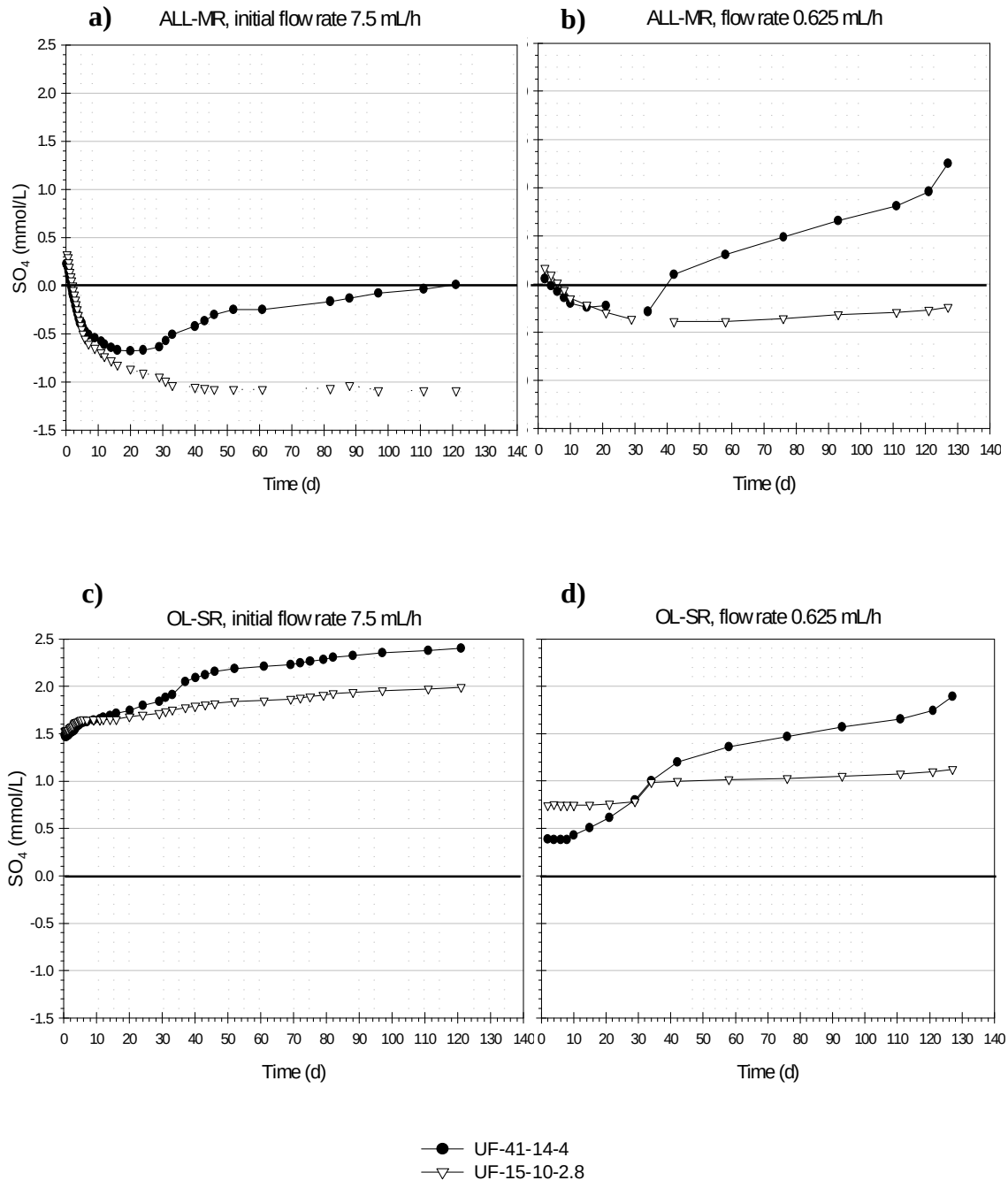

Figure A 7. Cumulative concentrations of SO_4^{2-} in fresh (ALL-MR) and saline (OL-SR) leachates. Note! The legend applies to all sub-figures. The sub-figures a and b as well as sub-figures c and d have same x-axis.

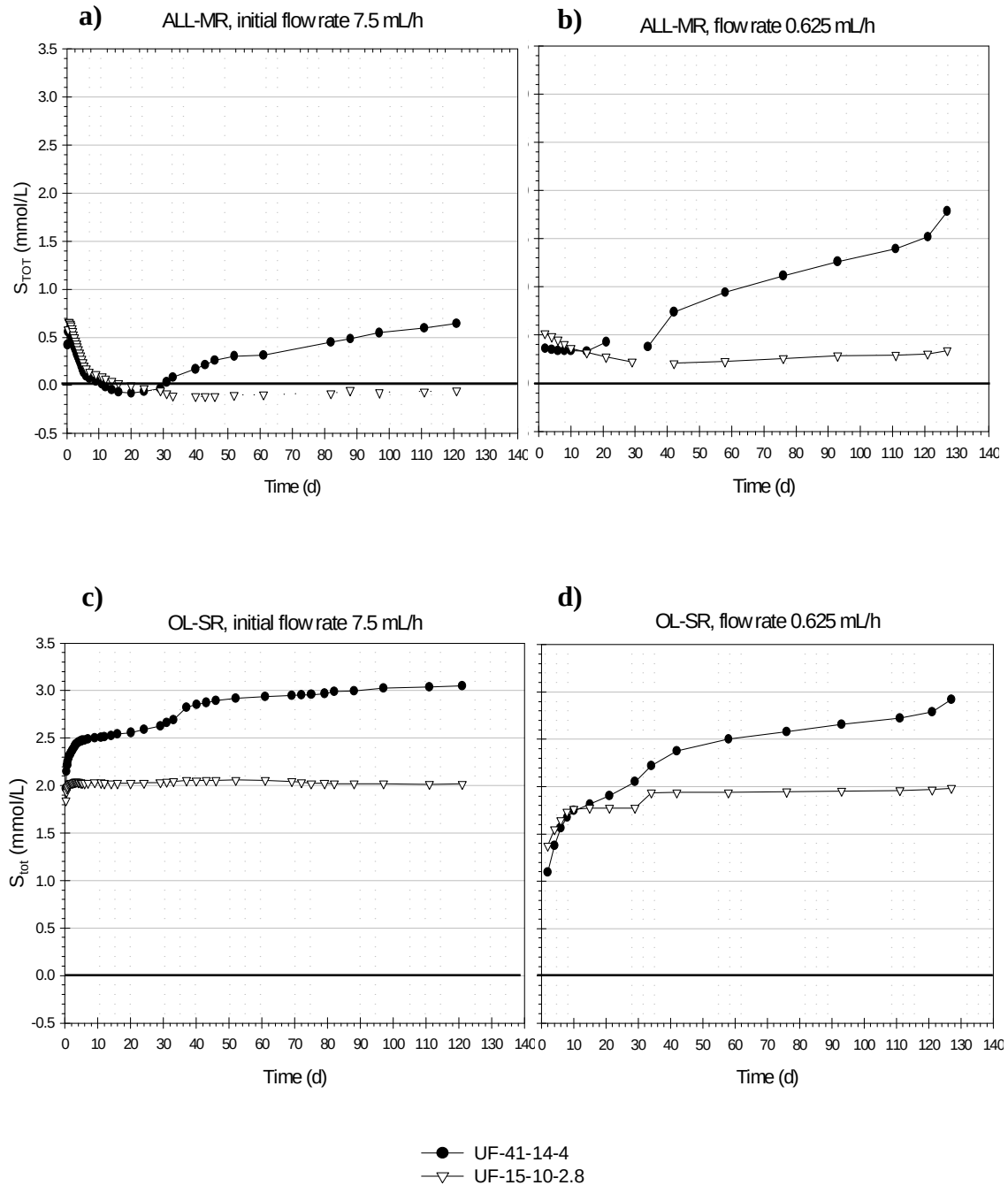

Figure A 8. Cumulative concentrations of S_{TOT} in fresh (ALL-MR) and saline (OL-SR) leachates. Note! The legend applies to all sub-figures. The sub-figures a and b as well as sub-figures c and d have same x-axis.

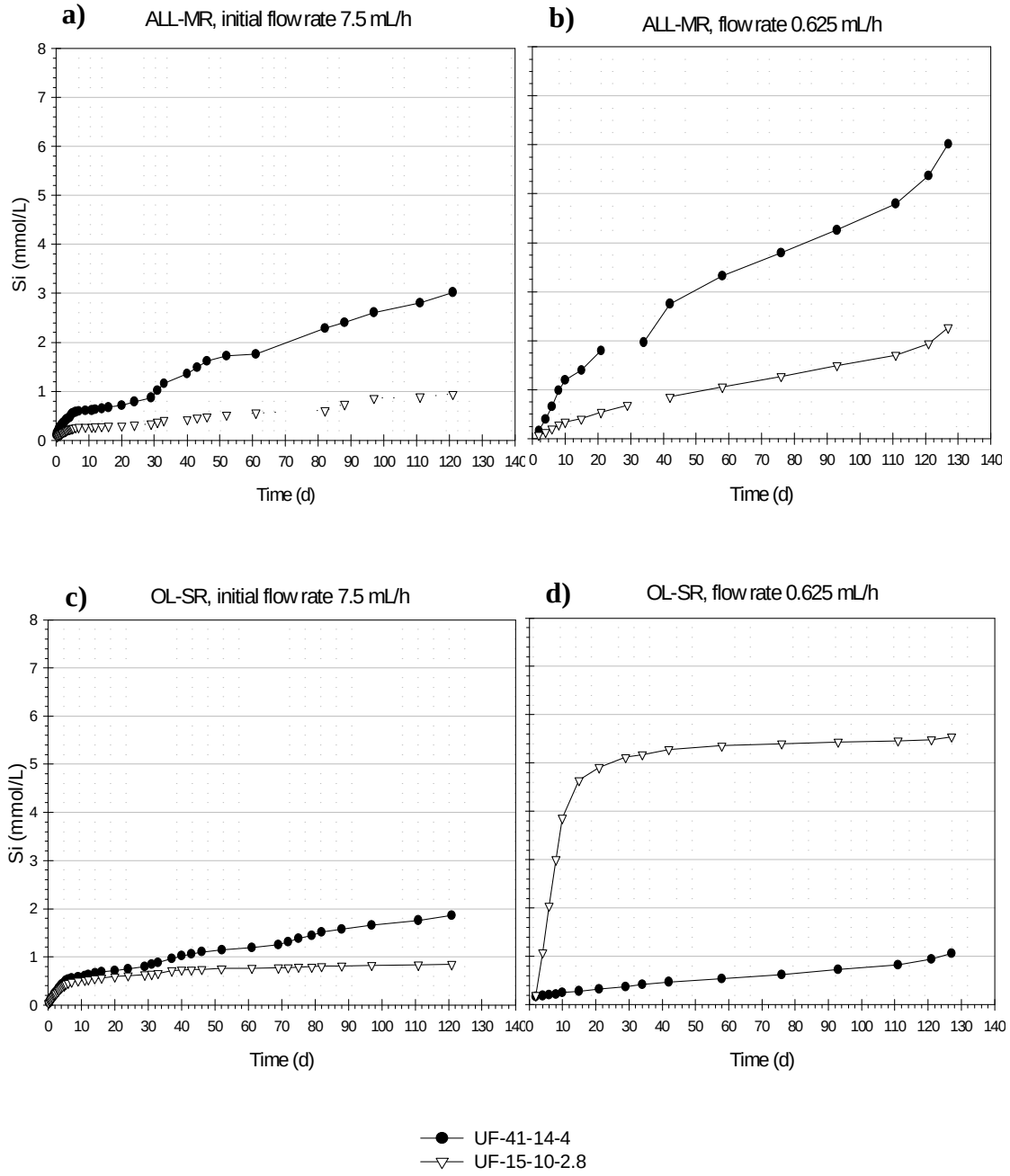

Figure A 9. Cumulative concentrations of Si in fresh (ALL-MR) and saline (OL-SR) leachates. Note! The legend applies to all sub-figures. The sub-figures a and b as well as sub-figures c and d have same x-axis.

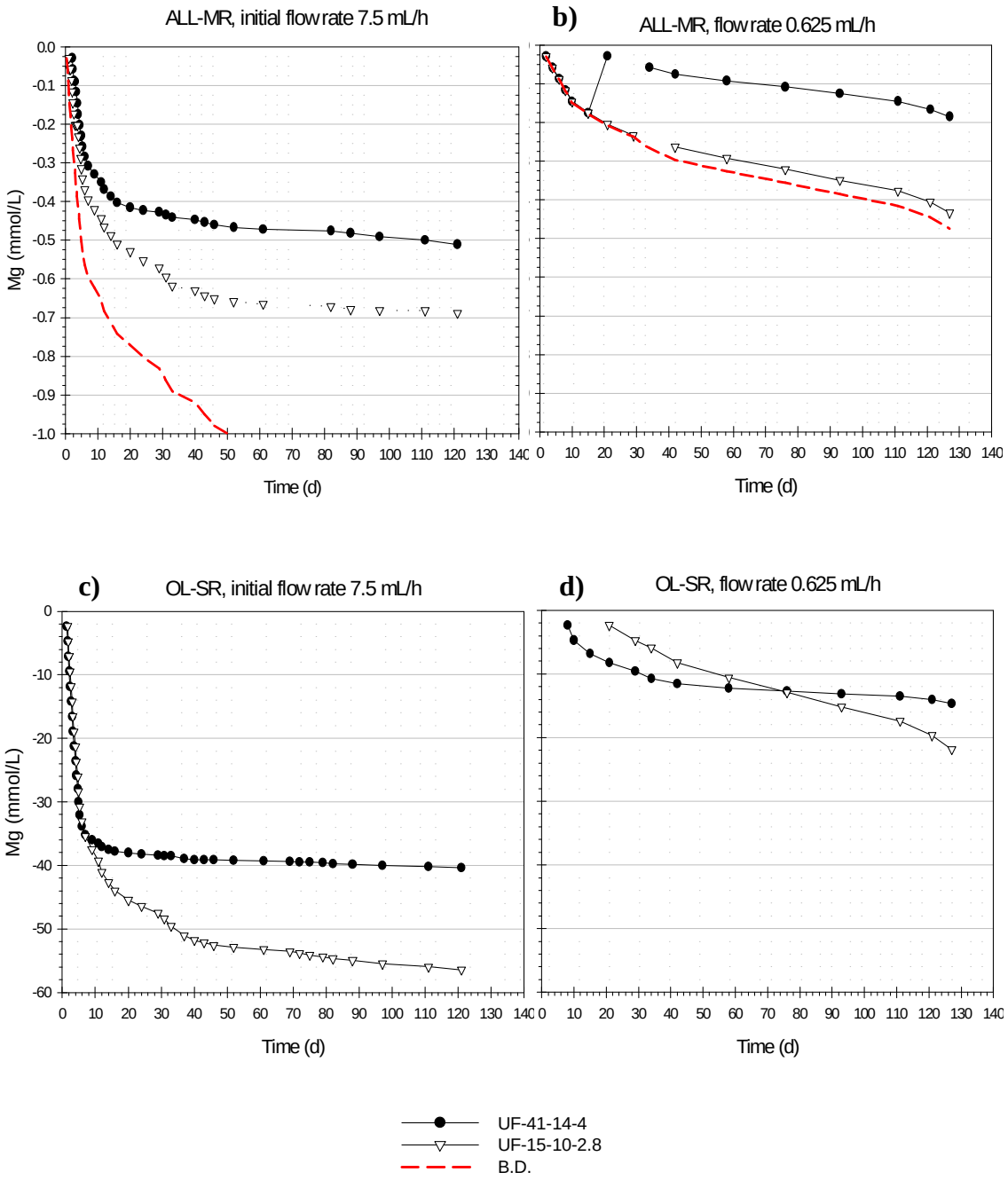

Figure A 10. Cumulative concentrations of Mg in fresh (ALL-MR) and saline (OL-SR) leachates. Note! The legend applies to all sub-figures. The sub-figures a and b have same x-axis as well as sub-figures c and d.

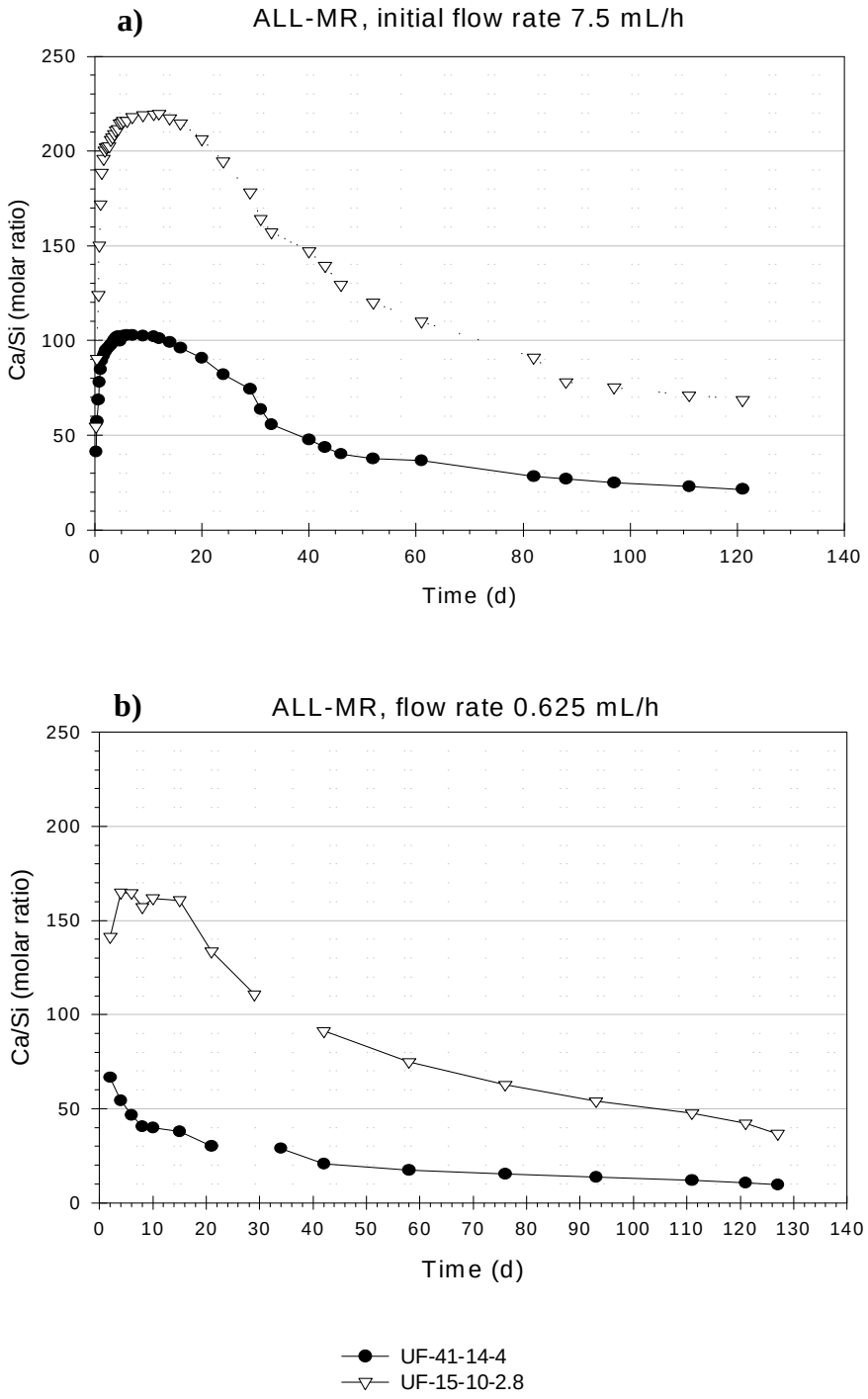

Figure A 11. Cumulative molar concentration ratio for Ca/Si in the leachates at different sampling points in fresh (ALL-MR) leachates. Note! The legend applies to both sub-figures.

APPENDIX 3

Thermal curves of the injection grout samples

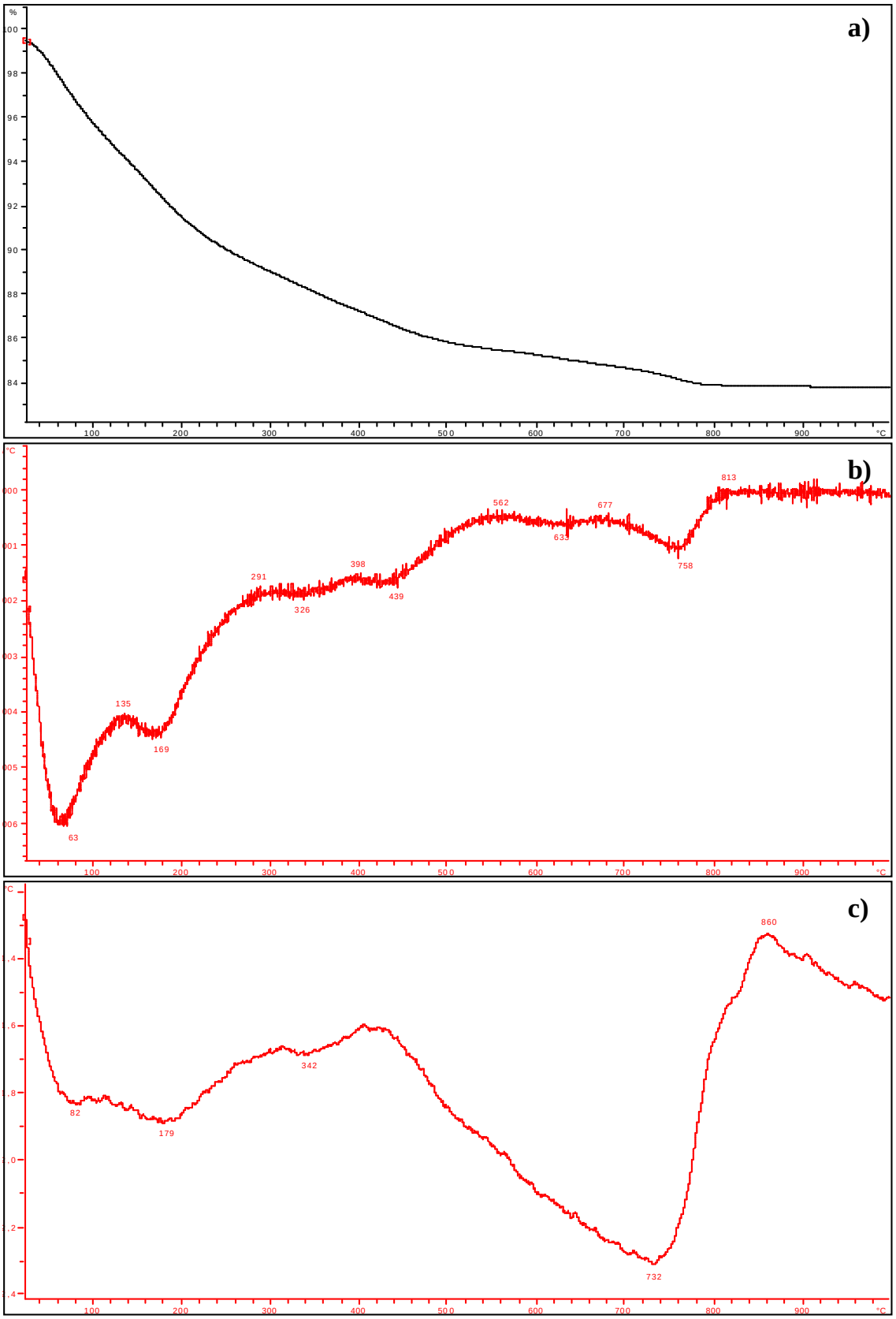

Figure A 12. Sample UF-41-14-4 surface, leached with fresh solution with initial flow rate 7.5 ml/h, a) TG-curve, b) DTG-curve and c) DTA-curve.

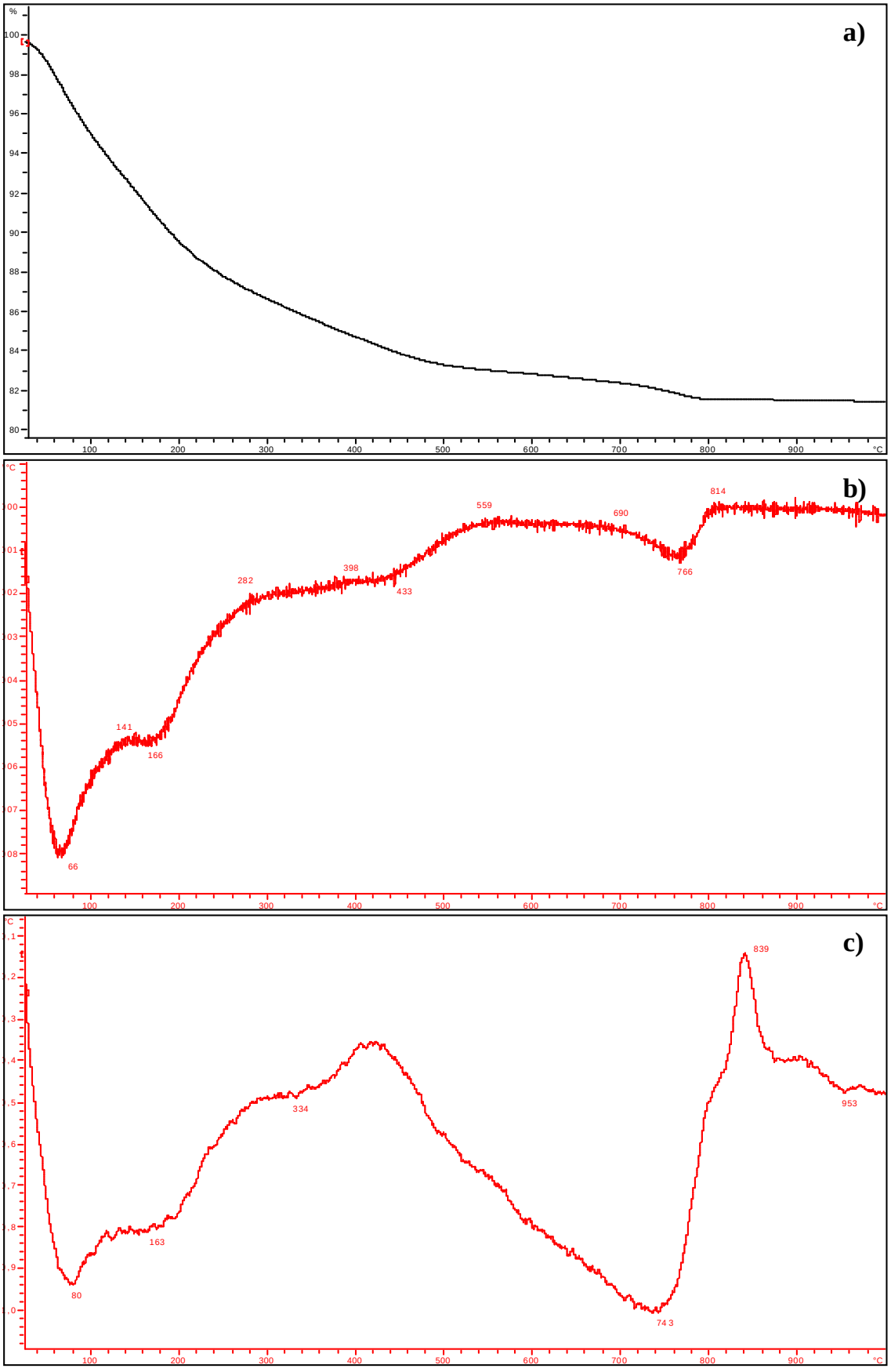

Figure A 13. Sample UF-41-14-4 base, leached with fresh solution with initial flow rate 7.5 ml/h, a) TG-curve, b) DTG-curve and c) DTA-curve.

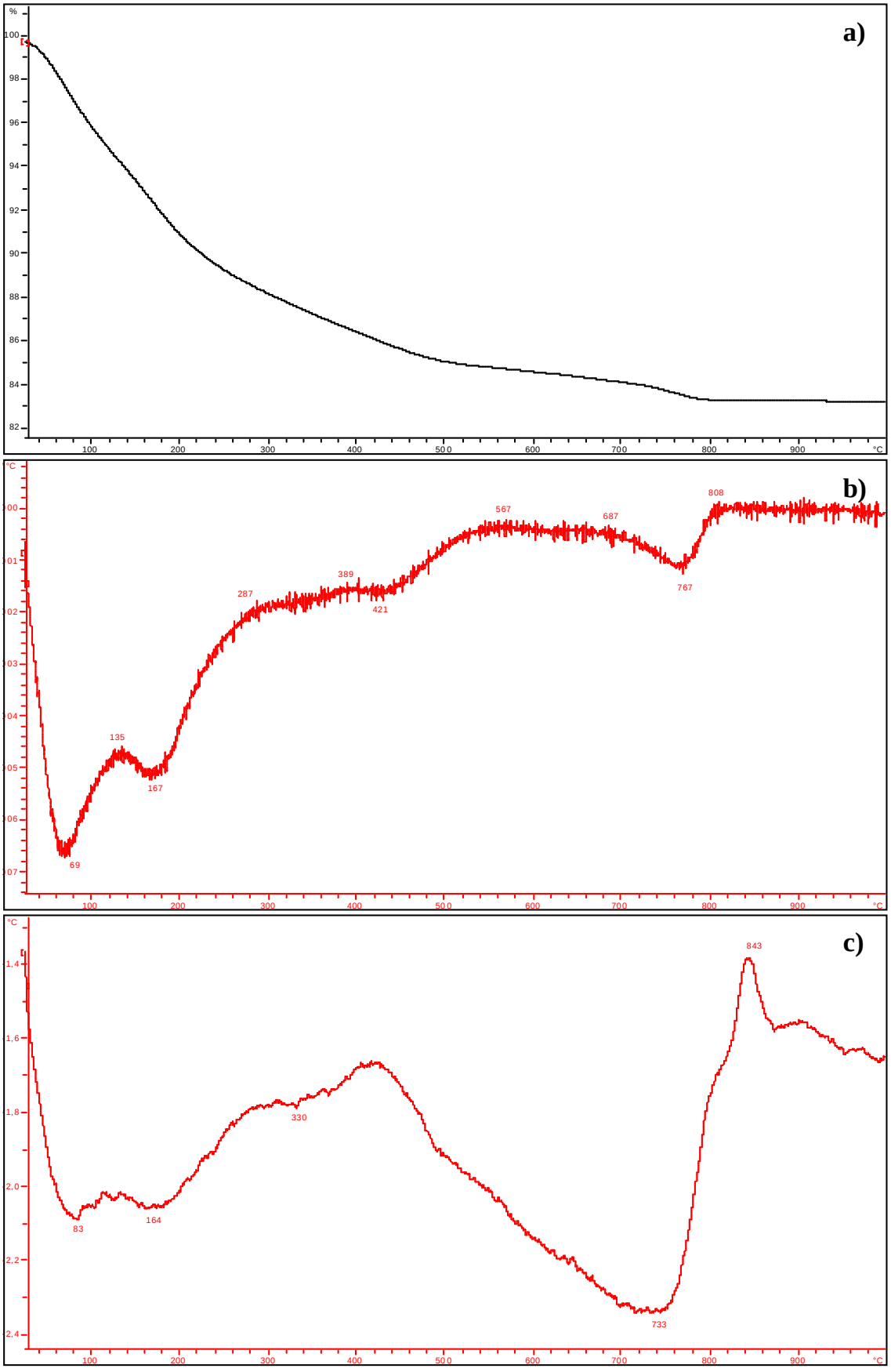

Figure A 14. Sample UF-41-14-4 surface, leached with fresh solution with flow rate 0.625 ml/h, a) TG-curve, b) DTG-curve and c) DTA-curve.

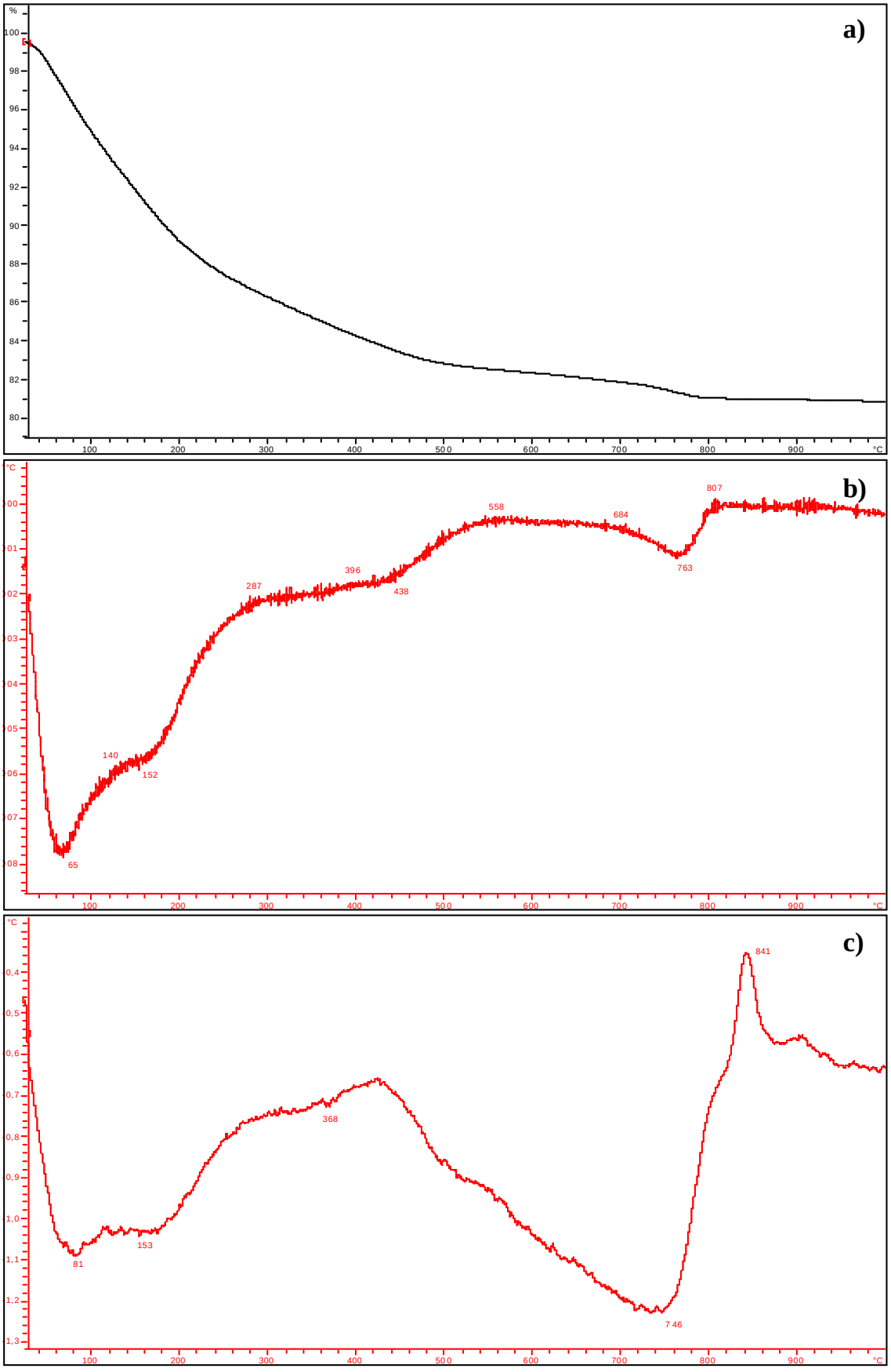

Figure A 15. Sample UF-41-14-4 base, leached with fresh solution with initial flow rate 0.625 ml/h, a) TG-curve, b) DTG-curve and c) DTA-curve.

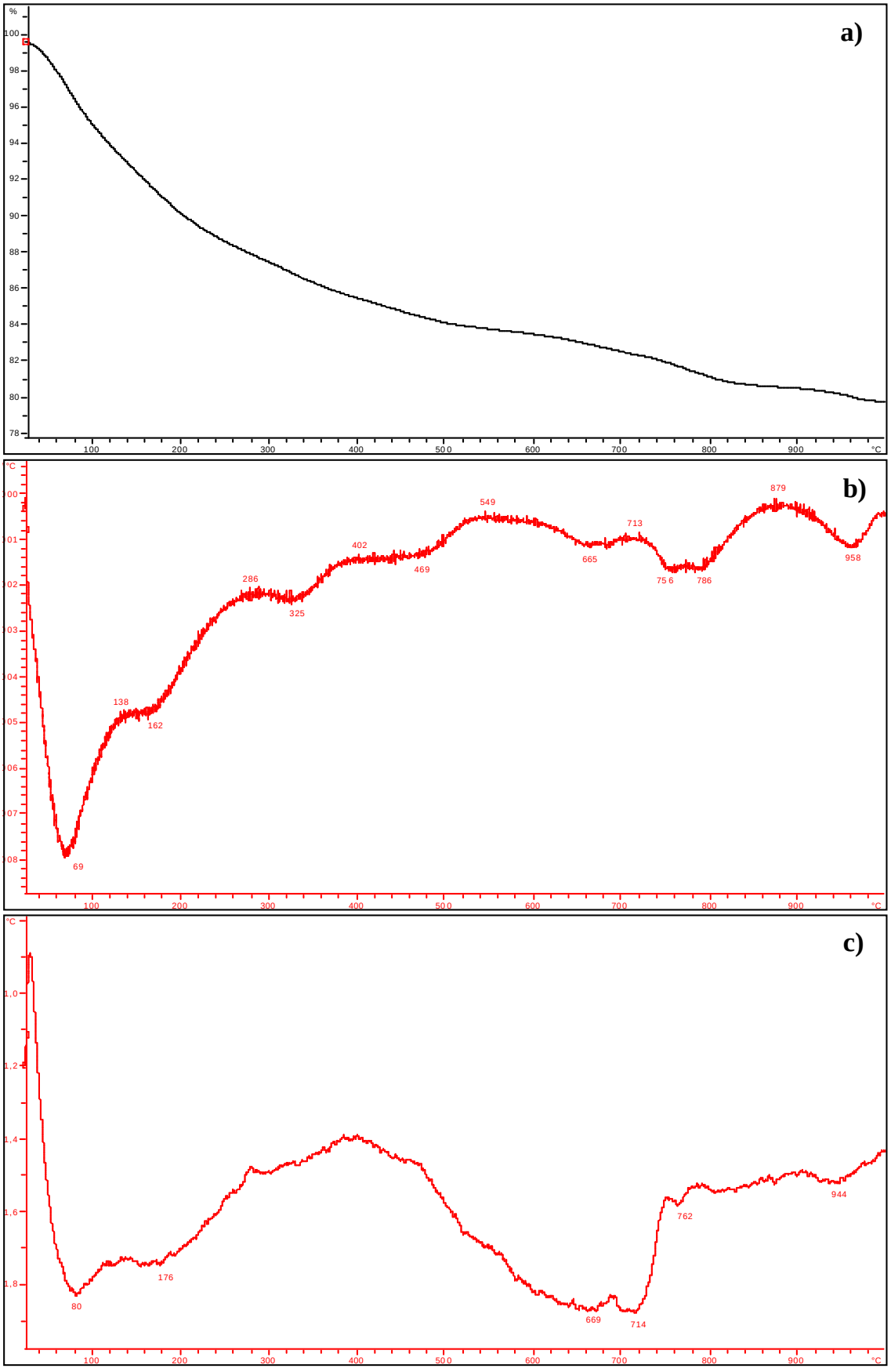

Figure A 16. Sample UF-41-14-4 surface, leached with saline solution with initial flow rate 7.5 ml/h, a) TG-curve, b) DTG-curve and c) DTA-curve.

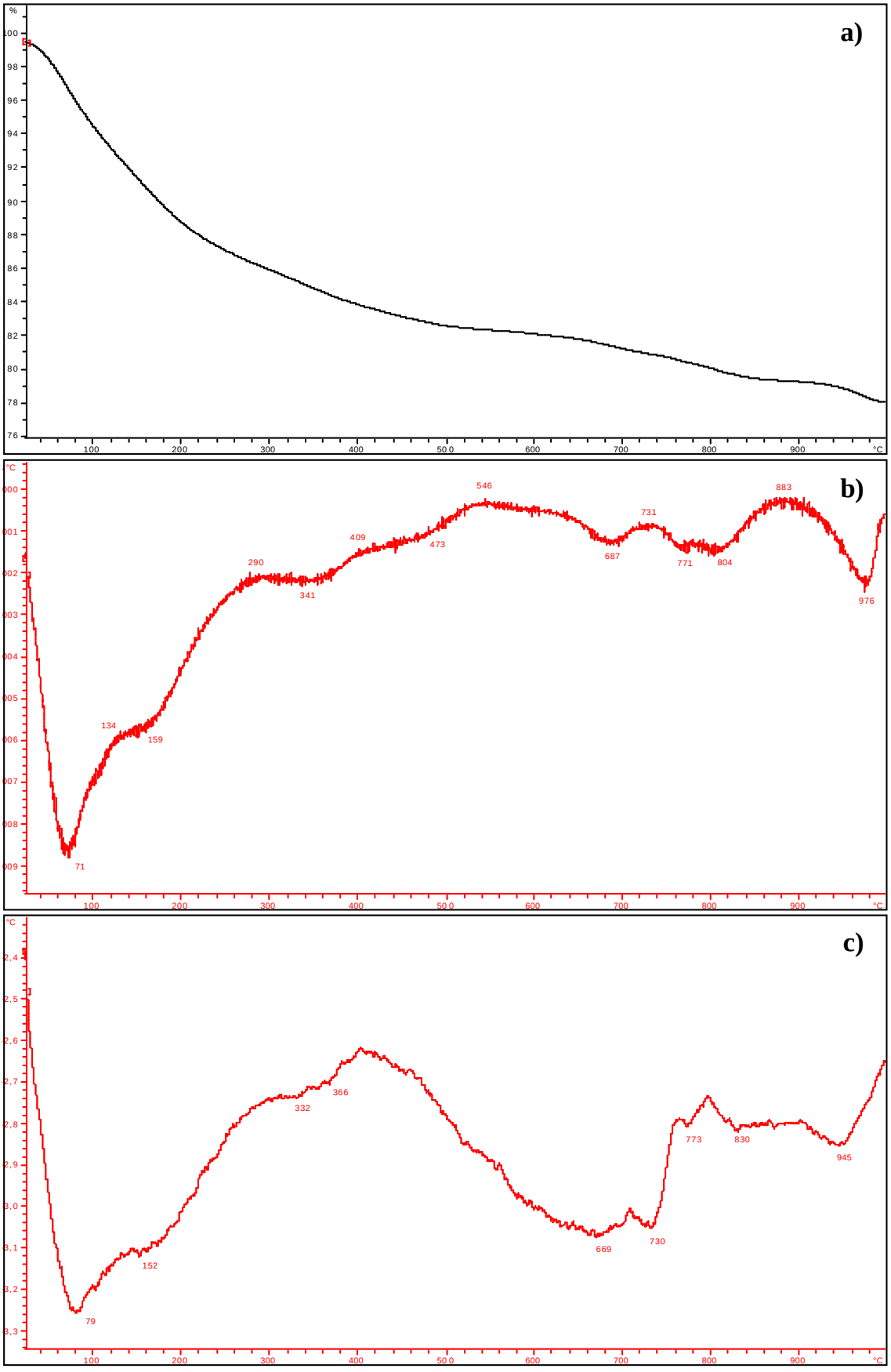

Figure A 17. Sample UF-41-14-4 base, leached with saline solution with initial flow rate 7.5 ml/h, a) TG-curve, b) DTG-curve and c) DTA-curve.

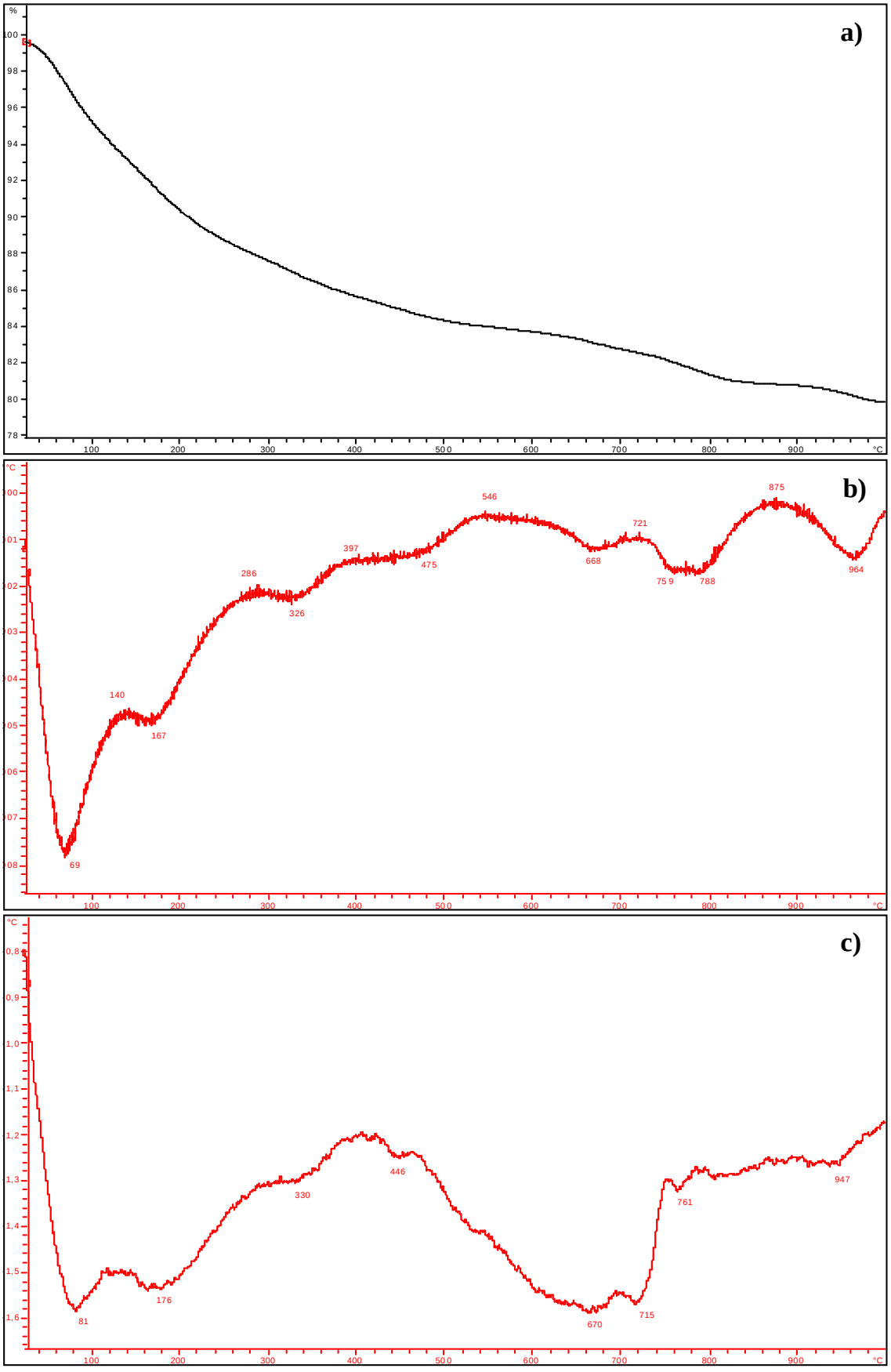

Figure A 18. Sample UF-41-14-4 surface, leached with saline solution with flow rate 0.625 ml/h, a) TG-curve, b) DTG-curve and c) DTA-curve.

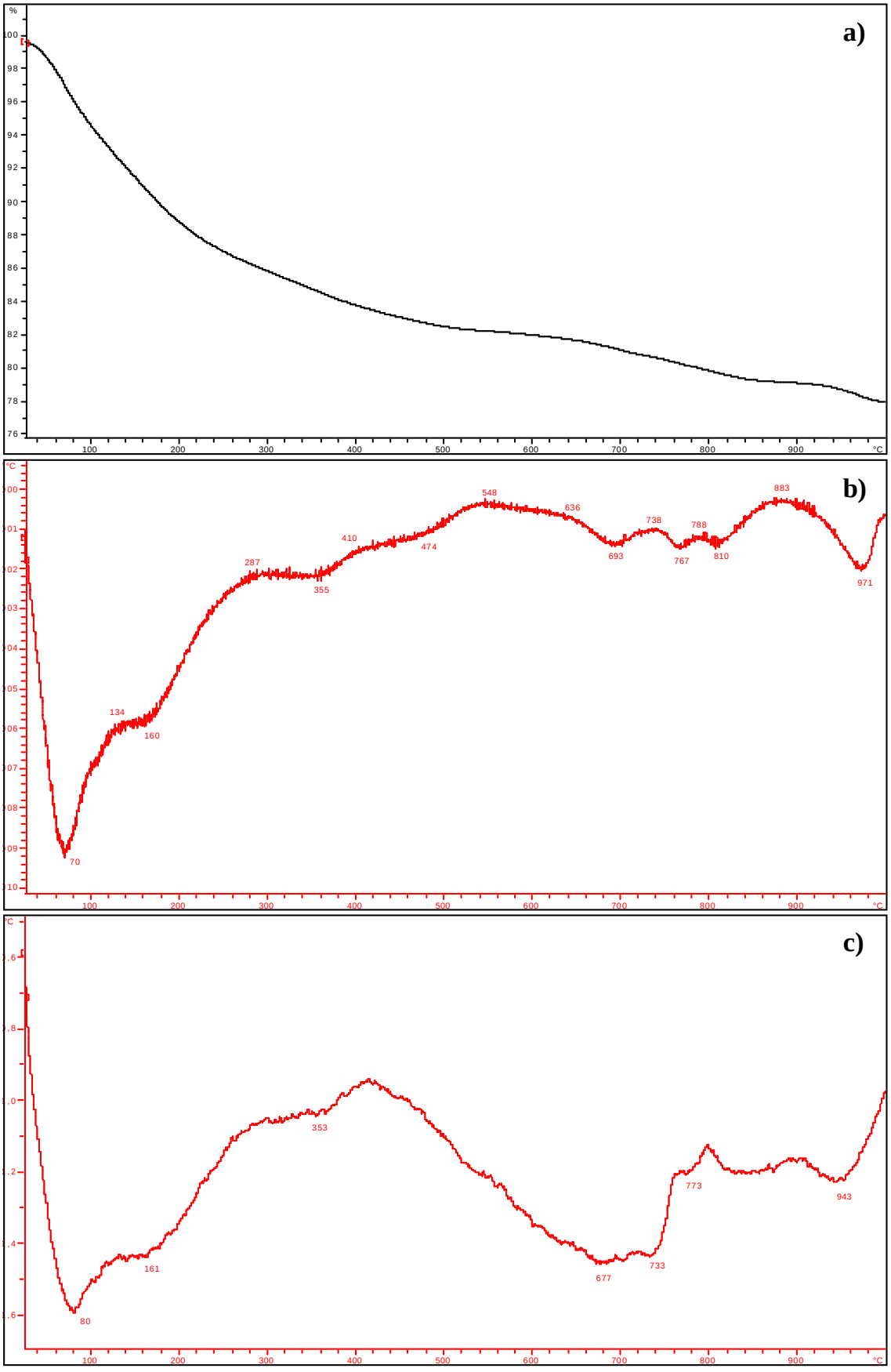

Figure A 19. Sample UF-41-14-4 base, leached with saline solution with flow rate 0.625 ml/h, a) TG-curve, b) DTG-curve and c) DTA-curve.

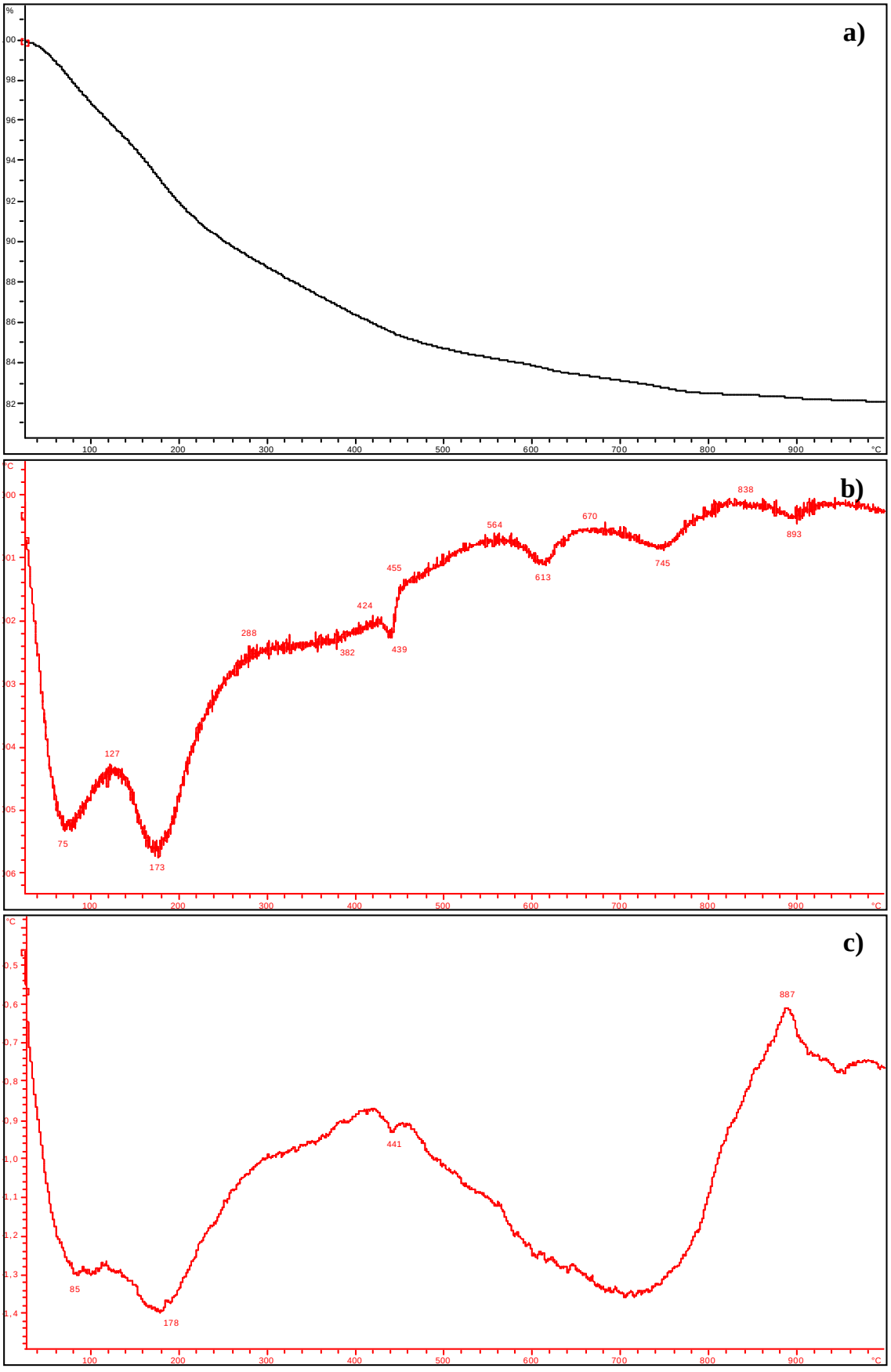

Figure A 20. Sample UF-15-10-2.8 surface, leached with fresh solution with initial flow rate 7.5 ml/h, a) TG-curve, b) DTG-curve and c) DTA-curve.

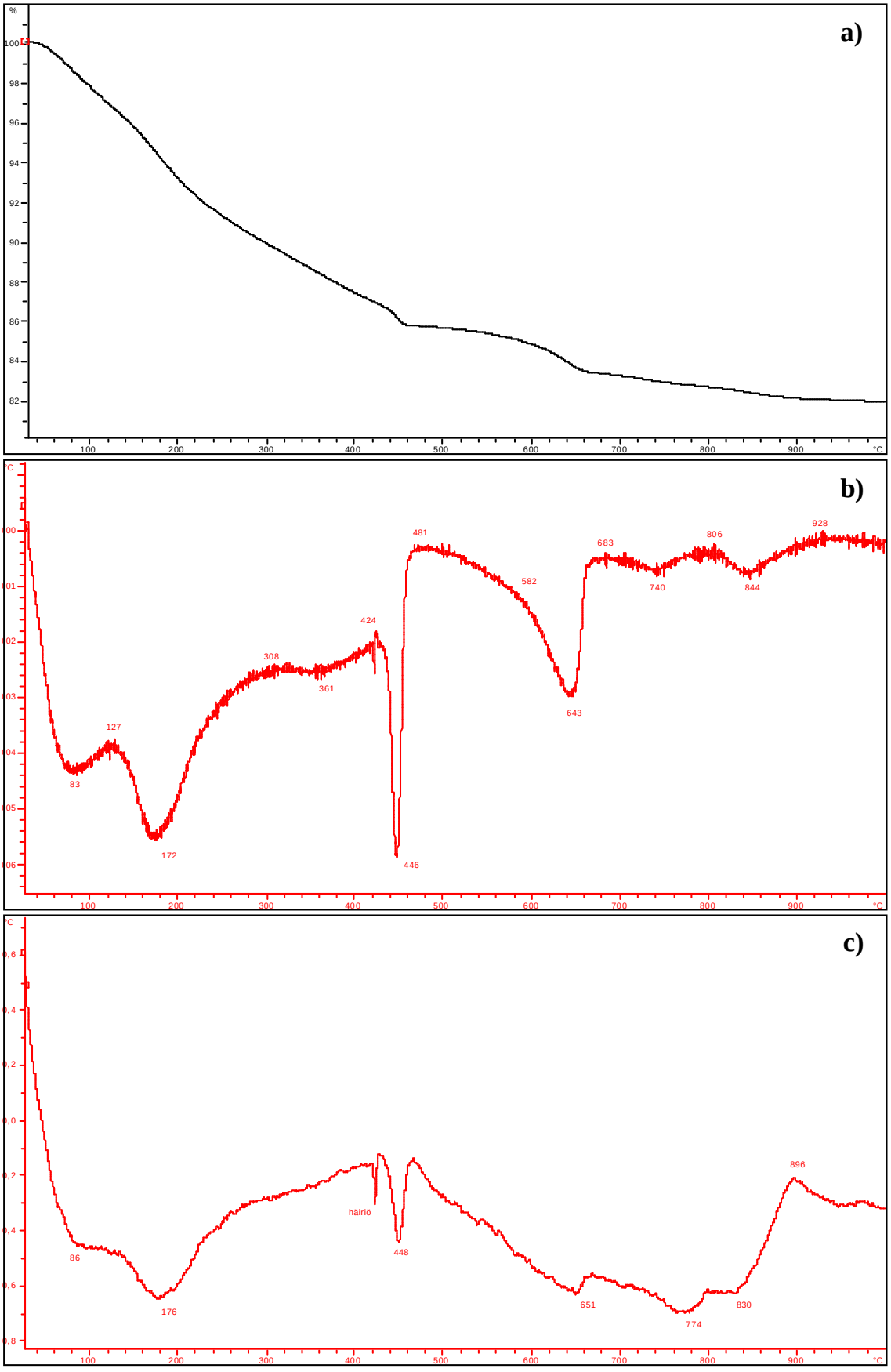

Figure A 21. Sample UF-15-10-2.8 base, leached with fresh solution with initial flow rate 7.5 ml/h, a) TG-curve, b) DTG-curve and c) DTA-curve.

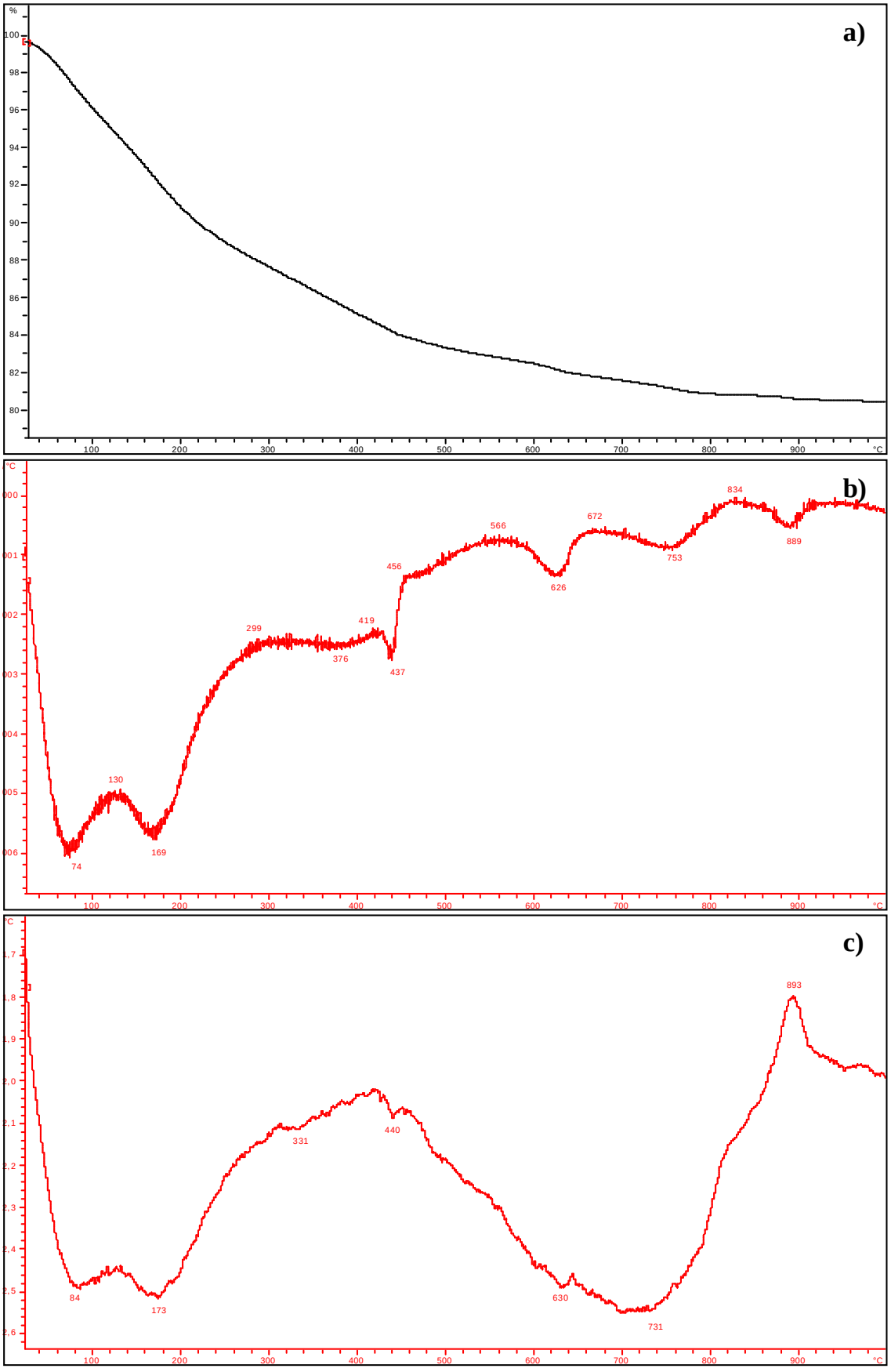

Figure A 22. Sample UF-15-10-2.8 surface, leached with fresh solution with flow rate 0.625 ml/h, a) TG-curve, b) DTG-curve and c) DTA-curve.

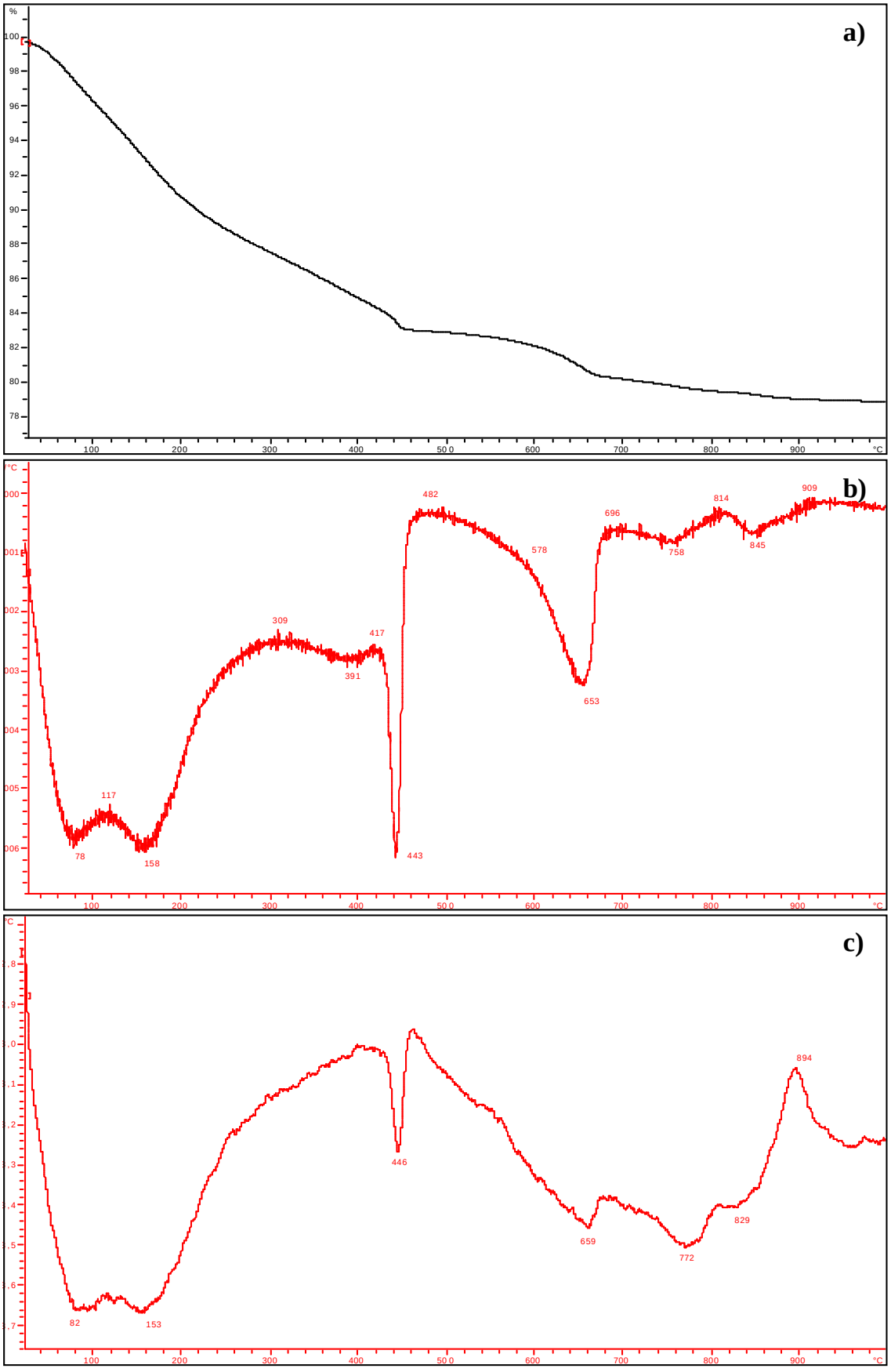

Figure A 23. Sample UF-15-10-2.8 base, leached with fresh solution with flow rate 0.625 ml/h, a) TG-curve, b) DTG-curve and c) DTA-curve.

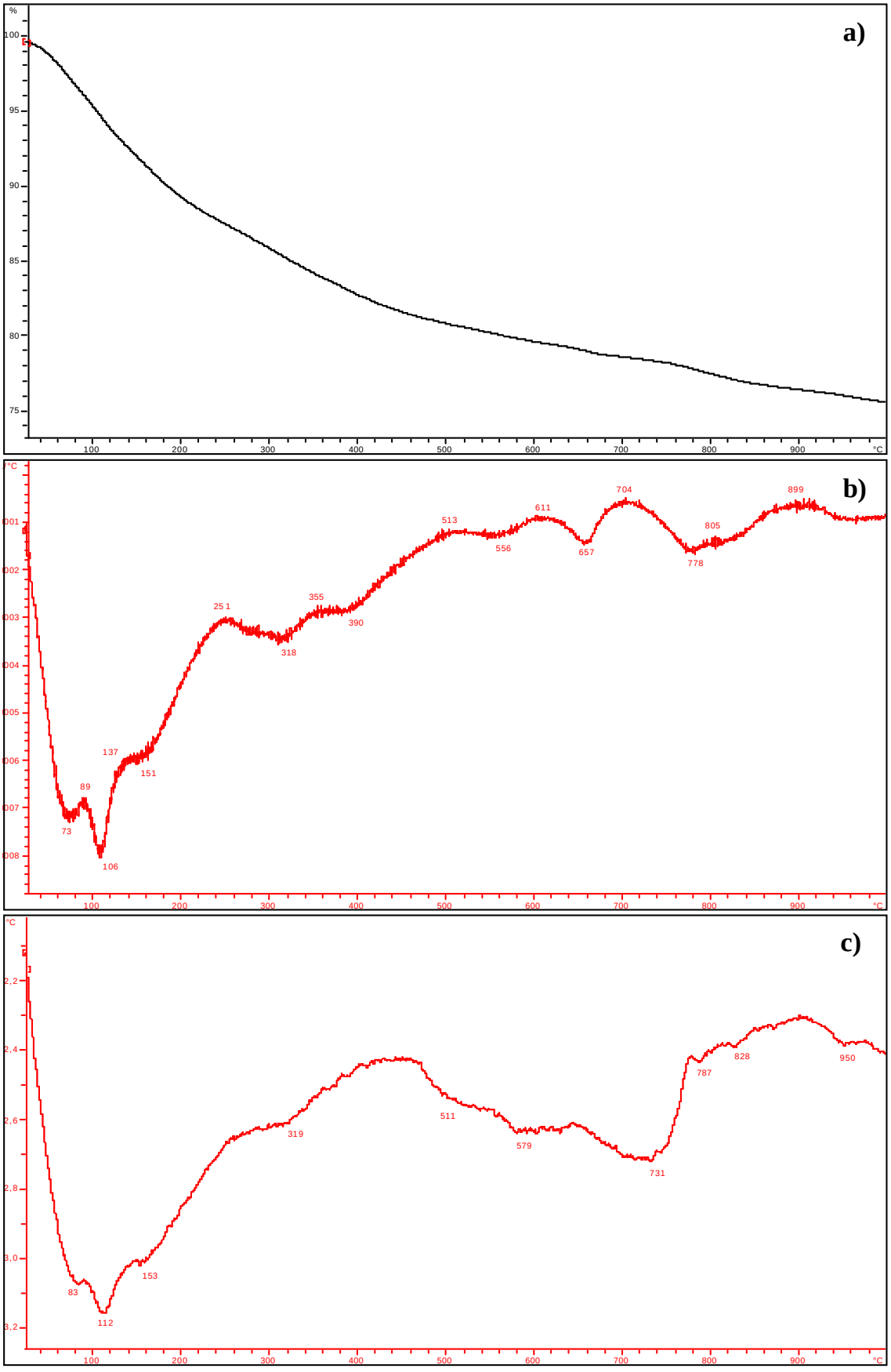

Figure A 24. Sample UF-15-10-2.8 surface, leached with saline solution with initial flow rate 7.5 ml/h, a) TG-curve, b) DTG-curve and c) DTA-curve.

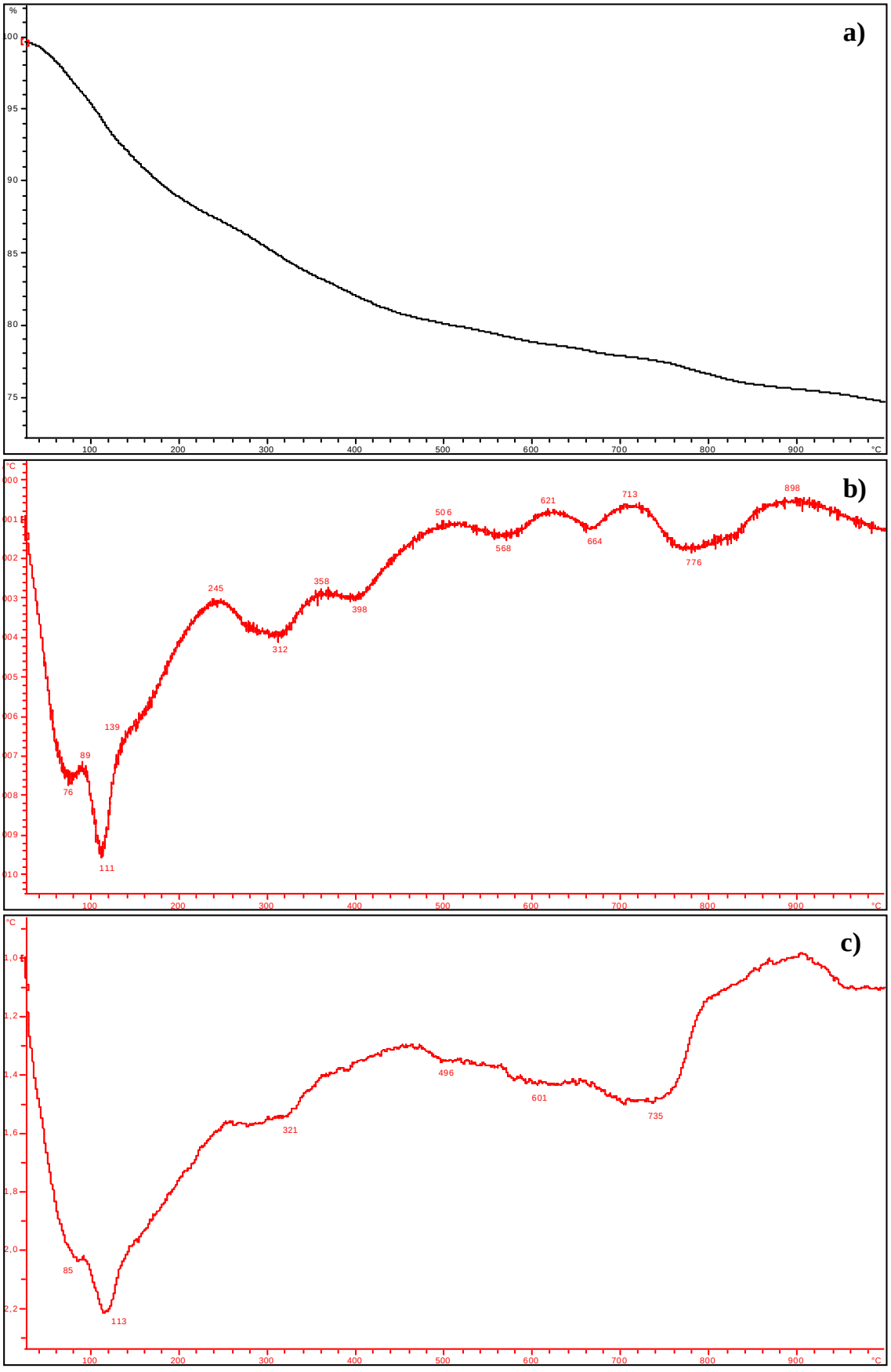

Figure A 25. Sample UF-15-10-2.8 base, leached with saline solution with initial flow rate 7.5 ml/h, a) TG-curve, b) DTG-curve and c) DTA-curve.

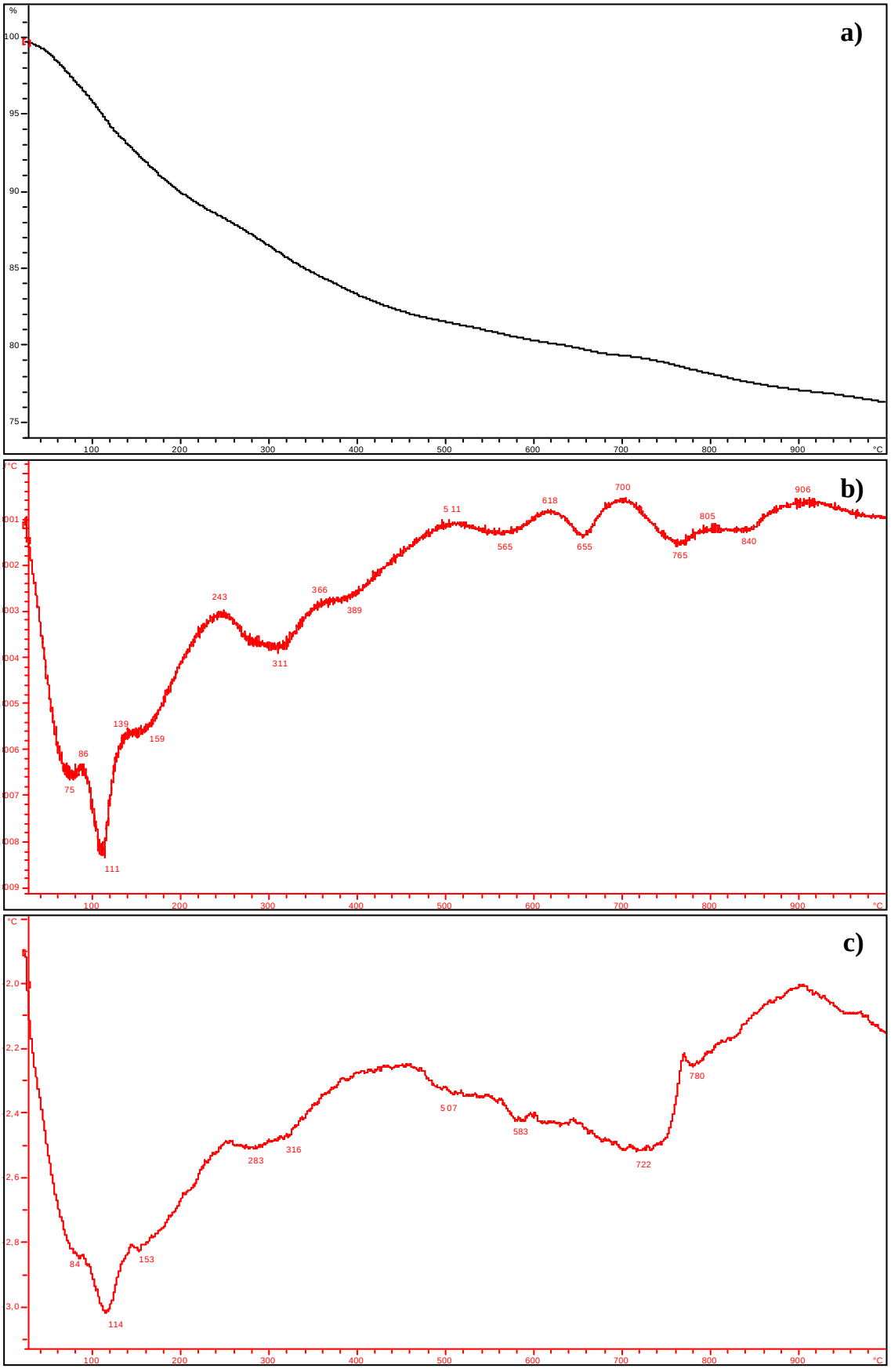

Figure A 26. Sample UF-15-10-2.8 surface, leached with saline solution with flow rate 0.625 ml/h, a) TG-curve, b) DTG-curve and c) DTA-curve.

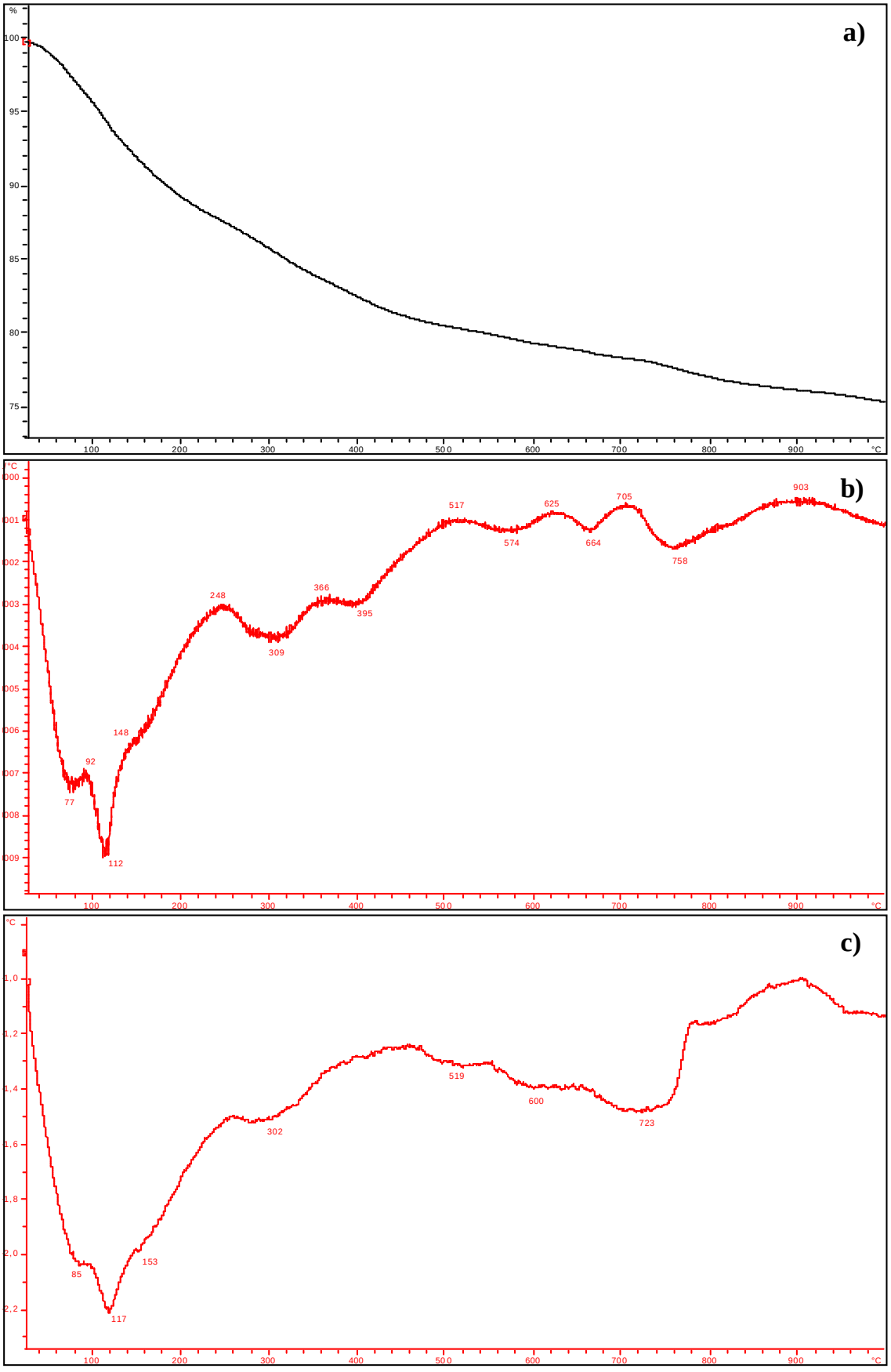

Figure A 27. Sample UF-15-10-2.8 base, leached with saline solution with flow rate 0.625 ml/h, a) TG-curve, b) DTG-curve and c) DTA-curve.

APPENDIX 4

X-Ray diffraction diagrams of the injection grout samples

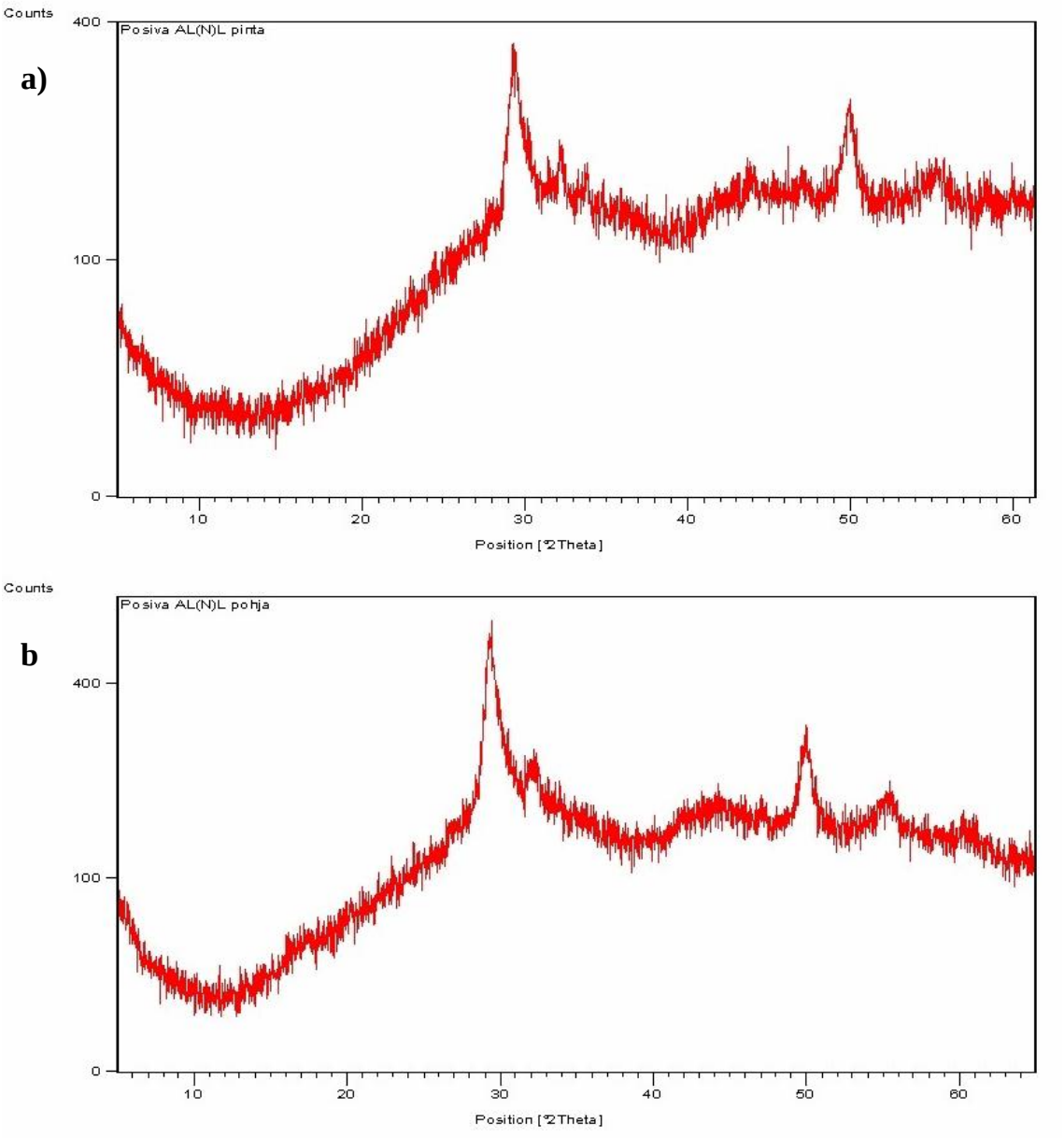

Figure A 28. X-Ray diffraction diagrams of injection grout UF-41-14-4 leached with fresh (ALL-MR) solution with initial flow rate 7.5 ml/h, a) surface and b) base sample.

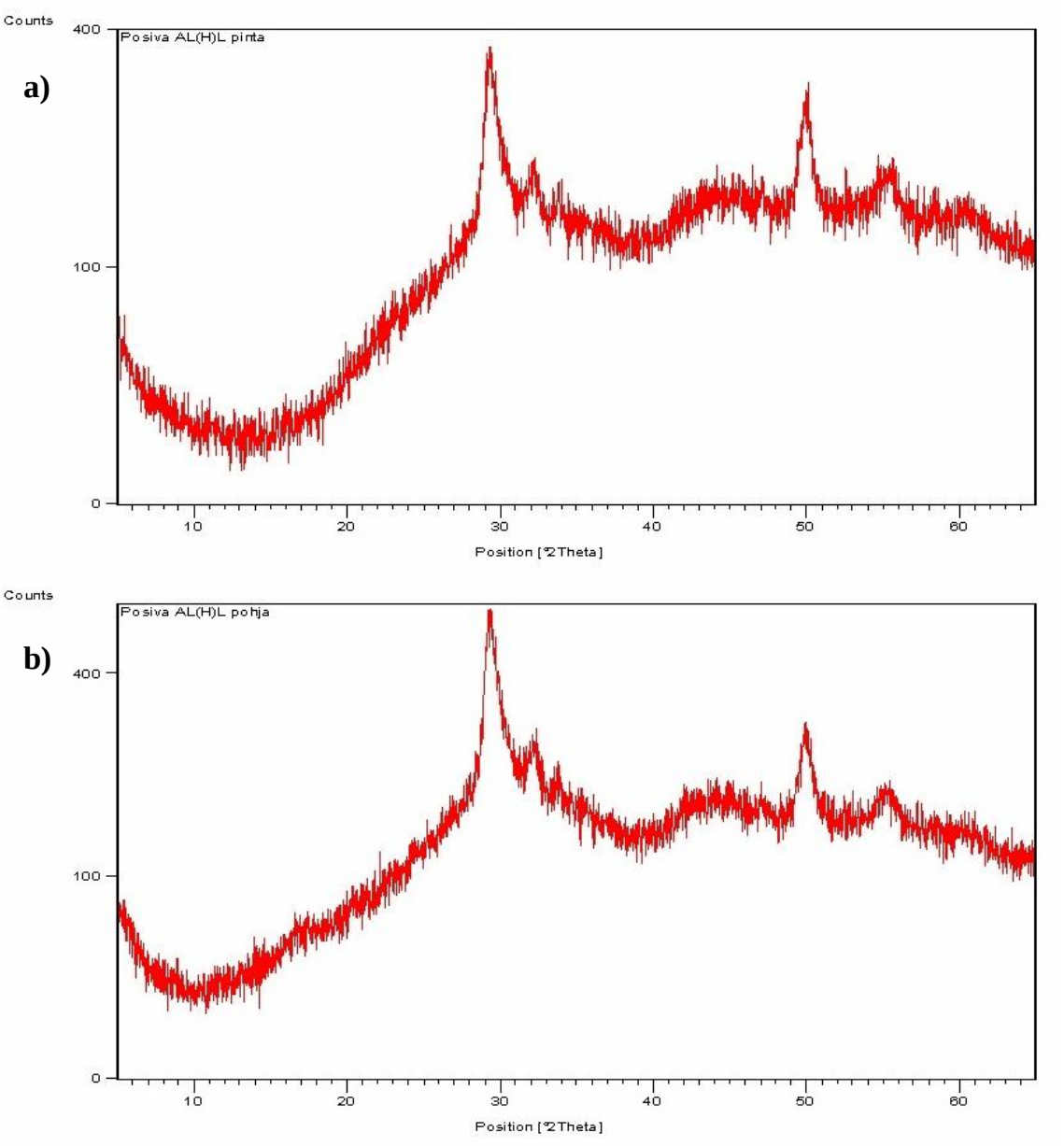

Figure A 29. X-Ray diffraction diagrams of injection grout UF-41-14-4 leached with fresh (ALL-MR) solution with flow rate 0.625 ml/h, a) surface and b) base sample.

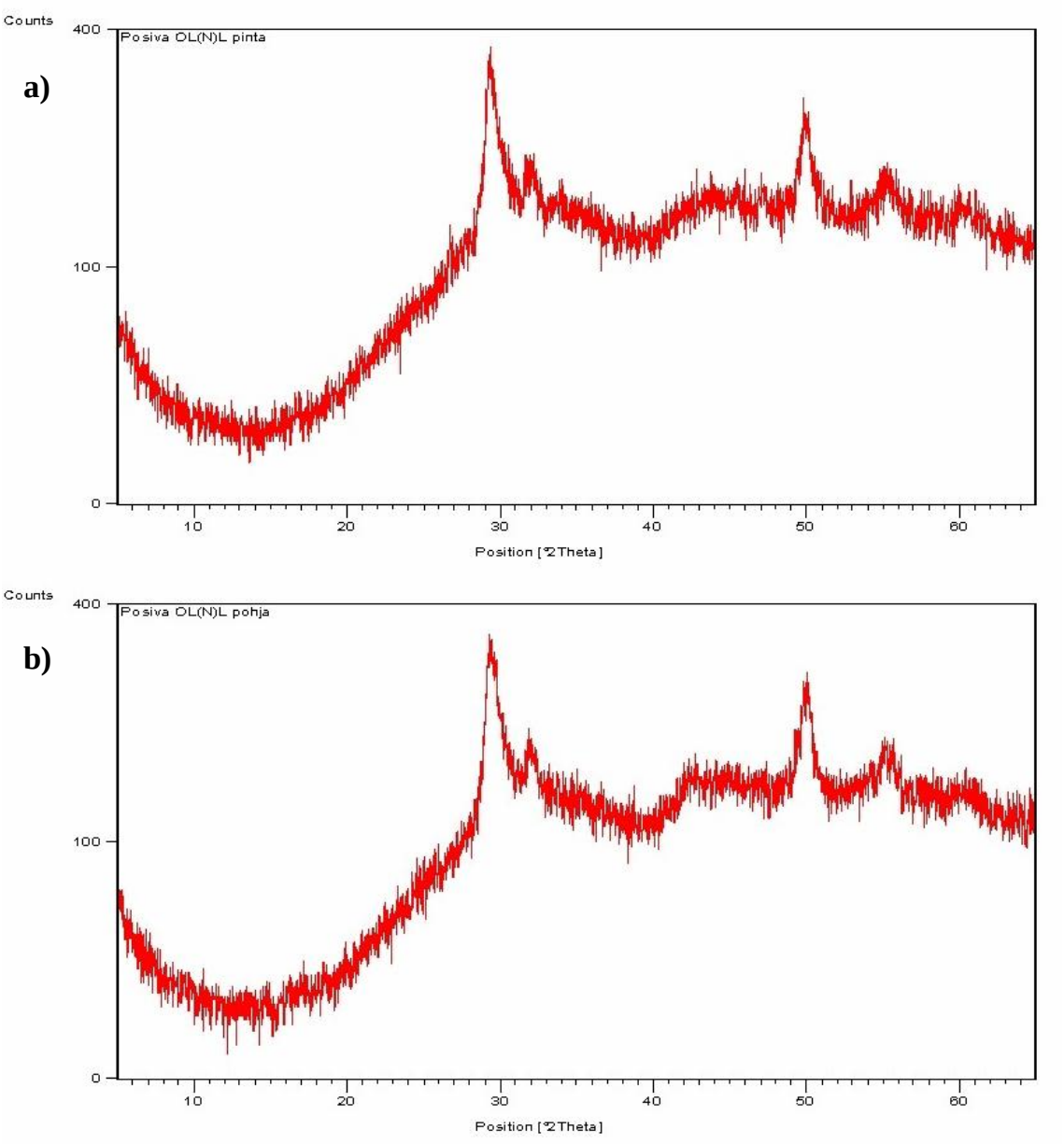

Figure A 30. X-Ray diffraction diagrams of injection grout UF-41-14-4 leached with saline (OL-SR) solution with initial flow rate 7.5 ml/h, a) surface and b) base sample.

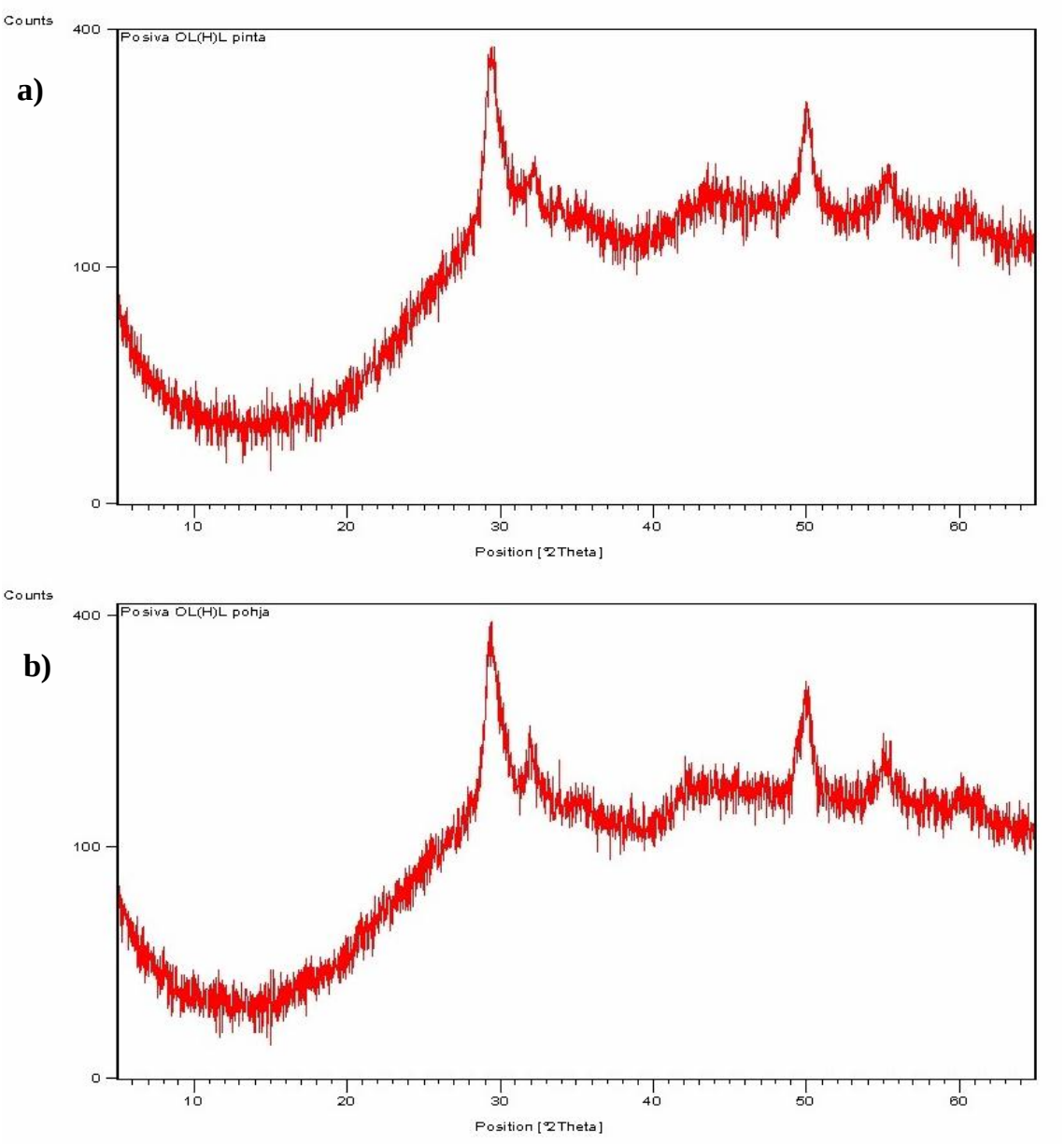

Figure A 31. X-Ray diffraction diagrams of injection grout UF-41-14-4 leached with saline (OL-SR) solution with flow rate 0.625 ml/h, a) surface and b) base sample.

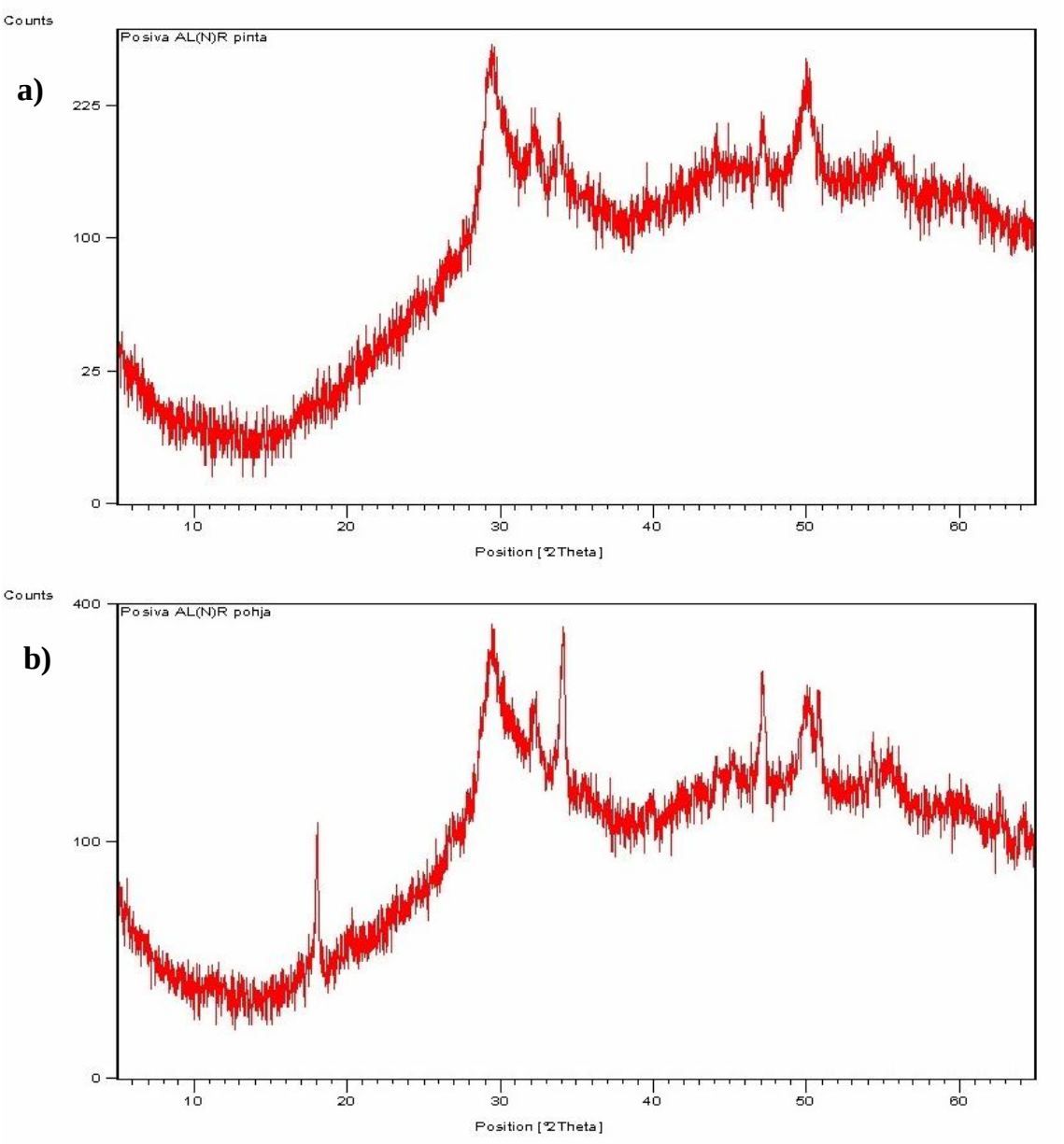

Figure A 32. X-Ray diffraction diagrams of injection grout UF-15-10-2.8 leached with fresh (ALL-MR) solution with initial flow rate 7.5 ml/h, a) surface and b) base sample.

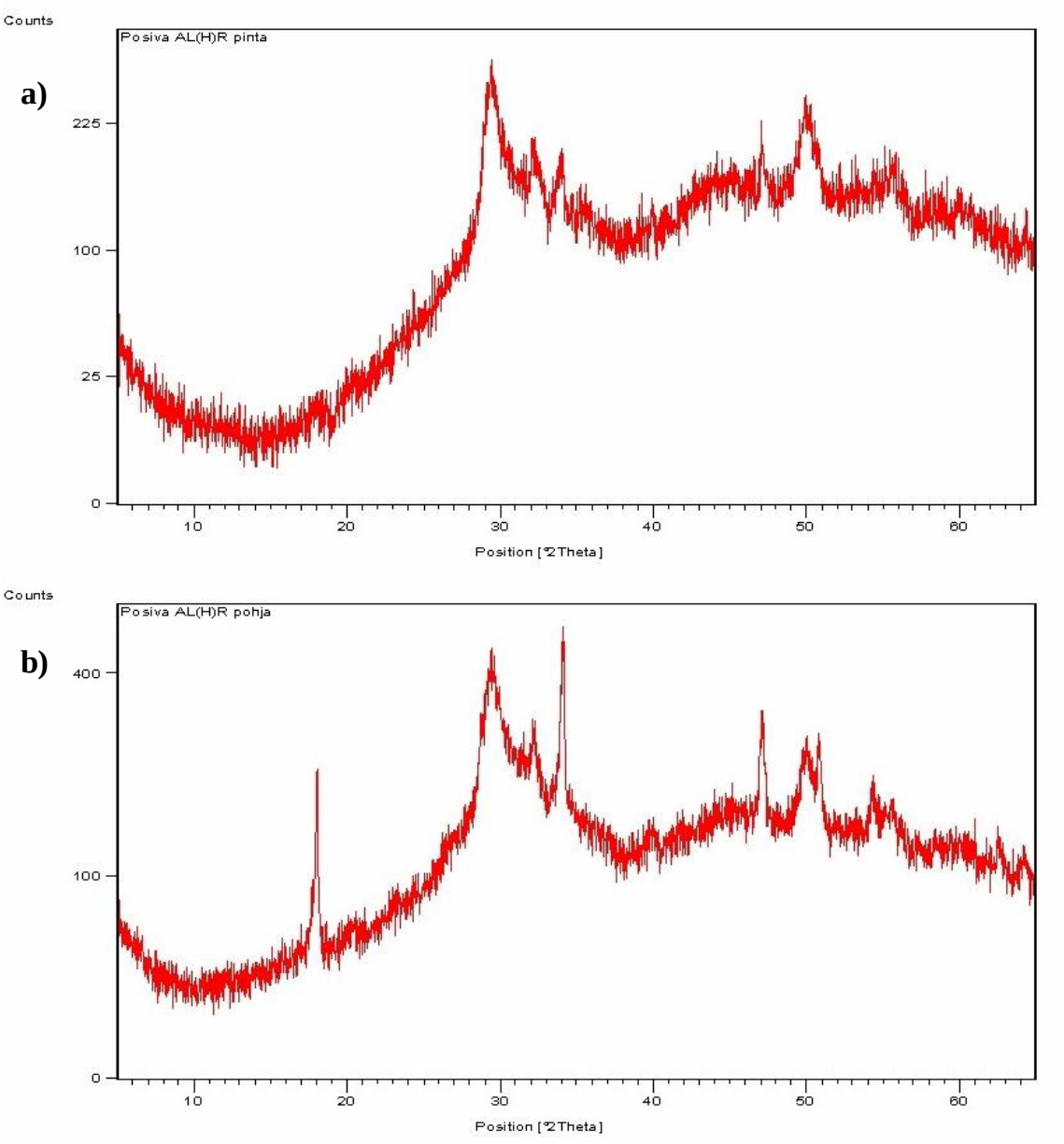

Figure A 33. X-Ray diffraction diagrams of injection grout UF-15-10-2.8 leached with fresh (ALL-MR) solution with flow rate 0.625 ml/h, a) surface and b) base sample.

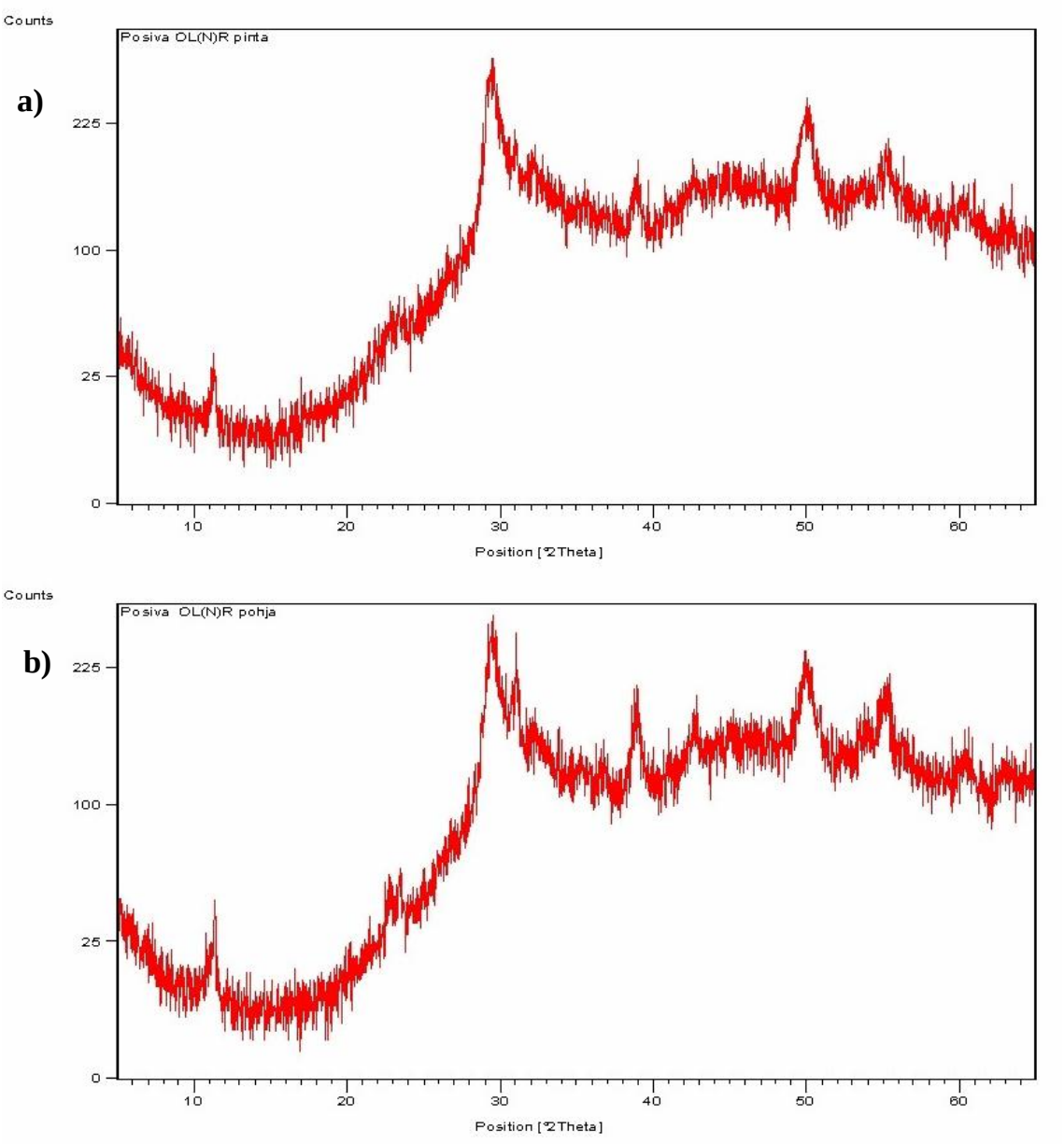

Figure A 34. X-Ray diffraction diagrams of injection grout UF-15-10-2.8 leached with saline (OL-SR) solution with initial flow rate 7.5 ml/h, a) surface and b) base sample.

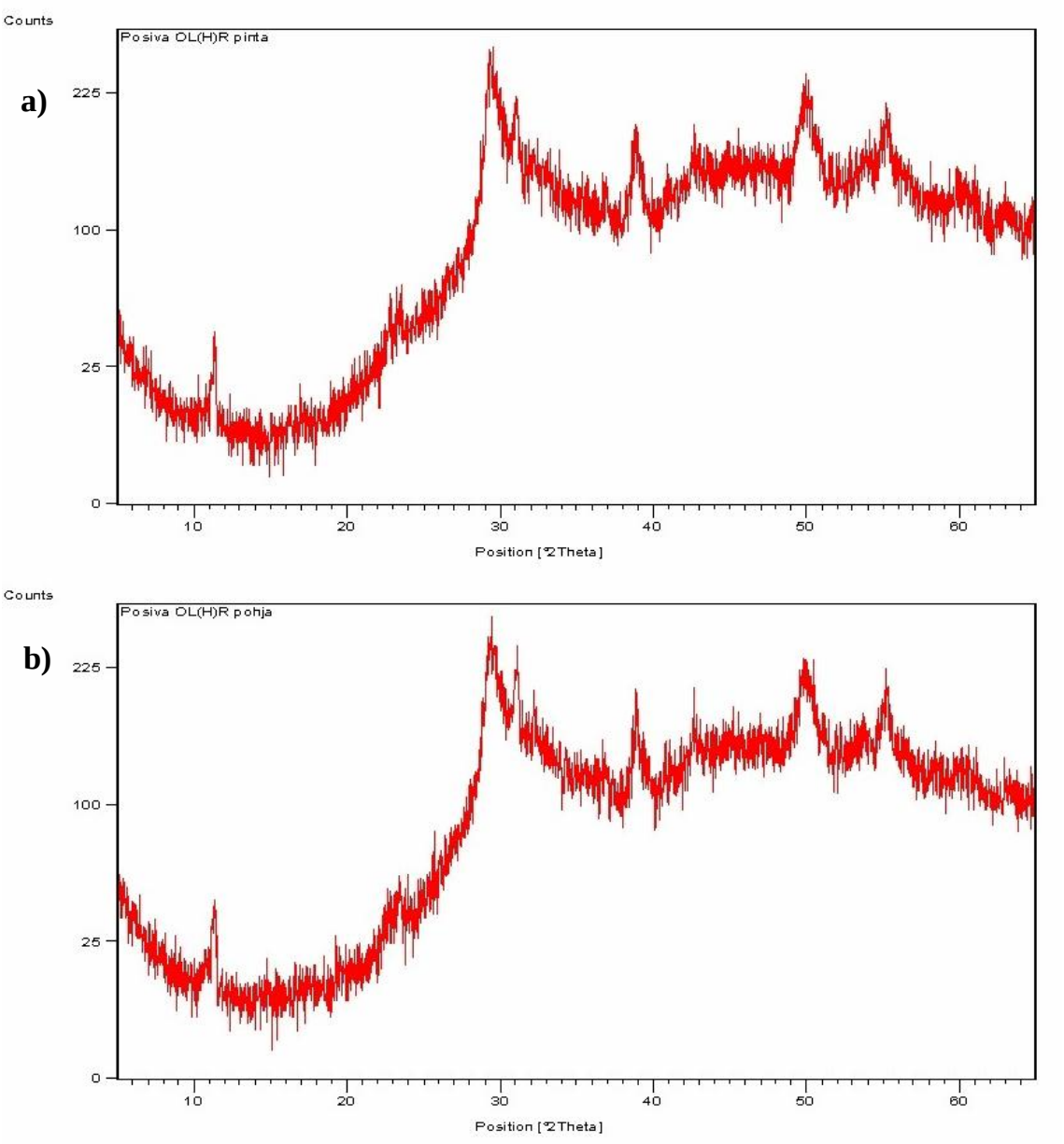

Figure A 35. X-Ray diffraction diagrams of injection grout UF-15-10-2.8 leached with saline (OL-SR) solution with flow rate 0.625 ml/h, a) surface and b) base sample.

APPENDIX 5

pH Measurement

In aqueous solutions the nature of chemical reactions such as complex formation and oxidation-reduction depends closely on the pH of the solution, there for it is essential to understand the behaviour of acids and bases.

pH theory

An acid is a substance that increases the concentration of H_3O^+ (hydronium ion) when added to water and conversely addition of a base decreases the concentration of H_3O^+ and increases the concentration of OH^-(hydroxide) ions.

Pure water is an interesting substance it undergoes self-ionization, called autoprotolysis, in which it acts as both an acid and base:

$$H_2O + H_2O \Leftrightarrow H_3O^+ + OH^- \quad (14)$$

which is generally written:

$$H_2O \Leftrightarrow H^+ + OH^- \quad (15)$$

The autoprotolysis constant (equilibrium constant) for H_2O has the special symbol K_w, where w stands for water. Table A 2 shows how K_w varies with temperature.

Table A 2. Temperature dependence of K_W.[60]

Temperature (°C)	K_w	pK_w
0	1.14×10^{-15}	14.944
5	1.85×10^{-15}	14.734
10	2.92×10^{-15}	14.535
15	4.51×10^{-15}	14.346
20	6.81×10^{-15}	14.167
25	1.01×10^{-14}	13.996
30	1.47×10^{-14}	13.833
50	5.47×10^{-14}	13.262
100	5.45×10^{-13}	12.264

An approximate definition of pH is the negative logarithm of the H^+ concentration in the solution.

$$pH \approx -\log [H^+] \quad (16)$$

This is not exactly correct. The more accurate definition is:

$$pH = - \log a_{H+} = - \log [H^+]\gamma_{H+} \quad (17)$$

When measuring the pH of the solution with a pH meter, we are in fact measuring the negative logarithm of the hydrogen ion activity, also regarded as an effective concentration, not its actual concentration. For dilute solutions, the effective and actual concentrations are equal and the activity coefficient is one. For solutions with high concentrations of ions, the crowding and presence of other charges reduces the activity coefficient to less than one and the effective concentration becomes less than the actual concentration. For most purposes equation 16 is a good working definition. In pure water at 25 °C with $[H^+] = 1.0\times10^{-7}$ M, the pH is $-\log (1.0\times10^{-7}) = 7.00$. When the concentration of H^+ ions in the solution is known the OH^- concentration can be calculated from the equations below:

$$-\log K_w = \log[H^+] - \log[OH^-] \quad (18)$$

$$14.00 = pH + pOH \quad (19)$$

A solution is acidic if $[H^+] > [OH^-]$ and basic if $[OH^-] > [H^+]$. Although pH generally falls in the range 0 to 14, the negative pH values are not unthinkable, for example for concentrated solution of strong acid like HCl.

Practical pH measurement, interference

Electrodes

Electrode is an electrochemical two-phase system where ions or electrons can cross the phase boundary: an electrochemical cell consists of two electrodes which are connected by one or several electrolytes.[61] At the boundary between the electrode and the solution there will be an electrochemical potential μ_i^* as a result of substance i. It differs from the chemical potential by the addition electrical work necessary when ions leave their phase. For a mole of substance, the electrochemical potential is:

$$\mu_i^* = \mu + z F \phi \quad \text{(J/mol)} \quad (20)$$

where: z = charge number of the ion

F = Faraday's constant ($F = 9.6485\times10^4$ C/mol)

ϕ = unmeasurable electrical potential of the individual phase

The galvanic potential $\in$ of the electrode in equilibrium with the solution is:

$$\in = \frac{{}_A\mu_i^0 - {}_B\mu_i^0}{zF \lg e} + \frac{RT}{zF \lg e} \lg \frac{{}_B a_i}{{}_A a_i} \qquad (21)$$

The factor RT/(F lg e) is known as the Nernst potential and is written U_N. Nernst potential is an important factor in quantitative electrochemistry. Table A 3 lists some values of U_N for a range of temperatures.

Table A 3. Effect of temperature on the Nernst potential.[61]

Temperature (°C)	**U_N (mV)**
0	54.20
5	55.19
10	56.18
15	57.17
20	58.16
25	59.16
30	60.15
50	64.12
100	74.04

Hydrogen electrode

To compare the results of different electrodes, such as a calomel electrode and a silver-silver chloride electrode, it is necessary to use a particular electrode as reference point. A standard hydrogen electrode was introduced for this purpose. Its potential under standard conditions (pressure 1 atm, concentration 1 M, and temperature 25 °C) is defined as zero for all temperatures. The standard hydrogen electrode is a platinum electrode exposed to hydrogen at a pressure of 1 atm, which is immersed in a solution with hydrogen ion activity of one. Potentials of any other electrodes are compared with that of the standard hydrogen electrode at the same temperature.

Reference electrode

Reference electrode is an electrode which has a stable and well-known electrode potential. It is designed to provide a stable reference potential and provide an electrical path between the process and measuring electrode. The mercury/calomel and silver-silver chloride electrodes are the most important reference electrodes used today. The silver-silver chloride reference electrodes (Figure A 36) have a silver-silver chloride inner electrode and a potassium chloride electrolyte. The potassium (K^+) and chloride

(Cl^-) ions have about the same mobilities, which minimizes the junction potential.[61] The standard reduction potential for the AgCl | Ag half-cell is +0.222 V at 25 °C, if the activity of chloride ions is unity. This not a case in a saturated solution of KCl at 25 °C, and potential of the silver-silver chloride electrode in Figure A 36 is found to be +0.197 V with respect to a standard hydrogen electrode at 25 °C.[60]

AgCl | Ag electrode:

$$AgCl(s) + e^- \Leftrightarrow Ag(s) + Cl^- \qquad E° = +0.222\ V$$
$$E(\text{saturated KCl}) = +0.197\ V$$

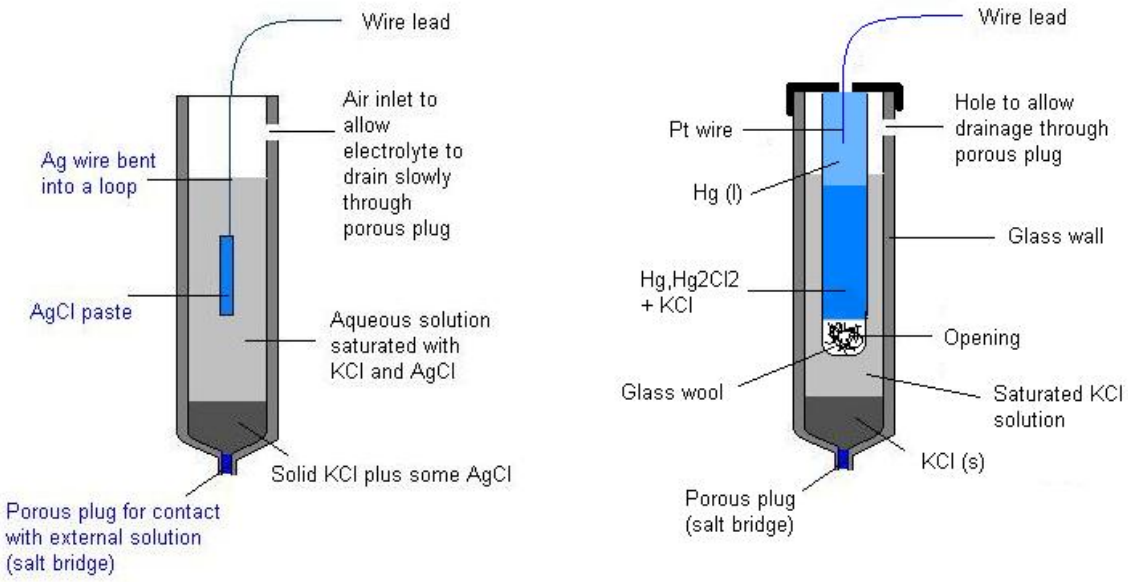

Figure A 36. Diagrams of a silver-silver chloride reference electrode (on the left) and a saturated calomel electrode (S.C.E.) (on the right).[60]

The calomel electrode is based on the reaction:

$$\tfrac{1}{2}\ Hg_2Cl_2(s) + e^- \Leftrightarrow Hg(l) + Cl^- \qquad E° = +0.268\ V$$
$$E(\text{saturated KCl}) = +0.241\ V$$

In the same way as in case of silver-silver chloride electrode the potential of a calomel electrode saturated with KCl solution is less than its standard reduction potential. The mercury-calomel electrode is more readily polarized than silver-silver chloride

electrode; it also regenerates itself much more slowly after being overloaded. Drying and exposure to the air cause irreversible destruction of the electrode.

Indicator electrodes

The indicator electrode, also referred as a working electrode, is the electrode in an electrochemical system on which the reaction of interest is occurring. Ion Selective Electrodes (ISE) fall in to a class of indicator electrodes. They are membrane electrodes that respond selectively to ions in the presence of other ions. The most commonly used ISE is the pH probe. Other ions that can be measured include metals (fluoride, bromide, cadmium, and cupric to name a few) and gasses in solution such as ammonia, carbon dioxide, nitrogen oxide, and oxygen. The key feature of an ion-selective electrode is a thin membrane across which only the intended ions can migrate.[61] The actual sensor of a standard glass electrode is spherical membrane at the tip of the electrode. It is a filled with internal buffer electrolyte and contact with the external solution (Figure A 38). The basic principle of the ion-selective electrode is to measure the electric potential generated across a membrane by "selected" ions, and comparing it to a reference electrode, a net charge is determined. The electric potential difference across the membrane can be expressed with equation 22. The equation applies to any ion-selective electrodes, including the glass pH electrodes. In case of an ideal glass pH electrode, factor-of-10 difference in activity of H^+ (one pH unit) across the electrode membrane builds a difference of 59.16 mV (at 25 °C) across the glass pH electrode (Figure A 37).

$$E = \frac{RT}{nF}\ln\left(\frac{a_1}{a_2}\right) = \frac{0.5916}{n}\log\left(\frac{a_1}{a_1}\right) \qquad \text{(volts at 25 °C)} \qquad (22)$$

where F is the Faraday constant and n is the charge of the ion, R is the gas constant, T is temperature (K) and *a* is activity of specimen.

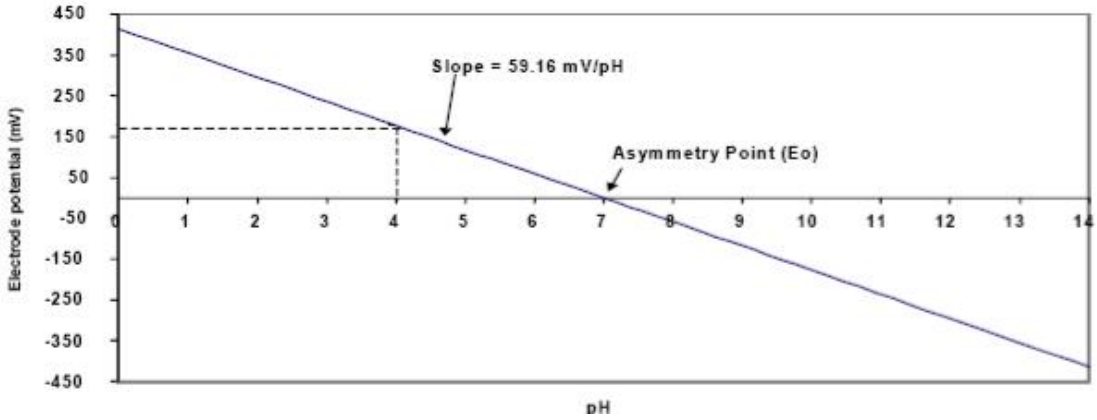

Figure A 37. Slope of an ideal electrode at 25 °C.

In the real pH combination electrode, the both glass and reference electrodes are incorporated in one body (Figure A 38). The potential difference between the inner and outer silver-silver chloride electrodes in combination electrode depends on the chloride concentration in each electrode compartment and the potential difference across the glass membrane. Because the chloride and H^+ concentrations inside the glass membrane are fixed, the only variable factor is the pH of the analyte solution outside the glass membrane, thus the response of the real glass electrodes can be described by the equation 23.

$$E = \text{constant} + \beta\,(0.05916)\log\left(\frac{a_{H+}(outside)}{a_{H+}(inside)}\right) \quad \text{(at 25 °C)} \qquad (23)$$

The value of β, the electromotive effiency, is close to 1.00 (typically > 0.98). The constant term, called the *asymmetric potential*, E_0, arises from the fact that the two sides of the membrane are not identical and a small voltage exists even if a_{H+} is the same on both sides of the membrane.

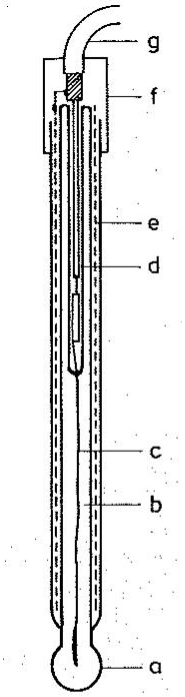

Figure A 38. Diagram of a glass combination electrode. **a** glass membrane, **b** internal buffer, **c** internal reference electrode, **d** lead connection space, **e** screening, **f** electrode head, **g** electrode lead.[61]

Calibration

Before measuring the pH of the sample, the pH electrode should be calibrated with two (or more) standard buffer solution. The buffers should be selected so that the pH of the sample lies within the range of the standards. Both measurements that make up the calibration must be made at the same temperature at which the samples will be investigated. It is essential that the difference between the two calibration buffers should be no more than 2–3 decades of difference in pH value.

Errors in pH measurement

When two dissimilar electrolyte solutions are in contact, a voltage difference called junction potential develops at their interface.[60] The junction potential puts a fundamental limitation on the accuracy of direct potentiometric measurements (at least 0.01 pH unit). The precipitation of AgCl and Ag(s) in the porous plug near the bottom of the electrode affects the junction potential, causing a slow drift of the pH reading over a long period of time.

When an electrode is transferred from one sample or buffer solution to another then the sample solution that has already diffused into the junction still remains within it

initially.[61] It might take several minutes to displace all the old sample solution within the plug. So that during this time the new sample solution will make contact with the old one rather than making direct contact with the reference electrolyte. The test cell exhibits a changing diffusion potential known as a memory effect increasing the equilibrium time of the electrode.

When the concentration of H^+ is very low and the concentration of Na^+ or Li^+ ions in sample solution is high, the electrode responds to Na^+ and Li^+ as well as to H^+.[60] Since cation errors are mainly observed in the presence of sodium, they are usually referred to as alkali or sodium error. The electrode behaves as if Na^+ were H^+, and apparent pH is lower than the true pH. In the present experiment, the concentration of sodium in the solutions is relatively low, so the alkali error can be excluded. Just as there is cross-sensitivity towards cations there are measurement errors in the presence of some anions. In strong acids, the measured pH is higher than the actual pH, perhaps because the glass surface is saturated with H^+ and can not be protonated at any more. The error is difficult to recognize and is usually small compared to alkali error.

The diffusion potentials of concentrated solutions are lower than those for solutions of moderate strength because the rates of migration of ions are diminished at concentrations of $b > 1$ mol/kg and the differences between ions of different species are also partially reduced.[61] At high salt concentrations the high mobilities of H^+ and OH^- ions contribute only a small portion of the diffusion potential. In such cases, it might be necessary to eliminate the relatively large residual diffusion potential by using a buffer solution whose composition is comparable with sample solution.

pH measurements are temperature dependent. An increase in temperature of solution will cause a decrease in its viscosity and an increase in the mobility of its ions. Temperature has also variety of effects on pH electrodes of both physical and chemical nature, such as:

- Temperature effects on electrode slope
- Calibration isothermal point
- Thermal equilibrium
- Chemical equilibrium
- Membrane balance.

An increase in buffer and/or sample solutions' temperature increases the hydrogen ion activity and thus increases the pH value. The temperature coefficient variation of buffer and sample solutions is minimal over a wide span of temperature in the acid region but can be quite dramatic in the alkaline region with significant variation in the neutral area. In practice it is important to report the temperature at which the measurement is done. This facilitates comparability and reduces the potential for error or misunderstanding.[62]